Assistance Regulation in Wearable Robots

by

Aliasgar Morbi

A Thesis submitted to
the Faculty of Graduate Studies and Research
in partial fulfilment of
the requirements for the degree of
Master of Applied Science

Ottawa-Carleton Institute for
Mechanical and Aerospace Engineering

Department of Mechanical and Aerospace Engineering
Carleton University
Ottawa, Ontario, Canada
September 16, 2009

Your file Votre référence
ISBN: 978-0-494-60218-8
Our file Notre référence
ISBN: 978-0-494-60218-8

Abstract

Actuated assistive devices (ADs) such as powered orthoses and exoskeletons can dramatically enhance the quality of life of individuals suffering from motor impairments, and have the potential to promote neuromuscular recovery as a result of prolonged use. However, most research in the area of powered ADs has focussed on designing and controlling wearable robots that amplify the user's strength. While appropriate for military and search and rescue applications, prolonged use of ADs that amplify muscle strength may result in unanticipated detrimental effects such as muscle atrophy - muscle amplification controllers (MACs) drastically reduce the muscle effort required to perform both high and low intensity tasks. Additionally, it is a well known and proven fact that patient involvement in rehabilitation therapy is fundamental in improving both the level and rate of a patient's recovery. Thus, active assistance regulation is essential in allowing any wearable robot or powered AD to promote neuromuscular recovery. At minimum, all such ADs should be controlled to provide assistance only when required.

This thesis presents a novel AD controller capable of achieving this goal. The assistance regulation controller (ARC) reported in this thesis consists of a modified impedance control algorithm that ensures that the user is provided with assistance only when required, and that allows the user to retain full control over the orthosis-assisted limb or joint motion. Simulations of orthosis-assisted knee motion confirm both of these beneficial features of the ARC, and indicate that the ARC encourages significantly more user effort than a MAC. This thesis also describes the design of a single degree of freedom experimental apparatus developed to verify and validate the simulation results. Knee and elbow

extension experiments conducted with seven healthy male participants confirm the benefits predicted in simulation, and suggest that the ARC may be better suited than the MAC for rehabilitation applications of wearable robots.

To my parents. Your sacrifices made this opportunity possible.

Acknowledgments

I would like to thank my supervisors, Mojtaba Ahmadi, Adrian Chan, and Robert Langlois for their patience, guidance and advice in matters technical and otherwise, and for giving me the freedom to go down paths that sometimes led nowhere. I would also like to thank Kevin Sangster and Alex Proctor for their assistance during my time in the machine shop, and all the students in the ABL Lab for their input and suggestions, and for making the long hours in the lab enjoyable.

Table of Contents

List of Tables

List of Figures

List of Abbreviations

AD	Assistive device
ARC	Assistance regulation controller
DAC	Data acquisition card
DOF	Degree of freedom
EMG	Electromyography
ICR	Instantaneous centre of rotation
IDB	Inverse-dynamics-based
LLF	Lower leg frame
MA	Motor assembly
MAC	Muscle amplification controller
RART	Robot-assisted rehabilitation therapy
ULF	Upper leg frame

Chapter 1

Introduction

1.1 Overview

Muscle loss and motor skill degradation, two common outcomes of neurological disorders such as stroke and Parkinson's disease, affect millions of individuals around the world. Motor skill impairments in particular can substantially limit the ability of many individuals to work, participate in recreational activities, or even perform the activities of daily living. Assistive devices (ADs) have been shown to increase the autonomy and quality of life of individuals suffering from such impairments while simultaneously reducing home care costs and caregiver burden [1].

Devices such as canes, walkers, and powered exoskeletons are all examples of the broad range of devices classified as ADs. However, powered ADs such as actuated orthoses and exoskeletons have been the focus of substantial recent research and have received particular interest from the robotics community (see [2] for a review). In addition to the benefits described above, powered ADs also have the potential to lower rehabilitation therapy costs, and to promote neuromuscular recovery. However, this last benefit - promotion of neuromuscular recovery - is unlikely to be realized using the muscle amplification control strategies typically employed on most powered ADs (see [3–8] for examples).

Muscle amplification control strategies amplify the user's strength (or drastically

minimize the effort required to complete a particular task). Prolonged use of such devices may result in unintentional detrimental effects such as muscle atrophy if these devices provide users with excessive levels of assistance. Furthermore, it is also well known that maintaining an appropriate level of exercise intensity is fundamental in facilitating neuromuscular recovery during rehabilitation therapy [9]. Accordingly, powered ADs intended for rehabilitation applications need to strike a balance between providing the immediate assistance required to perform the desired activity and persistently challenging the user to exert more effort. This thesis presents the development and experimental validation of an AD controller capable of achieving this balance.

1.2 Motivation

1.2.1 Factors that Influence the Rate and Magnitude of Recovery during Rehabilitation Therapy

Loosely speaking, neural plasticity refers to the adaptive capacity of the brain to physically reorganize itself as a result of thinking, learning, and doing. Neural plasticity and rehabilitation therapy are intimately linked since experience-dependent neural plasticity is the mechanism that allows rehabilitation therapy to restore or compensate for lost function [9]. A recent review of experience-dependent neural plasticity suggests ten principles that should be used to guide clinical research and practice, and to optimize rehabilitation therapy [9]. These principles are defined using statements such as, *use it or lose it*, *use it and improve it*, *time matters*, *age matters*, etc. However, three of these principles - the importance of intensity, repetition, and salience - are most relevant to the the field of robot-assisted rehabilitation therapy (RART). The implications of these principles are summarized below.

- Experiments with animals have shown that exercise intensity is a strong factor in

inducing functional recovery through neural plasticity [9]. More importantly, though, experiments with animals have also shown that significant behavioural changes may not always be accompanied by lasting neuronal changes. In fact, repetition of newly learned or relearned tasks is essential for inducing plasticity [9].

- Experiments with animals also suggest that exercise repetition and intensity alone are not enough to guarantee lasting changes; experience-dependent plasticity is an equally strong function of salience (i.e., the importance of one experience relative to other experiences). Thus, active participation, emotional engagement, and experiencing a sense of accomplishment during the rehabilitation process are essential in promoting - and perhaps even optimizing - functional recovery [9]. Studies with human participants have also confirmed the importance of patient participation during RART [10].

Extrapolating these ideas to AD control yields the following observations:

- ADs may be capable of inducing functional recovery through prolonged use;
- AD controllers should only provide users assistance when assistance is required; and
- AD controllers should be designed to ensure active user participation.

The concepts of salience and active participation also have broader implications for RART in general. The types of robots typically used with RART, *rehabilitation robots*, are designed to provide specific and repetitive therapy and typically consist of large, stationary devices used in hospitals or rehabilitation therapy clinics (e.g., as in [11–16]). An example of such a device, the pneumatically-actuated upper extremity exoskeleton, Pneu-WREX is shown in Figure 1.1 (a).

Most approaches to RART rely on requiring patients to track pre-defined trajectories. These trajectories are chosen to correspond to the specific actions or behaviours that require rehabilitation. Another key feature of RART, especially for upper extremity

(a) Pneu-WREX, a pneumatically actuated upper extremity rehabilitation robot (from [11])

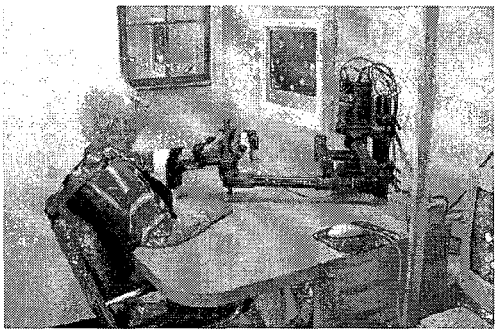

(b) The visual interface used with MIT-MANUS a rehabilitation robot designed for planar reaching tasks (from [13]).

Figure 1.1: Examples of rehabilitation robots, and the visual interfaces used to administer RART.

rehabilitation, is the use of video-game-like interfaces for administering the therapy (e.g., as in [11–14]). An example of such an interface can be seen in Figure 1.1 (b).

Asking users to follow the pre-defined trajectories may be appropriate in the early stages of rehabilitation therapy, especially for individuals suffering from extreme motor impairments. However, trajectory-driven approaches naturally become limiting at later stages in rehabilitation therapy when focused, task-specific therapy may be necessary (e.g., for walking on uneven terrain or brushing teeth). Designing trajectories for such complex (but routine) tasks is impractical. These trajectories would be extremely context and environment specific, and designing a sufficiently robust trajectory database would be very time-consuming and challenging. Additionally, the process of choosing the appropriate trajectory from a vast database would itself require complex and involved logic.

Using video-game-like interfaces to administer RART may also be undesirable. With this approach to RART, the task performed by the user only simulates the task which requires rehabilitation. Though there is no direct evidence available to date, it is likely that RART would be most effective if the therapy required performing the actual task that require rehabilitation. Therapy salience - perhaps the key factor that controls the rate and

magnitude of functional recovery [9, 10] - would be maximized with such an approach to RART.

ADs, on the other hand, are much more likely to be used in representative environments and contexts (e.g., in the user's home rather than in a hospital or clinic) since they are designed to be sufficiently light and compact enough to be fully integrated with the user's body. Examples of such devices can be seen in Figures 1.2 and 1.3. It is also important to note that powered ADs are developed to assist users in performing a variety of tasks. In contrast, most rehabilitation robots are developed to allow users to perform simulated versions of a particular task in controlled environments. Since salience is clearly linked to the ability to successfully complete a task - and the accompanying gains in motivation and confidence - powered ADs may prove to be superior at promoting recovery if designed and controlled expressly for that purpose.

1.2.2 Common Approaches to AD Control

As discussed above, ADs are designed to assist users in performing a wide range of different tasks. As a result, the desired motion of an AD is typically prescribed in real time using user-supplied input signals such as interaction forces measured at user-device interfaces or surface electromyography (EMG) signals (see [3–6, 8, 17, 18] for examples). User-device interfaces consist of any regions of contact between the user and orthosis. Thus, the key challenge in AD control is in predicting the user's desired motion, i.e., the desired trajectory of the user's joint or limb that corresponds to what the user is thinking about doing. Accurate estimates of desired motion provide a means for systematically prescribing the appropriate assistance magnitude and timing. However, both interaction forces and EMG signals are poor predictors of desired motion. EMG signals indicate the level of muscle activation, while interaction force measurements indicate how much the exoskeleton interferes with the user's natural motion. EMG signals are best used as predictors of user effort (e.g., as in [3,6,19]) or muscle force/joint torque (e.g., as in [4,5,20,21]).

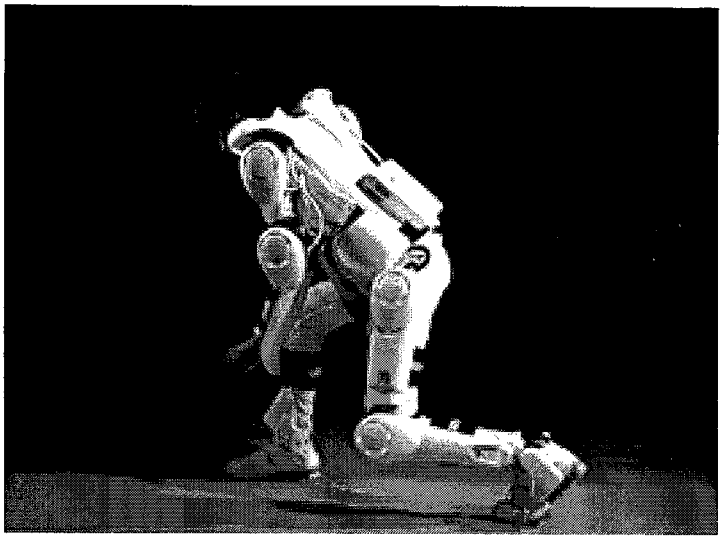

Figure 1.2: The electrically actuated HAL5 exoskeleton from Cyberdyne Inc.\(from http://www.cyberdyne.jp/english/).

Figure 1.3: ReWalk exoskeleton from Argo Medical Technologies Ltd.\(from http://www.argomedtec.com/downloads.asp).

In some cases, it is possible to estimate the user's desired motion from EMG-based joint torque estimates [22]. These estimates may be obtained by assuming the EMG-based joint torque estimates to be equal to the actual joint torques required to generate the user's desired motion. Accordingly, these estimates along with any relevant kinematic measurements (i.e., joint positions and velocities) may be used as inputs into a limb or body dynamic model. The position trajectory obtained by integrating the dynamic model may be assumed to reflect the desired motion of the user [22]. However, this approach for estimating the desired motion is only applicable to healthy individuals. Individuals suffering from neuromuscular impairments may be unable to generate the joint torques required to perform the desired motion. In this scenario, the EMG-based torque estimates would likely only reflect what the user can do, rather than to accurately predict what the user would like to do.

The challenges in predicting the user's desired motion have in part led to the development of the muscle amplification control strategies used on most ADs. It is also important to note that many ADs were originally designed for military or industrial applications (e.g., [7] and [4]), where the need to regulate user effort did not arise as an explicit concern. This too, has contributed to the predominance of muscle amplification control strategies. Figure 1.4 illustrates how a typical muscle amplification controller (MAC) works. The basic premise behind muscle amplification is to estimate user effort, and to provide assistance directly in proportion the magnitude of the estimated effort.

Some muscle amplification control strategies use EMG signals to predict joint torque, and command joint actuator torques proportional to the estimated joint torque (e.g., as in [4, 20, 21]). Simpler approaches that involve commanding actuator torques proportional to EMG signal amplitudes have also been considered in [6, 8]. Alternatively, more complex methods employing function approximators and learning algorithms to learn the relationship between EMG signals the user's intended motion have also been considered

in [3, 23].

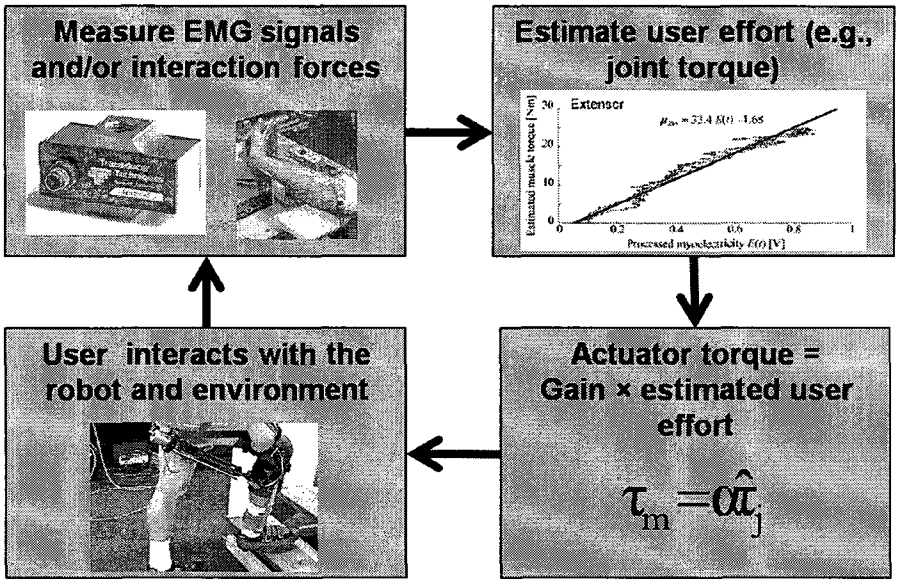

Figure 1.4: A flow chart describing the typical application of the MAC

In general, EMG-based AD controllers are attractive because EMG signals precede muscle contraction. This lead time provides an opportunity to complete control calculations and compensate for actuator dynamics prior to the onset of the user's motion [20]. However, inter- and intra-patient variability in EMG signals due to factors such as electrode placement and condition, skin moisture, muscle fatigue, blood circulation, EMG cross-talk, etc., [22] mean that extensive and possibly regular re-calibration of some elements of the control system may be necessary (e.g., as in [3], [22], and [20]).

These challenges have prompted some researchers to avoid the use of EMG for control altogether. The RoboKnee [24], for example, uses knee orientation and ground reaction force measurements along with a simple body dynamic model to estimate the assistance required at the user's knee joint. In [18], impedance control was used to assist the user's knee joint motion by making the user perceive a reduced joint impedance, while the novel AD controller described in [7] used positive kinematic feedback to increase the mechanical

admittance of a full body exoskeleton. This model-based controller behaved like a high gain amplifier that generated large motions from small force inputs (without requiring explicit measurements of the force inputs).

In summary, most AD's effectively employ online trajectory generators to specify their motion. While this approach is more flexible than forcing a user to track a pre-specified trajectory, most AD controllers are only designed to behave as muscle amplifiers. The problem of selectively assisting the user based on their need for assistance remains outstanding, and warrants further investigation. As discussed below, ADs that achieve this goal may have a tremendous impact on how rehabilitation therapy is administered.

1.2.3 Approaches to Active Assistance Regulation in Rehabilitation Robots and ADs

It has been proven that stiff position controllers that force users to follow a pre-defined motion discourage patient participation and limit the therapeutic benefits of RART [10]. Additionally, experimental results in [11] also indicate that stiff position controllers may encourage *slacking* behaviour during the course of the therapy. Patients will take a more passive role during therapy by reducing their effort and letting the robot do the work if given the opportunity.

These types of observations regarding the pitfalls of stiff position control have prompted the development of numerous *assist-as-needed* controllers for rehabilitation robots. Typically, these controllers are designed to selectively alter the assistance provided to the user at particular instances of the robot's desired trajectory. Some approaches rely on varying controller parameters such as stiffness and damping at different points along the trajectory [25], after successive runs of the same trajectory [14], or in relation to the tracking error at any given instant of time [11–13, 16]. Other approaches focus on varying the desired trajectory in order to modulate the assistance provided by the robot. These

approaches include changing the shape of the desired trajectory if the user is unable to complete a task within a pre-specified amount of time [12], or reshaping the desired trajectory in ways that minimize interaction forces over the entire trajectory [15], or in ways that a generate a pre-specified relationship between the measured interaction forces and tracking error [15]. While effective, these approaches for intelligently assisting users are only suitable for devices that are designed to follow pre-specified trajectories. Additionally, many of these controllers rely on repeating a particular motion numerous times, or on therapist input for proper calibration. As such, these approaches cannot be transferred or easily manipulated to work with ADs because ADs do not rely on tracking pre-specified trajectories, and may be used without therapist supervision in a variety of different environments and contexts.

Few researchers have attempted to develop assist-as-needed controllers for ADs. In fact, the AD controller in [19] represents one of the only attempts at addressing this problem. The controller described in [19] was designed to increase the assistance provided to the user anytime the user's muscle activity (i.e., processed EMG data from the extensor and flexor muscles controlling the joint) exceeded a pre-defined threshold. This approach was effective because it forced the user to initiate and sustain any motion that did not generate sufficient muscle activity. However, this approach did not provide a precise method for regulating user effort, and was susceptible to phenomena such as muscle co-contraction and EMG cross-talk.

1.3 Objectives

Clinical studies with rehabilitation robots have shown that RART can be at least as effective as traditional rehabilitation therapy [10]. This naturally begs questions about how RART can be optimized to provide even more effective rehabilitation therapy.

Conventional approaches to RART, even those that employ algorithms for intelligently

assisting users based on their need, are fundamentally limited due to their reliance on tracking pre-defined trajectories. Trajectory-driven control approaches are simply not robust enough to be used in unstructured environments or for complex tasks which humans complete with ease on a daily basis. Furthermore, trajectory-driven control approaches coupled with the use of video-game like interfaces for administering RART result in therapies that merely simulate the task and environment for which the rehabilitation therapy is required.

ADs are attractive since they are designed to assist users in the completion of a wide range of tasks rather than to force them to follow pre-defined motions. However, ADs have not explicitly been designed and controlled to simultaneously assist users and promote neuromuscular recovery. To the contrary, most ADs have been designed to amplify muscle strength without regard for the long-term ramifications of providing users with excessive assistance. As an analogy, consider that astronauts can lose up to 10% of their muscle mass over a 17 day mission in space due to reduced body loading in the microgravity conditions of space [26]. Given the fact that ADs facilitate the ability to perform more relevant therapies in representative environments without the need for therapist supervision, there is a good chance that such devices can become the de facto vehicles for providing rehabilitation therapy in the near future, provided that the outstanding challenges regarding their design and control can be solved in an economically viable fashion. Accordingly, the objectives of this research were chosen to address some of these outstanding challenges in AD control, and can be summarized as follows.

1. Design an AD controller that allows the user to control the motion of the orthosis-assisted joint or limb (i.e., no pre-defined joint trajectories) and provides assistance only when assistance is required. The controller must be simple to implement and calibrate, must use the same types of actuators and sensors typically used on other ADs, and must be robust enough to be used without modification for a large variety

of different tasks and/or task intensities; and

2. Demonstrate through simulation and experiments that such a controller would be more effective at encouraging user effort than the MAC.

1.4 Contributions

The following research contributions are presented in this thesis:

1. **Control strategy:** This thesis introduces the *assistance regulation controller* (ARC), a novel AD controller that satisfies the research objectives.

2. **Design and development of a powered orthosis:** This thesis describes the development of a single degree-of-freedom (DOF) experimental apparatus designed to assist knee motion. This apparatus was used to conduct controller validation experiments with human participants.

3. **Controller Verification and Validation:**

   (a) Simulation of orthosis-assisted knee flexion and extension was used to verify that the ARC satisfies the research objectives. These results indicate that the ARC allows the user to remain in control of the orthosis-assisted limb motion, but ensures that assistance is provided only when required.

   (b) Elbow extension experiments conducted with a single participant (the author) confirmed that the benefits of the ARC observed in simulation could be reproduced in a real human-robot interaction.

   (c) Knee extension experiments conducted with six healthy male participants confirmed that the results observed in simulation and from the elbow extension experiments could be reproduced with other healthy participants.

1.5 Outline

This section provides an overview of the contents of the remaining chapters of this thesis.

Chapter 2: Emulating Assistance Regulation and Muscle Amplification Behaviour using Impedance Control

This chapter begins with introductory material concerning joint dynamics modelling, joint torque estimation, and impedance control. The discussion then focusses on describing how impedance control may be used to make an orthosis exhibit both the muscle amplification and assistance regulation behaviours. The chapter concludes with simulation experiments of AD assisted knee flexion and extension that highlight the benefits of using assistance regulation instead of muscle amplification in rehabilitation applications of ADs.

Chapter 3: Design of a Single DOF Powered Exoskeleton for Controller Validation

The chapter begins with a general discussion about the key challenges in designing wearable robotics systems, and specifies the design requirements that guided the design of the single DOF experimental apparatus that was developed for validating the performance of the ARC with human participants. This chapter also describes the mechanical, electrical, and software design of the experimental apparatus.

Chapter 4: Verification Experiments with Elbow Extension

This chapter discusses the results from numerous elbow extension verification experiments performed using the experimental apparatus described in Chapter 3. The results from these experiments provide evidence that confirms many of the benefits of the ARC observed in simulation. This chapter also includes a discussion about the implications of using inaccurate joint torque estimates in the control loop.

Chapter 5: Validation Experiments with Knee Extension

This chapter describes the results from knee extension experiments conducted with six healthy male participants using the experimental apparatus described in Chapter 3. In addition to confirming the results observed in simulation and from the elbow extension

experiments, the validation experiments also provided an opportunity for recording and analyzing user perceptions regarding the use of both the MAC and ARC. This chapter also discusses how the ARC presented in this thesis compares to existing approaches to active assistance assistance regulation found in literature.

Chapter 6: Conclusions and Recommendation

This chapter summarizes the research conclusions and discusses possible improvements and directions for future work.

Chapter 2

Emulating Assistance Regulation and Muscle Amplification Behaviours using Impedance Control

The first half of this chapter covers the preliminaries regarding joint dynamics modelling, joint torque estimation, and impedance control. The remainder of this chapter is devoted to describing how impedance control can be used to generate muscle amplification and assistance regulation behaviours in a single-joint powered orthosis. The chapter concludes with simulation experiments that compare both the MAC and ARC during AD assisted knee flexion and extension.

2.1 Modelling Joint Dynamics

Accurate human joint dynamics models are essential for analyzing the behaviour of particular AD control strategies, and for ensuring the stability and performance of controllers employing inverse-dynamics-based (IDB) joint torque estimates in the control loop.

The two primary items that contribute to the joint dynamics include, the rigid body motion of the links (i.e., the combination of muscles, bones, and connective tissue) that make up the joint, and the nonlinear viscoelastic properties of the joint that result from the combined elasticity, viscosity, and Coulomb friction in the muscles, tendons, and connective tissue of the joint [27]. In reality, the connective tissue and muscles deform

as a function of joint orientation and velocity [28]. However, neglecting this deformation does not appear to limit control performance in wearable robotic systems in practice [4,5,7].

It is also important to distinguish between passive and active joint viscoelastic properties. Passive joint viscoelastic properties consist of the fundamental joint viscoelastic properties observed when only external forces and torques excite the motion of the joint [29]. Active joint viscoelastic properties observed during voluntary motions may be substantially different due to the muscle contraction velocity-dependence of muscle force, and changes in reflex muscle activation characteristics during voluntary motions and under different external loading conditions [30,31].

While joint dynamics are obviously non-linear, they are reasonably modelled by second order linear time-invariant systems for small variations in joint angle and muscle activation [32]. Due to the challenges associated with modelling the complex muscle and tissue dynamics, some researchers opt to model joint dynamics as second order linear time-varying systems [4, 33]. These models require the use of time-varying system identification methods for estimating the variation in the stiffness and damping properties of the joint over time. Some research has also focused on identifying non-linear lumped parameter models of joint dynamics [29,34]. Such models are desirable since they are valid for larger ranges of motions and muscle activation levels.

The types of motions performed in the experiments described in Chapters 4 and 5 were limited to knee and elbow extension. These motions are described in Figures 2.1 and 2.2, and may be modelled as constant coefficient, non-linear pendulums with viscous friction (i.e., as second order nonlinear time-invariant systems). In particular, the knee joint may be modelled as,

$$J_k\ddot{\theta}_k + b_k\dot{\theta}_k + m_k g L_k \sin(\theta_k) = -\tau_{int} + \tau_m, \tag{2.1}$$

and the elbow joint may be modelled as,

$$J_e\ddot{\theta}_e + b_e\dot{\theta}_e + m_e g L_e \sin(\theta_e) = -\tau_{int} + \tau_m, \tag{2.2}$$

where θ is the joint angle, τ_{int} is the interaction torque (i.e., the reaction torque generated when the user pushes or pulls against the orthosis), τ_m is the joint torque generated by the muscles, and J, b, m, g, and L represent the mass moment of inertia of the limb segment about the centre of rotation, the viscous damping of the muscoskeletal system, limb segment mass, gravitational acceleration constant, and limb segment centre of mass offset, respectively. The subscripts k and e denote the knee joint and elbow joint, respectively. Joint dynamic model parameters are highly user-specific and must be estimated using system identification methods or using guidelines similar to those presented in [35,36].

As discussed above, large changes in joint angle (and muscle activation) are also accompanied by significant variations in the viscoelastic properties of the joint. This effectively implies that the viscous damping parameter, b, is not constant in (2.1) and (2.2). However, model-based AD controllers are often designed, analyzed, and implemented using similar or equivalent constant coefficient models without significant consequences (e.g., as in [5,18,37]). This is likely because the user is capable of compensating for the disturbances introduced by using inaccurate joint dynamic models in the control loop. The implications of joint dynamics model parameter estimation errors are further discussed in Section 4.2.4.

2.2 Joint Torque Estimation via Inverse Dynamics

Human joint torque measurements are often required for implementing model-based controllers and for evaluating both the controller's and user's performance. However, there

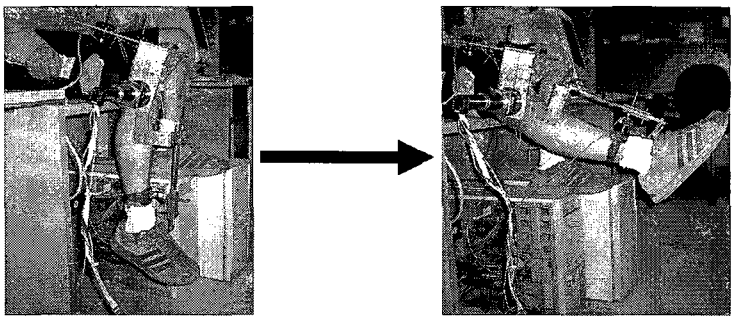

Figure 2.1: The type of knee motion considered during the validation experiments.

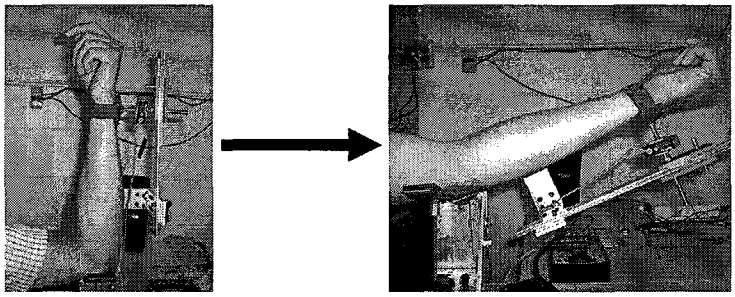

Figure 2.2: The type of elbow motion considered during the verification experiments.

is no direct method for measuring joint torque because it is unsafe and impractical to install torque sensors within a human joint. Joint torque is typically estimated by inverse dynamics or empirical models that relate EMG signals to joint torque [4, 20–22].

EMG-based joint torque estimates are desirable because EMG signals precede the onset of motion [21]. This lead time provides an opportunity to synchronize the torque generated by the actuator with the torque generated by the muscles. However, the inter- and intra-patient variability in EMG signal characteristics discussed in Section 1.2.2 imply that extensive and possibly frequent (re-)calibration of such models may be necessary. Furthermore, EMG-based joint torque models are typically estimated using IDB joint torque estimates [22]. As such, they can only be as accurate as the the IDB joint torque estimates used to generate them.

IDB joint torque estimates require a dynamic model of the user's joint. For the types

of knee motion considered in this thesis, IDB joint torque estimates can be obtained by isolating for τ_m in (2.1). These estimates would be calculated as,

$$\hat{\tau}_m = \hat{J}\ddot{\hat{\theta}} + \hat{b}\dot{\hat{\theta}} + \hat{m}g\hat{L}\sin\hat{\theta} + \hat{\tau}_{int}, \tag{2.3}$$

where $\hat{\tau}_m$ is the estimated joint torque, $\hat{J}$, $\hat{b}$, $\hat{m}$, $\hat{g}$ and $\hat{L}$ are estimates of joint model parameters, $\hat{\theta}$ is the measured joint angle, and $\hat{\tau}_{int}$ is the measured interaction torque.

A similar process can also be used for complicated motions involving entire limbs by deriving appropriate dynamic models of the combined limb-orthosis system. It can be seen from (2.3) that joint torque estimation accuracy is a function of the accuracy of the model parameters and of the measurements of interaction torque, and joint angular position, velocity, and acceleration. Kinematic and interaction torque measurement errors can be limited to acceptable values using appropriate sensors. Thus, the accuracy of an IDB joint torque estimate is primarily limited by the accuracy of the dynamic model itself.

In the experiments described in this thesis, joint dynamic models such as those shown in (2.1) and (2.2) were used to estimate joint torque according to (2.3). As noted in Section 2.1, such dynamic models are only suitable for small variations in muscle activation and joint angle. However, the experimental results described in Chapters 4 and 5 - which did not satisfy these assumptions - indicated that such models were adequate for allowing successful implementation of an AD controller that satisfied the research objectives. Approximate values of joint torque estimation uncertainty, and the implications of using inaccurate joint torque estimates in the control loop are further discussed in Section 4.2.4.

2.3 Impedance Control

Impedance control refers to a general approach to robot control that has been used quite extensively in wearable robotic systems (see [4,11,15,18,19,25] for examples). The primary advantage of impedance control is its ability to simultaneously accommodate position tracking and dynamic robot-environment interactions [38]. This feature of impedance control is most easily illustrated using a simple example. Consider, a second order linear time-invariant system whose representation in the Laplace domain is given by,

$$(s^2 + as + b)X(s) = \tau_{act}(s) + \tau_{ext}(s), \tag{2.4}$$

where X is the output of the system, a and b reflect the open-loop dynamic properties of the system, τ_{act} is the actuator input, and τ_{ext} is the input provided by the environment due to the system-environment interaction.

The goal of impedance control is to make the controlled system (i.e., the closed-loop dynamics) behave according to the target, or desired dynamics given by,

$$(s^2 + a_d s + b_d)(X(s) - X_d(s)) = \tau_{ext}(s), \tag{2.5}$$

using the control law,

$$\tau_{act}(s) = (a_c s + b_c)X(s) + (s^2 + a_d s + b_d)X_d(s), \tag{2.6}$$

where X_d is the desired output, and $a_c = a - a_d$ and $b_c = b - b_d$ correspond to compensatory damping and stiffness parameters.

Thus, for appropriate values of a_d and b_d that ensure the stability of target dynamics (i.e., for values that ensure that $s^2 + a_d s + b_d$ is a Hurwitz polynomial), and assuming that $\tau_{ext} = 0$, the controlled system asymptotically approaches the desired output X_d. In case of contact with the environment (e.g., collision with an obstacle), the control law given by (2.6) sacrifices tracking error for a safer interaction with the environment. Using a regular position control scheme in the same scenario would likely result in the generation of dangerously large interaction forces at the contact point since a position controller is not explicitly designed to safely accommodate contact with the environment.

Impedance controllers are typically implemented as either torque-based or position-based implementations [38]. The torque-based impedance controller implementation calculates the desired actuator input assuming that the open-loop system dynamics are known (i.e., that a and b in the example above are known). The main advantage of this implementation of impedance control is that it does not require a measurement of the external input. For the example considered above, the desired actuator input would be calculated by the time-domain equivalent of (2.6). In practice, a low-level force (or torque) controller at the actuator would be used to track the desired actuator input trajectory.

The position-based impedance controller implementation requires measurements of the external input. This implementation requires integrating (2.5)to generate a reference trajectory, $x_r(t)$, that defines the system output that would be observed if the system exhibited the desired impedance. Perfectly tracking the reference trajectory (using a low-level position controller at the actuator) ensures that the controlled system exhibits the desired impedance specified by (2.5). The primary advantage of this impedance control implementation is that it requires no information about the open-loop dynamics of the system. The position-based impedance controller implementation was used throughout

this research primarily for this reason.

It is also important to note that making the controlled system exhibit the desired impedance using either type of implementation requires having an actuator with a sufficiently high bandwidth. It is impossible to make the controlled system emulate the desired closed-loop dynamics if the actuator lacks the bandwidth to track either the desired torque command or reference trajectory. Furthermore, the stability properties of both impedance control implementations are different [39]. The position-based implementation is unable to make the controlled system safely observe *small* impedances, while the torque-based implementation is unable to make the controlled system observe *large* impedances. However, it is difficult to make more specific statements regarding stability of either implementation, since the stability of both depends on the open-loop dynamics of the system to be controlled, the desired closed-loop dynamics, environment stiffness and damping, and any time delays in the system [40].

2.3.1 Muscle Amplification via Impedance Control

As discussed in Section 1.2.2, muscle amplification control strategies for ADs consist of a variety of different control approaches that are designed to assist the user directly in proportion to an estimate of their effort. This section describes how a MAC similar to the one presented in [4] can be implemented via a modified impedance controller. This controller will be compared with the ARC presented in Section 2.3.2 using the simulation experiments discussed in Section 2.4.2 and the experiments described in Chapters 4 and 5. The development below focuses on the knee joint. However, the same approach was also used to develop an implementation suitable for the elbow joint extension experiments described in Chapter 4.

Joint and Orthosis Models

Consider the situation in which a user sitting on a chair uses a 1 DOF powered orthosis to assist knee flexion and extension. The dynamics of the lower leg may be modelled according to (2.1), while the dynamics of the orthosis may modelled as,

$$J_o\ddot{\theta}_o + b_o\dot{\theta}_o + m_o g L_o \sin(\theta_o) = \tau_{int} + \tau_{act}, \tag{2.7}$$

where θ_o is the orthosis orientation, and J_o, b_o, m_o, and L_o represent the mass moment of inertia of the orthosis about its articulation joint, the viscous damping coefficient, orthosis mass, and orthosis centre of mass offset, respectively. This simplified model does not account for nonlinearities such as backlash, static friction, or actuator dynamics. However, similarly simple orthosis models have been shown to be adequate for analyzing and implementing impedance controllers on other powered knee orthoses (see [4, 18] for examples).

Virtual Impedance Model

The virtual impedance model specifies the desired dynamic behaviour of the orthosis and is given by,

$$K_1\ddot{\theta}_r + K_2\dot{\theta}_r + K_3 \sin(\theta_r) = \tau_{int} + \tau_v \tag{2.8}$$

where θ_r is the reference trajectory, K_1, K_2, and K_3 are therapist/user defined constants that specify the desired dynamic behaviour of the exoskeleton, and τ_v, the *virtual torque input*, is an additional input that will be chosen to shape the magnitude and timing of the assistance provided to the user. Equation (2.8) is the analog of (2.5) in the

simple impedance control example described above. The virtual impedance model can be integrated in real-time to specify the reference trajectory of the orthosis. Tracking the reference trajectory perfectly ensures that the orthosis exhibits the desired impedance specified by (2.8). As shown in Section 2.3.1, the coupling between the user and the orthosis can be exploited to make the user perceive a desired closed-loop joint impedance by properly specifying the values of K_1, K_2, and K_3.

Using the Virtual Torque Input to Emulate Muscle Amplification Behaviour

The virtual torque input, τ_v, may be used to control the behaviour of the robot and the amount of assistance it provides. In particular, the orthosis can emulate muscle amplification behaviour when τ_v is specified as,

$$\tau_v = \alpha \tau_m \tag{2.9}$$

where α, the *amplification gain*, controls the magnitude by which the MAC amplifies the user's muscle-generated joint torque. Assuming perfect tracking of the orthosis reference trajectory (i.e., $\theta_r(t) = \theta_o(t)$), a rigid connection at the user-robot interface (i.e., $\theta_o(t) \approx \theta_k(t)$) and specifying τ_v according to (2.9) results in the following approximate closed-loop (i.e., orthosis-assisted) joint dynamics,

$$\begin{aligned} (J_k + K_1)\ddot{\theta}_k + (b_k + K_2)\dot{\theta}_k + (m_k g L_k + K_3)\sin(\theta_k) &= \tau_m + \tau_v \\ &= (1+\alpha)\tau_m \end{aligned} \tag{2.10}$$

This result can be verified by assuming that $\theta_r = \theta_o$ and $\theta_o \approx \theta_k$ in (2.8), and substituting the result along with (2.9) into (2.1). In short, defining τ_v according to (2.9)

effectively scales the user's muscle-generated joint torque by a factor of $1 + \alpha$.

Equation (2.10) clearly shows how the virtual impedance model and its parameters can be used to control the assistance provided to the user. In particular, large positive values of K_1, K_2, and K_3 would make the user perceive increased joint inertia and damping, and gravitational loading; conversely, negative values of these parameters would reduce the joint inertia and damping and gravity loading perceived by the user. Furthermore, it can also be seen that the virtual torque input is reflected into the closed-loop joint dynamics due to the coupling between the orthosis and the user. As such, the virtual torque input provides a convenient method for controlling the assistance provided to the user. In fact, defining τ_v according to (2.9) results in a MAC similar to the one presented in [4].

It is important to note that any practical implementation of a MAC requires estimates of joint torque. IDB joint torque estimates generated according to the process described in Section 2.2 were used in all experiments conducted as a part of this research. The model of the user's muscle-generated joint torque used during simulation is described in further detail in Section 2.4.1.

2.3.2 Assistance Regulation via Impedance Control

As discussed in Section 1.1, the major drawback of the muscle amplification control strategy is that it does not take into account the need to selectively assist the user according to the user's need for assistance. As a result, the MAC may provide users with excessive assistance, and prolonged use may result in unanticipated detrimental effects such as muscle atrophy. This section presents a novel approach to active assistance regulation that directly addresses this concern, and satisfies the research objectives described in Section 1.3. In particular, the approach to active assistance regulation proposed in this thesis requires re-defining τ_v

according to,

$$\tau_v = \begin{cases} 0 & \text{if } \sigma_u \leq \tau_m \leq \sigma_l \\ \beta(\tau_m - \sigma_u) - \zeta\dot{\theta}_k & \text{if } \tau_m \geq \sigma_u \\ \beta(\tau_m - \sigma_l) - \zeta\dot{\theta}_k & \text{if } \tau_m \leq \sigma_l \end{cases} \tag{2.11}$$

where σ_u and σ_l correspond to the *upper and lower assistance triggers* that initiate additional assistance from the orthosis, and β, the *difference gain*, controls the magnitude of the assistance provided to the user when the user's joint torque exceeds either assistance trigger. Large values of β would likely result in rapid changes in assistance that would make the AD difficult to control. Accordingly, (2.11) also contains additional damping terms meant to minimize oscillations, and reduce the likelihood of an unstable interaction between the user and AD. The magnitude of this additional damping is controlled by ζ, the *assistance damping gain.*

Assuming perfect tracking of the reference trajectory (i.e., $\theta_r = \theta_o$), a rigid connection at the user-robot interface (i.e., $\theta_o \approx \theta_k$) and specifying τ_v according to (2.11) results in the approximate closed-loop knee joint dynamics given by,

$$\begin{cases} (J_k + K_1)\ddot{\theta}_k + (b_k + K_2)\dot{\theta}_k + (m_k g L_k + K_3)\sin(\theta_k) = \tau_m & \text{if } \sigma_u \leq \tau_m \leq \sigma_l \\ (J_k + K_1)\ddot{\theta}_k + (b_k + K_2)\dot{\theta}_k + (m_k g L_k + K_3)\sin(\theta_k) = (1+\beta)\tau_m - \beta\sigma_u & \text{if } \tau_m \geq \sigma_u \\ (J_k + K_1)\ddot{\theta}_k + (b_k + K_2)\dot{\theta}_k + (m_k g L_k + K_3)\sin(\theta_k) = (1+\beta)\tau_m - \beta\sigma_l & \text{if } \tau_m \geq \sigma_l \end{cases} \tag{2.12}$$

This result can be verified by assuming that $\theta_r = \theta_o$ and $\theta_o \approx \theta_k$ in (2.8), and substituting the result along with (2.11) into (2.1). Equation (2.12) indicates that the

ARC does not provide the user with any assistance anytime the user's knee torque remains bounded between the trigger values. However, as soon as the user's knee torque falls outside either trigger's range, the user is provided with additional assistance in proportion to the difference between the user's knee torque and the corresponding trigger's magnitude. Thus, (2.11) effectively attempts to regulate the user's knee torque to lie within the torque range specified by the upper and lower assistance triggers. Choosing the trigger magnitudes to be near (but below) the user's actual joint torque limits and assuming that $K_1 = K_2 = K_3 = 0.01$ (or some other small values close to zero that negligibly impact the joint impedance perceived by the user), ensures that the user is provided with assistance only when assistance is required.

It is important to note that choosing negative values for K_1, K_2, and K_3 would reduce the joint impedance perceived by the user. This would effectively negate some of the benefits of the ARC since reducing the perceived joint impedance is akin to reducing the muscle effort required to make the joint follow a particular trajectory. Thus, it is important to ensure that the values of K_1, K_2, and K_3 are greater than or equal to zero when using the ARC. Using values close to zero would be desirable since they would make the user's joint motion feel more natural, i.e., there would be little difference between the actual and perceived joint impedance. However, in practice, force (or torque) sensor noise in $\hat{\tau}_{int}$ is excessively amplified as the values of K_1, K_2, and K_3 approach zero, and the resulting oscillations tend to make the user-orthosis interaction unstable. Thus, it may be necessary to use large, positive values of K_1, K_2, and K_3 in order to ensure the user-device interaction remains stable when using the ARC.

The following list summarizes how the ARC defined by (2.11) satisfies the research objectives defined in Section 1.3.

- The ARC does not require the motion of the orthosis (or user) to be known ahead of

time. The interaction torque generated at the user-device interface is used to specify the desired motion of the robot via integration of (2.8).

- Proper specification of the assistance triggers and virtual impedance model parameters ensures that the ARC encourages more user effort than the MAC. This is because the ARC only provides the user with assistance when the user's effort (i.e., joint torque) exceeds a pre-specified threshold. In contrast, the MAC constantly provides the user with assistance. Simulation and experimental results that corroborate this claim follow in Section 2.4 and Chapters 4 and 5, respectively.

- The ARC relies on the same sensors and actuators that would be required by an AD that employs a MAC, and avoids the extensive calibration process common to many EMG-based approaches to muscle amplification. Simulation and experimental results will also reveal the ARC to be robust enough to be used for a large variety of different tasks and task intensities without modification of the controller gains β, ζ, σ_l, and σ_u.

2.4 Simulation Results

This section describes the results of several simulation experiments that compared the performance of the MAC and ARC. The primary purpose of these experiments was to observe how user effort (i.e., joint torque) varied when both controllers were implemented in a simulation of orthosis-assisted knee flexion and extension.

2.4.1 Method

Figure 2.3 provides an overview of how the combined user-orthosis system was simulated. Equations (2.1) and (2.7) were used to model the behaviour of the knee joint and orthosis. Knee model parameters ($\hat{J}_k = 0.220$ kg·m^2, $\hat{b}_k = 1.71$ Nm/(rad/s), and $\hat{m}_k g \hat{L}_k = 5.96$ Nm/rad) were estimated using data from [18, 41]. Orthosis model parameters ($\hat{J}_o = 1.30$ kgm^2, $\hat{b}_o = 3.00$ Nm/(rad/s), and $\hat{m}_o g \hat{L}_o = 0.99$ Nm/rad) were chosen to reflect the

design of the knee orthosis discussed in the following chapter.

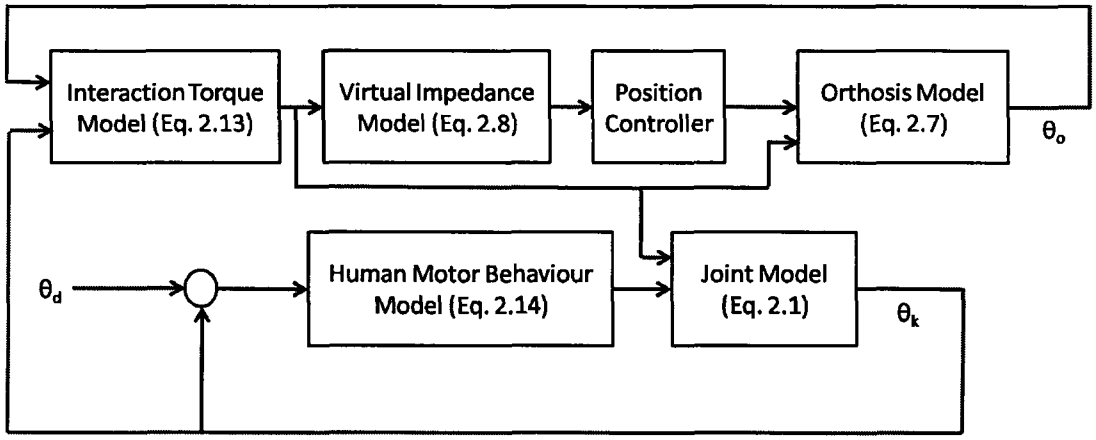

Figure 2.3: The process used to simulate the combined user-orthosis system.

The interaction torque between the user and orthosis was modelled as,

$$\tau_{int} = D(\dot{\theta}_o - \dot{\theta}_k) + P(\theta_o - \theta_k) \tag{2.13}$$

where P and D correspond to the expected stiffness and damping of the user-device interface. Only the mechanical design of the experimental apparatus was considered when approximating the values of these parameters as $P = 260$ Nm/rad and $D = 4$ Nm/(rad/s). In reality, the mechanical properties of the user's tissue would also influence the values of P and D. However, it was not possible to measure the tissue properties or to find relevant approximations from available literature.

The user's muscle generated joint torque (i.e., τ_m in (2.1)) was modelled as,

$$\dot{\tau}_m = -k_p(\dot{\theta}_k - \dot{\theta}_d) - k_i(\theta_k - \theta_d) - f\tau_m \tag{2.14}$$

where k_i and k_p are analogous to the integral and proportional terms in a typical proportional-integral controller, f is a positive constant that controls the characteristic muscle effort minimization behaviour of the human motor control system [42, 43], and θ_d is the desired orientation of the joint.

The human motor behaviour model described by (2.14) was first presented in [42] and has since been used in similar simulation studies of combined user-orthosis systems [43]. The first term on the right-hand side (RHS) of (2.14) models the spring-like impedance of human limbs, while the second term corresponds to an adaptive term that forms an internal model of the force (or torque) required to reach the desired position [43]. As discussed in [42], experimental studies in human motor adaptation suggest that the motor system attempts to find an optimal balance between minimizing kinematic error and muscle effort - the third term on the RHS of (2.14) models this muscle effort minimizing behaviour. Models of this form have been validated using different types of motor adaption experiments, and are primarily suitable for explaining steady-state behaviour after the motor system has adapted to an external force field (e.g., like the one generated by a powered orthosis) [42]. As in [43], the user's impairment was modelled by limiting τ_m between $\pm$ 1.5 Nm after integration of (2.14).

The virtual impedance model shown in (2.8) was used to define the desired orthosis impedance. The parameters of (2.8) were specified as $K_1 = 0.01$, $K_2 = 0.15$ and $K_3 = 0$, and a proportional-derivative controller was used to track the reference trajectory. The virtual torque input in (2.8) was specified according to (2.9) when implementing the MAC, and as (2.11) when implementing the ARC. Controller parameters were specified as follows: α = 3.1, β = 30, ζ = 7 Nm/(rad/s), σ_l = -1 Nm, and σ_u = 1 Nm. Additional details about how these values were selected are discussed is Section 2.4.2.

2.4.2 Results and Discussion

Figures 2.4 and 2.5 show the results for a large amplitude knee extension, and Figures 2.6 and 2.7 show the results of a small amplitude knee extension. Results for large and small amplitude sinusoidal knee motions are described in Figures 2.8 through 2.11. Experiments with sinusoidal motion were conducted to investigate whether the controller performance was altered during dynamic motions. In all figures, a 0° knee angle corresponds to the user sitting on a chair with feet touching the ground, while a 90° extension corresponds to the leg fully stretched with toes pointing upwards. The *no assistance* legend entry in each figure corresponds to the user's motion when the orthosis is fitted onto the user's leg without the servomotor active.

Both the muscle amplification and ARC gains (i.e., $\alpha = 3.1$, $\beta = 30$, and $\zeta = 7$ Nm/(rad/s)) were purposely chosen to provide similar joint torque profiles in the large amplitude knee extension simulation shown in Figures 2.4 and 2.5. The same controller gains were used throughout all the simulation tests. The following list summarizes the implications of the results.

1. The ARC allows adequate tracking of the user's desired motion without requiring any explicit information about the user's desired motion. The user's ability to adequately track the desired joint trajectory in Figures 2.4, 2.6, 2.8, and 2.10 provides proof of this behaviour. In these figures, the desired joint angle can be thought to correspond to a visual cue (e.g., a moving target on a computer screen) that provides a desired motion for the user to try and track. However, it is important to note that the desired joint angle is not explicitly required for implementing either the MAC or ARC.

2. The steady-state/tracking errors observed in these figures can largely be attributed to the dynamics of the human motor behaviour model. Observation of (2.14) indicates that statically holding a particular joint orientation under gravitational loading requires a non-zero tracking error [43]. More importantly, however, Figure 2.6 and

2.10 indicate that tracking errors at small amplitude motions are larger when using the ARC. Given that this behaviour was consistently observed in additional simulation runs, this phenomenon appears to be a specific consequence of using the ARC. Additionally, Figures 2.6 and 2.8 also suggest that the ARC results in a slower joint response in comparison to the MAC. Again, similar results were observed in additional simulation runs, and this phenomenon too, appears to be a consequence of using the ARC. In short, these results suggest that the ARC does not allow the user to control the orthosis-assisted motion as quickly or precisely as with the MAC.

3. The MAC provides excessive assistance because it provides assistance at all times (even when not required). In practice, the amplification gain of the MAC would be chosen to ensure that the user is provided with sufficient assistance to complete high-intensity tasks (e.g., the large amplitude motion simulation experiments). However, when the same amplification gain is used when performing a low intensity tasks (e.g., the small amplitude simulation experiments), the MAC provides excessive assistance. In contrast, the ARC ensures that the user is provided with adequate assistance when completing high intensity tasks (e.g., those shown in Figures 2.5 and 2.9). However, the same controller gains can also be used in low-intensity tasks without the risk of providing the user with excessive assistance (e.g., compare the ARC and MAC joint torque trajectories in Figures 2.5 and 2.9 with those in 2.7 and 2.11). The ARC's ability to better encourage and regulate user effort makes it more suitable for rehabilitation applications of wearable robotic systems.

4. The results of these simulation experiments suggest that the performance of the ARC is not strongly dependent on the specifics of the motion (e.g., slow-moving versus dynamic), or on the torque requirements of the activity. As such, the ARC is fairly robust in the sense that its controller parameters do not require re-tuning when either the task or task intensity is varied.

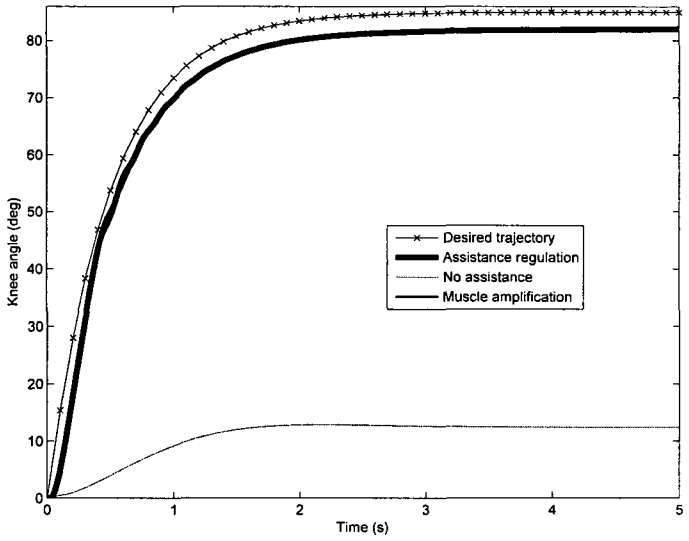

Figure 2.4: Comparing ARC and MAC tracking performance for a simulated large amplitude knee extension. The trajectories under assistance regulation and muscle amplification are nearly identical and cannot be distinguished in this figure.

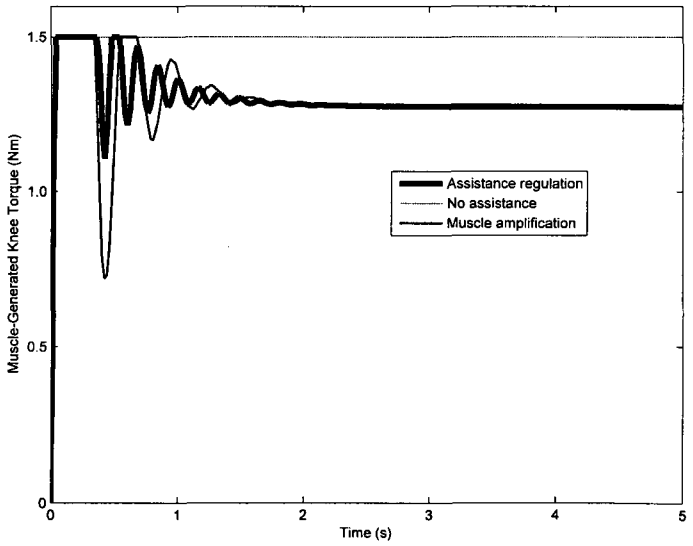

Figure 2.5: Comparing ARC and MAC muscle-generated knee joint torque for a simulated large amplitude knee extension.

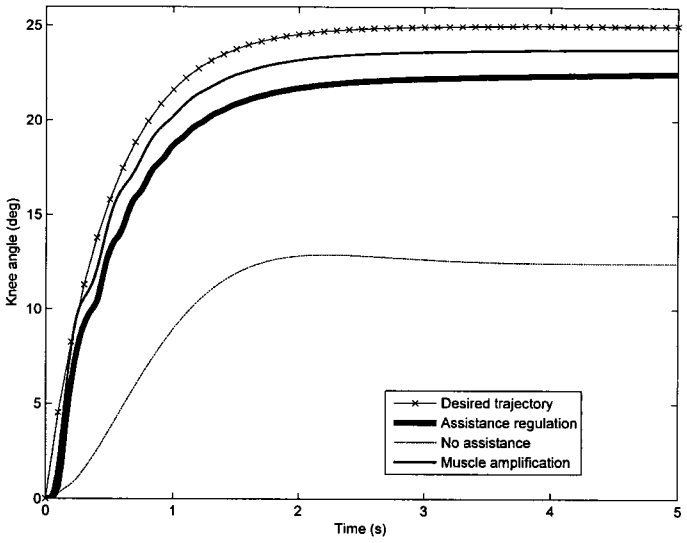

Figure 2.6: Comparing ARC and MAC tracking performance for a simulated small amplitude knee extension.

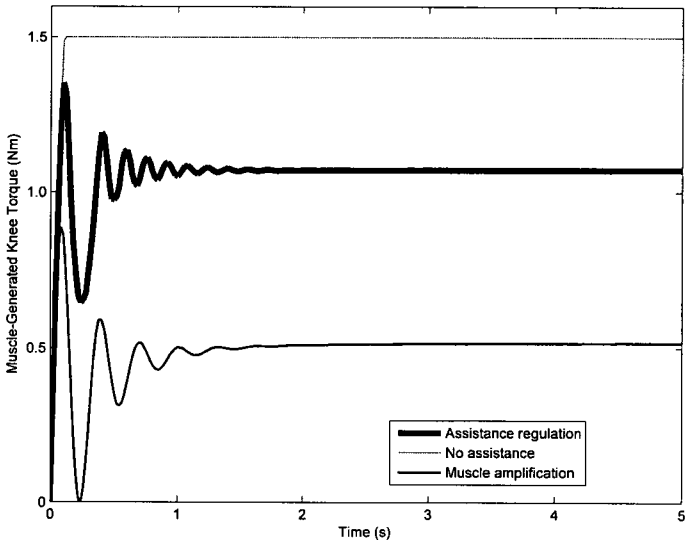

Figure 2.7: Comparing ARC and MAC muscle-generated knee joint torque for a simulated small amplitude knee extension.

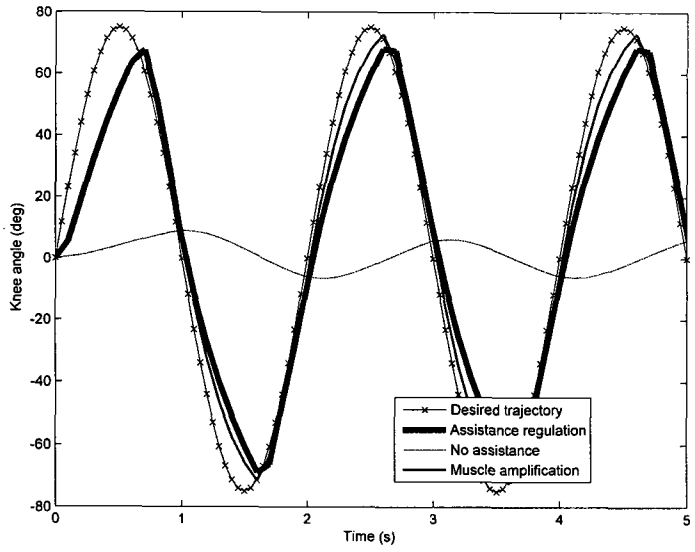

Figure 2.8: Comparing ARC and MAC tracking performance for a simulated large amplitude sinusoidal knee motion.

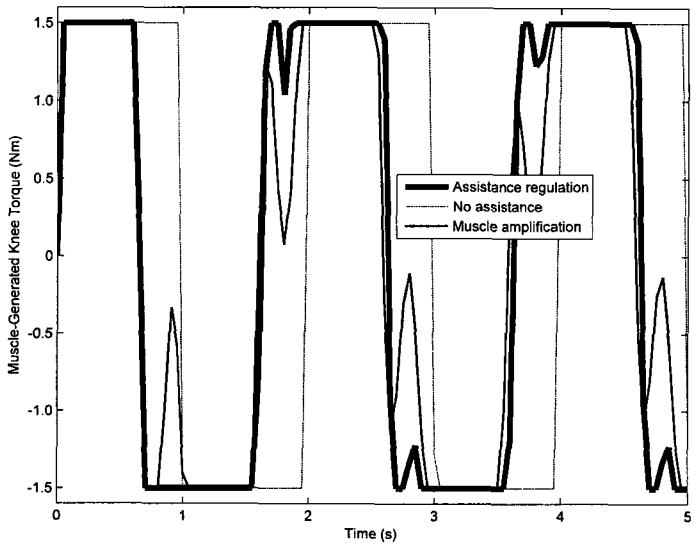

Figure 2.9: Comparing ARC and MAC muscle-generated knee joint torque for a simulated large amplitude sinusoidal knee motion.

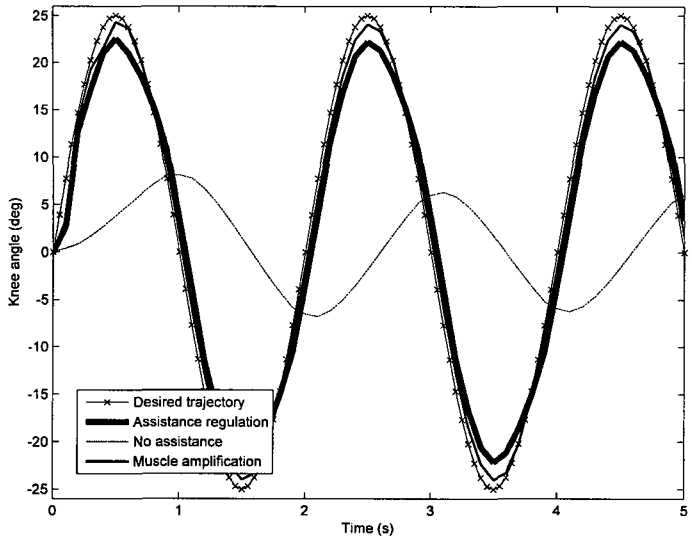

Figure 2.10: Comparing ARC and MAC tracking performance for a simulated small amplitude sinusoidal knee motion.

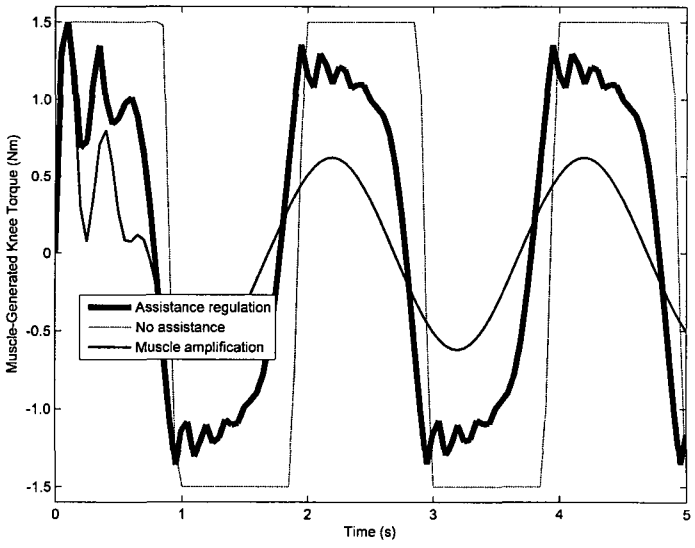

Figure 2.11: Comparing ARC and MAC muscle-generated knee joint torque for a simulated small amplitude sinusoidal knee motion.

2.5 Summary

This chapter provided some background information regarding joint dynamics modelling, joint torque estimation, and impedance control, and showed how impedance control can be used to generate muscle amplification and assistance regulation behaviours in a combined user-orthosis system. Simulation results of orthosis-assisted knee flexion and extension highlighted the key benefits of the ARC over the MAC: when the gains of the ARC are appropriately chosen, the ARC ensures that the user is provided with assistance only when assistance is needed. Additionally, the ARC is capable of achieving this goal while still allowing the user to remain in full control of his (or her) motion. While the simulation results suggested some minor drawbacks to using the ARC (i.e., the possibility of a reduced joint bandwidth and larger tracking errors relative to the MAC), its benefits seem to suggest that it may be more suitable than the MAC for rehabilitation applications of wearable robots.

Chapter 3

Design of a Single Degree-of-Freedom Powered Exoskeleton for Controller Validation

The previous chapter described the ARC and several simulation experiments that indicated its benefits in comparison to the commonly used MAC. This chapter describes the design of a single degree-of-freedom powered orthosis that was used to carry out similar comparison experiments between the assistance regulation and muscle amplification controllers with human participants.

Section 3.1 begins with a general discussion about the challenges in designing powered orthoses and outlines the key design requirements specified for the experimental apparatus developed for this research. This discussion is followed by detailed information about the electromechanical design of the orthosis and its software and control architecture in Section 3.2.

In the following sections, the terms experimental apparatus, orthosis, device, and robot are used interchangeably to refer to a powered orthosis such as the one developed for this research.

3.1 Design Requirements

Building a sufficiently light device remains one of the most substantial challenges in designing wearable robotic systems. This challenge exists primarily because the power to weight ratios of most common actuation systems (e.g., servomotors, hydraulic actuators, etc.) are substantially inferior to that of a human muscle [44]. Thus, any robot designed to provide a comparable power output to a normal human joint using typical actuation systems is likely to be too heavy to be supported about the same joint. Minimizing the actuation system's weight remains a key outstanding challenge in the field of wearable robotics [2], and some researchers focus solely on the development of novel actuation technologies for these devices (e.g., [17]).

In addition to minimizing weight, compactness and comfort are two other important design requirements for devices to be used for long periods of time [45]. Ideally, the robot should also be designed to adapt to the anatomy of many different users as this would significantly reduce development costs [45]. However, this requirement substantially complicates the design, and most devices are specifically designed - or modified after development - to fit each particular user. It is also important to use an anthropomorphic design [46] and to design the robot to present a low impedance to the user [24]. Both ensure minimal interference to the user's natural motion [24], [46].

In addition to the general requirements mentioned above, it is possible to define numerous other device and application specific design requirements (see [2, 45, 47] for a more exhaustive review of these requirements). However, it will be noted that the primary objective of this research was to develop and test new control algorithms suitable for use with wearable AD. As such, the experimental apparatus discussed in this chapter was designed to allow implementation and evaluation of the ARC presented in Section 2.3.2, rather than to address all of the design challenges discussed above.

Additionally, the experimental apparatus was designed to assist knee flexion and extension in order to allow more direct comparisons with the simulations discussed in Section 2.4.

The key design requirements for the experimental apparatus were specified as follows.

1. The orthosis must be able to provide 25% assistance in common high intensity knee flexion/extension tasks (e.g., descending a stairway).
2. The orthosis must be designed to easily adapt to different body morphologies.
3. The orthosis mass must be under 3.5 kg (excluding the power supply).
4. Backlash in the transmission must be kept below 10 arcmin.

The first design requirement ensured that the actuation system would be capable of providing sufficient assistance for common high intensity tasks such as walking up or down a flight stairs. While only able-bodied participants were allowed to participate in experiments, high levels of robot assistance were still required since the estimates of muscle-generated joint torque used to evaluate controller performance were subject to high levels of uncertainty (see Section 4.2.4 for details). Thus, it was necessary to ensure that the assistance provided by the orthosis exceeded the uncertainty in the joint torque estimates. This ensured that the joint torque estimates provided reliable information about changes in muscle joint torque between the assistance and no assistance conditions. Providing 25% assistance in high-intensity knee flexion/extension tasks was estimated to be sufficient to allow reliable controller comparisons using IDB joint torque estimates.

The second design requirement was essential since one of the goals of this research was to investigate the performance of the ARC on a large number of different individuals. Custom part fabrication or device alteration for each user would be too costly and time consuming.

The third design requirement was chosen to ensure the user's comfort. The value of 3.5 kg was chosen based on the design of other powered knee orthoses that have been used in similar studies (see [17, 24, 48] for examples).

Backlash in gear transmissions can to lead oscillations and instability. As discussed in [18], backlash induced oscillation is of particular concern in the design of wearable robotic systems. When using impedance control, the amplification of the noise in force/torque sensor used to estimate $\hat{\tau}_{int}$ can lead to oscillatory user-device interactions when there is a large amount of backlash in the gear transmission system [18]. As such, the maximum gear transmission backlash requirement for the experimental apparatus was specified close to the typical levels that may be expected from commercially available precision planetary gear transmissions used in backlash sensitive applications.

3.2 Experimental Apparatus

The key design requirements discussed at the end of the previous section formed the basis of the mechanical, electrical, and software design of the single DOF powered knee orthosis used to carry out controller comparison tests with human participants. All aspects of the design, fabrication, and construction of the device, including sensor and actuator selection, were completed by the author.

The experimental apparatus is shown in Figure 3.1. It consists of a robotic device that can be attached about either the left or right knee joint of an individual. The device only allows for motor-assisted (or resisted) flexion and extension. Rotations about any other axis are limited to the mechanical joint tolerances in the system, or due to deformation of the tissue surrounding any user-device interfaces. The motor assembly (MA), upper leg frame (ULF), and lower leg frame (LLF), the key mechanical constituents of the device, are shown in Figure 3.1.

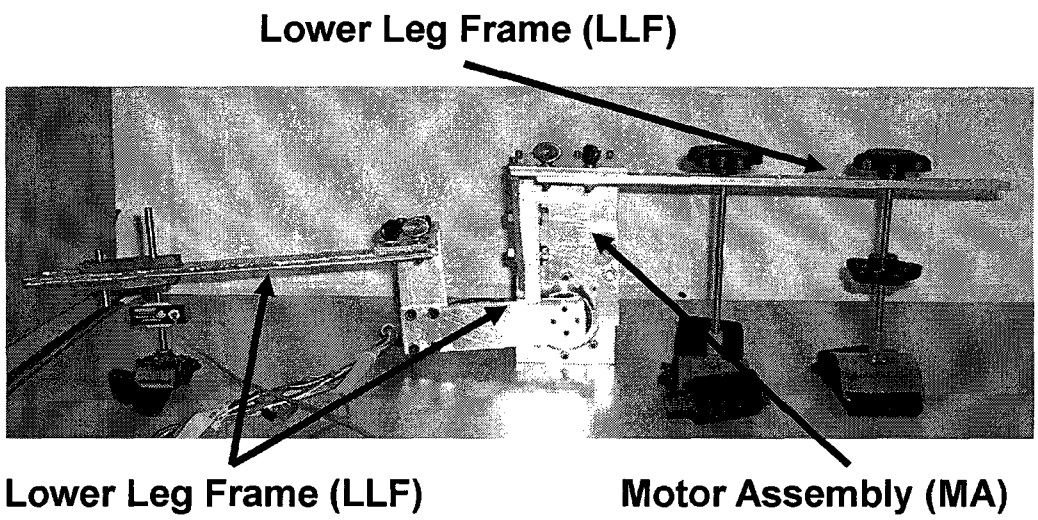

Figure 3.1: Key mechanical components of the experimental apparatus.

Figure 3.2 provides an overview of the entire system. Some of the key features of the system are briefly described below. Additional details are provided in subsequent sections.

- Assistance (or resistance) is provided by a servomotor.
- Joint and orthosis orientation is measured using an encoder mounted directly on the motor shaft
- Interaction torque is estimated from interaction force measurements obtained from a force sensor mounted between the ankle attachment and LLF.
- Muscle activity is monitored by recording EMG data from surface electrodes placed over joint flexor and extensor muscles.
- The entire system is controlled using a PC-based real-time control system.

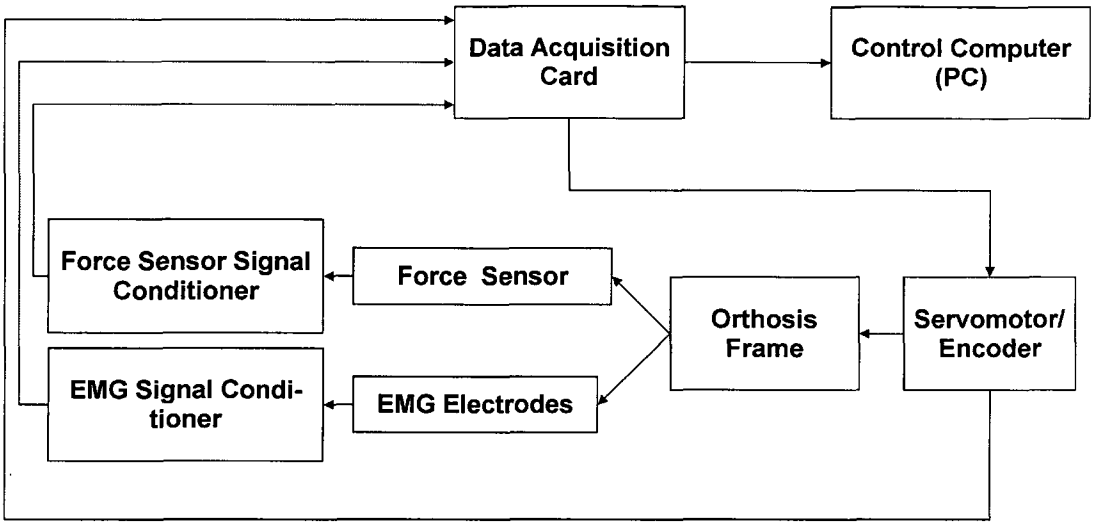

Figure 3.2: Overview of the key components that make up the entire experimental apparatus.

3.2.1 Mechanical Design

The dimensions of all mechanical components are chosen to ensure a minimum safety factor of 2 against yielding using a lightweight, high strength, 7075-T6 aluminum alloy. Stress calculations were based on a worst case scenario of the user fully resisting the maximum assistance torque that the servomotor was designed to provide. Details about the maximum assistance torque specification are provided in Section 3.2.3. Maximum stresses were calculated using elastic beam theory [49] and assuming that the various mechanical components behaved like cantilevered or simply supported beams.

Bolt spacings and sizes are designed to ensure a minimum safety factor of 2 against bolt yielding using standard bolt sizing procedures [49]. In order to simplify the construction of the device, and to increase device stiffness, all mechanical components are constructed using .635 cm aluminum sheet. Some components have been reinforced with additional material in order to reduce overall device flexibility.

Velcro strapping is used to strap the device onto the user's leg at three different connection points between the user's thigh and shank and the ULF and LLF. Each connection point is padded using foam to ensure the comfort of the user. The various adjustment mechanisms incorporated into the design of the device are highlighted in Figure 3.3. Their function is summarized below.

- The two hip connectors can be moved along the length of the ULF at discrete intervals of 1.9 cm over a total range of 25 cm. This feature accommodates differences in thigh lengths between users.
- The vertical distance between the hip connectors and the orthosis centre of rotation can be varied continuously within a 12.5 cm range to allow proper alignment of the knee and orthosis centres of rotation.
- The horizontal distance between the ULF and orthosis centre of rotation can be varied at discrete intervals of 1.3 cm over a total range of 12.5 cm. This feature accommodates differences in thigh circumference between users.
- The horizontal distance between the LLF and orthosis centre of rotation can be varied continuously within a 8.9 cm range. This feature allows the ankle connector to be properly aligned with the lower leg.
- The ankle connector can be placed at 4 different vertical positions with respect to the orthosis centre of rotation to accommodate differences in lower leg length between users.

3.2.2 Passive Translational Joint

The passive translational joint shown in Figure 3.4 allows the ankle connector to translate with respect to the LLF. This additional degree of freedom is necessary because the human knee joint does not behave like an ideal revolute joint. In fact, knee flexion (and extension) is generated by a combination of the rolling and sliding of the tibia and femur [50, 51], two

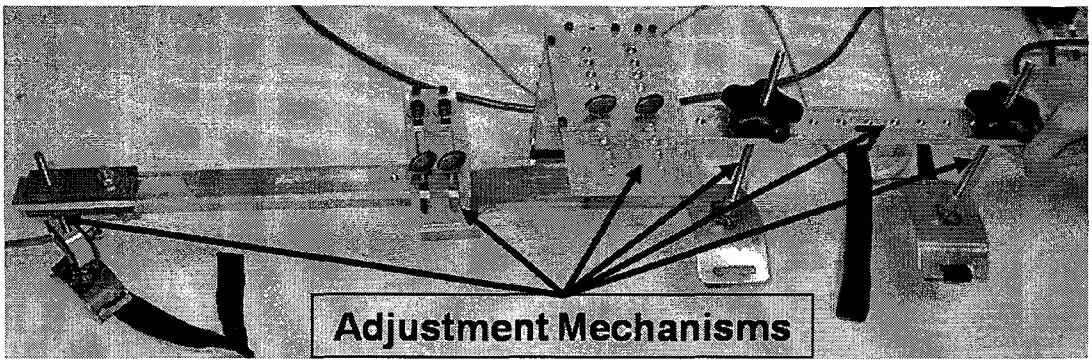

Figure 3.3: Adjustment mechanisms incorporated on the experimental apparatus.

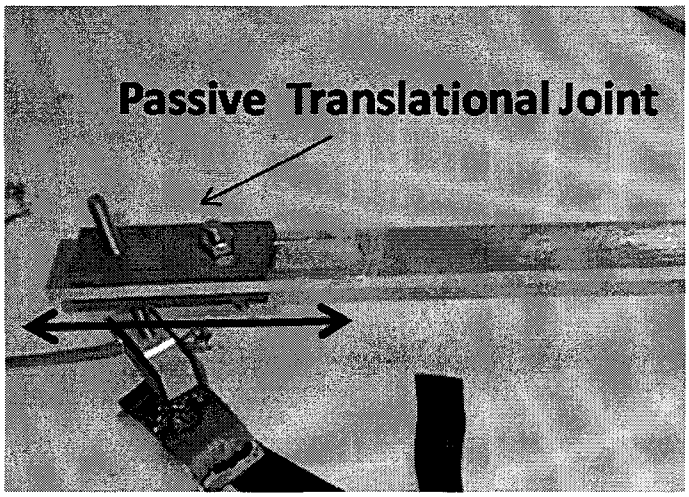

Figure 3.4: Passive translational joint on the LLF used to accommodate kinematic incompatibilities due to knee joint ICR variations.

of the three bones that make up the knee joint .

These complicated joint kinematics are generated as a result of the geometry of the contours on the tibia and femur, the constraints imposed by four ligaments that hold the joint together, and the way in which the muscles control the motion of the tibia and femur [52, 53]. While the exact nature and description of knee joint kinematics remains a topic of continued research [52], it is well known and accepted that the spatial position of the knee joint instantaneous centre of rotation (ICR) varies throughout flexion (and extension) [28, 50]. An AD that does not accommodate this variation will impede the user's

natural motion [46]. Typically, this kinematic incompatibility is manifested as a reduced range of motion due to excessive resistance to continued flexion or extension (i.e., joint locking), or slip at the connection points.

While evidence suggests that the motion of the knee joint ICR varies in a plane rather than along a particular line [28,51], passive translational joints such as the one employed in the design of this experimental apparatus have proved to be adequate even though they do not explicitly accommodate planar variations of the ICR (see [18,35] for examples). This is likely because the passive translational motion combined with local tissue deformation, device flexibility, and slip at the user-device interface allow the required relative motion between the orthosis and user necessary to correct any kinematic incompatibility.

3.2.3 Servomotor Sizing and Specification

As discussed in Section 3.1, the design requirements specified that the orthosis should provide 25% assistance in typical high intensity tasks. A review of different locomotion studies [54–58] indicated that descending a flight of stairs ranked among the most demanding of the common knee flexion/extension tasks. The results from these studies suggested that (on average) healthy individuals require a peak knee torque of approximately 1.4 Nm/Kg at an angular velocity of 30 RPM when descending a flight of stairs. Assuming a maximum user mass of 115 kg, it was determined that the servomotor must be capable of generating 40 Nm at 30 RPM in order to provide the minimum of 25% assistance while descending a flight of stairs.

The acutation system consists of a 200 Watt Maxon (Switzerland) EC Powermax Brushless DC motor coupled to a Maxon (Switzerland) GP 42C ceramic planetary gearbox with a 113:1 gear ratio. The output of this gearbox is passed through another precision, low backlash, 5:1 gear ratio planetary gearbox, the AD047-P1 from Apex Dynamics (Taiwan). The output bearing on this second gearbox directly mounts to both the MA and LLF.

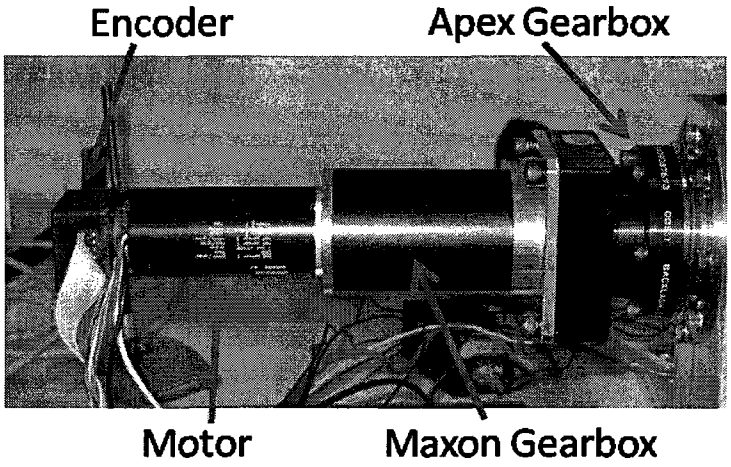

Figure 3.5: Assembled servomotor attached to the MA.

Figure 3.5 shows the assembled servomotor.

This particular choice of manufacturers, components, and gear ratios was carefully chosen to provide an optimal balance between low backlash, low weight, and maximum output torque. Using the specifications provided by the manufacturers, it is estimated that the servomotor has a total weight of 1.5 kilograms and a (no load) backlash of approximately 7.5 arcmin. Additionally, the entire system is capable of producing 40 Nm at 30 RPM continuously.

The servomotor is controlled using a Maxon (Switzerland) DES 70/10 digital servoamplifier and powered using a 48 V, 600 W DC power supply from Mean Well Electronics (USA). The amplifier employs sinusoidal commutation, operates in current control mode, and is used to track the desired torque command relayed from the control computer. Due to the low inductance of the motor, it is necessary to use an additional inductor (Maxon Motor Choke 309687) between the amplifier and the motor in order to ensure the stability of the amplifier current control loop. The servoamplifier, inductor, and power supply have not been mounted directly onto the orthosis in order to reduce its

weight. In practice, all these components would need to be mounted directly onto the device (or somewhere on the user's body) in order for the device to be truly portable. However, this experimental apparatus was only designed to be used in a controlled laboratory setting for validating the ARC. Furthermore, having these components separate from the orthosis frame has no impact on the performance of either the MAC or ARC.

3.2.4 Orientation Sensing

An Avago (USA) HEDL5540 500 PPR shaft encoder is mounted directly onto the motor shaft as shown in Figure 3.5. Due to the high gear ratio between the motor shaft and output bearing of the second gearbox, the encoder provides an angular resolution of approximately 0.0003 degrees. This sensor requires no calibration.

Since both the knee joint and motor are assumed to rotate about the same axis, the encoder-measured output bearing orientation is assumed to be equal to the knee joint orientation. As in other similar studies (see [18], [17], and [4] for examples) the motion of the orthosis with respect to the participant and the complex kinematics of the knee joint are assumed to introduce negligible error in this approximation.

3.2.5 Load Cell Calibration

A single-axis tension and compression load cell (Transducer Techniques, MLP 75) is mounted between the ankle connector and the LLF as shown in Figure 3.6. The load cell measures the interaction force between the user and the orthosis and has a rated capacity and output of 334 N and 2 mV/V, respectively. The interaction force measurement is used to estimate the interaction torque using (3.1).

$$\hat{\tau}_{int} = L_f \hat{F}_{int} \tag{3.1}$$

where L_f is the distance between the motor axis of rotation and ankle connector, and $\hat{F}_{int}$ is the measured interaction force. The nominal values of L_f used during each experiment are determined by measuring the distance between the motor axis of rotation and ankle connector after the orthosis is properly fitted onto the user. Variations in L due to the passive translational motion of ankle connector, or due to slip, are not accounted for in the estimation of the interaction torque since they are not measured.

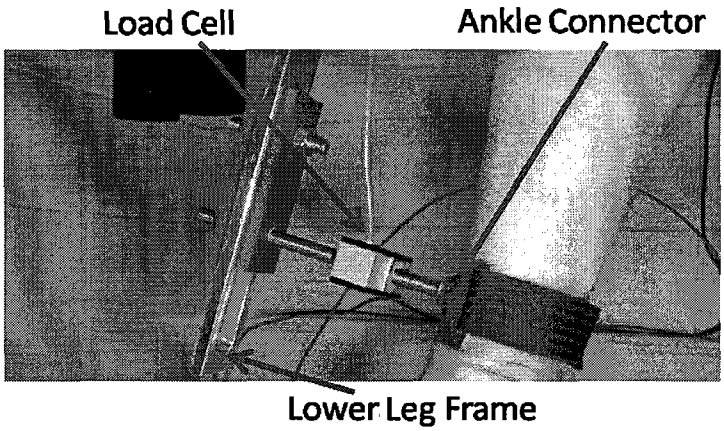

Figure 3.6: Load cell installation between ankle connector and LLF.

The raw load cell sensor signal is amplified and filtered using a TMO-2 signal conditioning unit from Transducer Techniques. This unit provides a variable amplification gain between 67 and 737, and includes a first-order analog filter with a 160 Hz cutoff frequency. The manufacturer also provides a calibration certificate and a precision resistor with the load cell that enable shunt calibration of the load cell.

Shunt calibration is the process of adding a known resistance to the load cell bridge circuit in order to simulate a physical load. If the physical load corresponding to the added resistance is known (i.e., if the manufacturer supplies this information in the

load cell calibration certificate), it is possible to calibrate the load cell and choose the appropriate amplification gain to achieve the desired resolution. Additional details about the calibration process can be found in [59]. Preliminary experiments indicated that the interaction force tended to remain below 10 N in most cases. Accordingly, the maximum amplification gain of 737 was used, and the sensor was calibrated to produce 0.05 V/N (the maximum allowable resolution). The calibration was verified by conducting tests with known weights.

High frequency noise in the sampled load cell signal is filtered using a second order low pass filter with an 80 Hz cutoff frequency. This noise is likely a result of the various sources of electromagnetic interference in the laboratory (e.g., numerous computers, power supplies, the servoamplifier, etc.). An example of the noise characteristics of the sensor can be seen in Figure 3.7 where a noticeable change in the noise of the sampled load cell signal is observed when the motor power supply is turned on approximately 4 seconds into the test. An 80 Hz filter bandwidth was used because it corresponds to 10 times the maximum bandwidth of a typical human joint [60].

3.2.6 EMG Data Recording and Processing

Muscle activation signals (i.e., EMG data), when appropriately processed, may be used as an indicator of user effort, muscle force, and/or joint torque. However, in the experiments discussed in this thesis, EMG data were exclusively used to evaluate the relative change in muscle activation when comparing different AD controllers or controller parameters. This information provides a coarser measure of user effort that can be used in conjunction with muscle joint torque estimates to evaluate and compare controller performance.

A Grass Telefactor (Pennsylvania, USA) 15A54 quad amplifier (0.01 - 6000 Hz, input impedance = 20 MΩ, CMRR = 90 dB at 60 Hz) is used to amplify and filter the raw EMG signals. The raw EMG signals are passed through a 60 Hz line filter, amplified by a

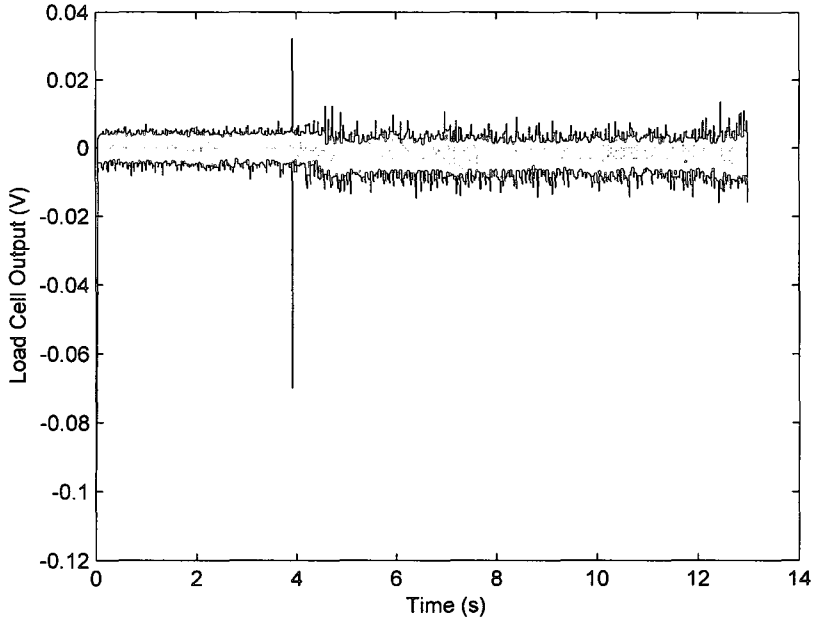

Figure 3.7: Load cell noise characteristics with and without the motor power supply on.

gain ranging between 2000-100000, and bandpass filtered between 30 Hz and 1 KHz using active, four-pole elliptic filters. The amplification gain used for each user and muscle is chosen to ensure that the amplifier's output does not saturate during the activity requiring the most muscle effort during any experiment session. Additionally, the high frequency components of the EMG signal are preserved during the hardware filtering process as they have been shown to be strongly correlated to muscle force [61].

The hardware-filtered EMG signals are sampled at 2 KHz using a data acquisition card and further processed using a procedure similar to the one described in [61]. This procedure is carried out after the completion of the experiment, and can be summarized as follows.

1. The mean of sampled signal is removed.

2. The signal from step 1 is highpass filtered using a first order filter with a cutoff

frequency of 375 Hz. As noted above, only high frequencies of the EMG signal tend to be correlated to muscle force [61].

3. The absolute value of the resulting signal is lowpass filtered with a first order filter with a cutoff frequency of 2 Hz. The absolute value of the highpass filtered signal is indicative of the number of muscle fibres that are active, while the final low pass filter mimics the dynamic response of the muscle in response to the activation inputs supplied by nerves [61].

This particular procedure - though modified from the original procedure described in [61] - is used since it has been shown to be effective at accurately estimating the relationship between EMG data and muscle force [61]. The processed signal was further filtered using a 200-sample (i.e., 200 millisecond window) moving average filter after the data had been collected. This additional filter was used to smooth the processed EMG signal for presentation purposes. Figure 3.8 highlights the transformation of the measured EMG signal as it passes through the different stages of processing.

EMG data for the elbow extension experiments described in the following chapter were collected using pre-gelled, circular 3M (USA) RedDot^{TM} Ag/AgCl electrodes with diameters of 1.75 cm. Duo-Trode ^{TM} Ag/AgCl electrodes (pre-gelled, circular, and with diameters 0.5 cm) from Myo-Tronics Inc. Washington, USA) were used with Grass Telefactor EC2 electrode cream during the knee flexion experiments. The two different types of electrodes were used only because a sufficient quantity of either type was not available for performing all experiments. Electrodes were placed on the belly of the flexor and extensor muscles of the joint in a bipolar configuration with a 2.5 cm separation between electrodes. The user's skin was cleaned with isopropyl alcohol and an abrasive skin preparation gel (Nuprep) prior to electrode application (and/or electrode cream application). Electrode locations varied between experiments and are specified in further detail in the Sections 4.1 and 5.1.

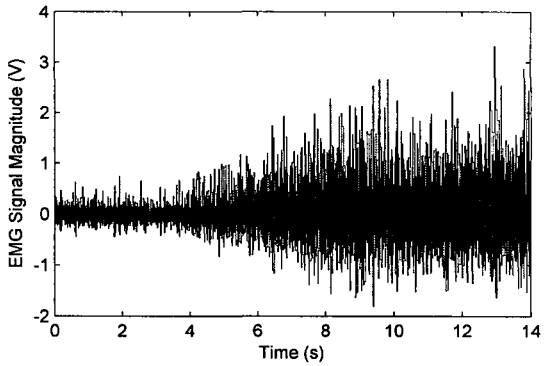

(a) Sampled EMG signal after amplification and active filtering.

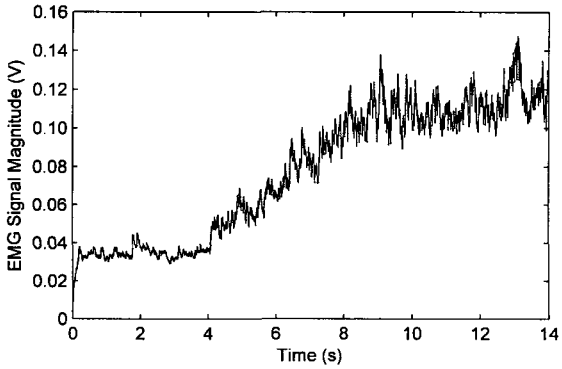

(b) Signal from (a) after high pass filtering, full-wave rectification (absolute value) and subsequent low pass filtering.

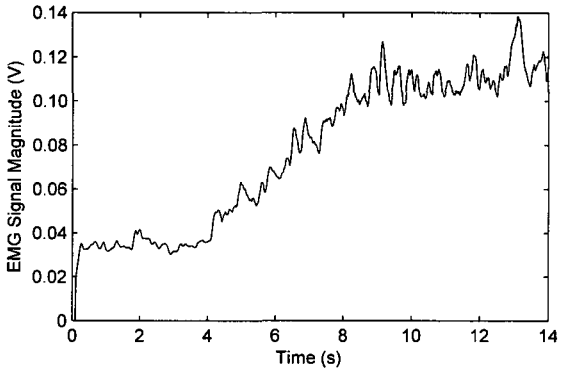

(c) Signal from (b) after 200 sample moving average filter.

Figure 3.8: Applying the EMG data processing technique to raw EMG data collected during an elbow extension experiment.

3.2.7 Safety Features

Injuries resulting from hyper-extension or hyper-flexion of the knee joint are the only serious physical risks associated with using the orthosis. A variety of safety features and precautions are included in both the design of the device and the experiments in order to mitigate this risk. This section describes the safety features incorporated into the experimental apparatus.

Two mechanical hard-stops are integrated into the design to prevent hyper-extension and hyper-flexion. During the experiment, the hard stops ensure that the joint range of motion while wearing the orthosis is limited to a value below the natural range of motion of the user's joint.

The experimental apparatus also includes two emergency pushbutton switches (Siemens 3SB38010DG3). Activation of either switch causes the servoamplifier to enter a disabled state. One switch is kept within the reach of the user, and the other is kept within the reach of the experimenter.

Finally, two different mechanisms are also used to limit the maximum servomotor torque to a safe value. Both fuses between the servoamplifier and motor, and the servoamplifier's adjustable current limiter are redundantly used to limit the maximum assistance (or resistance) torque to a safe value the user can resist.

3.2.8 Control Architecture

As shown in Figure 3.9, Matlab's xPC Target software is used to set up the real-time control system for the experimental apparatus. The process for generating the control software requires using a host PC to develop a Simulink model that performs all the necessary computations at each iteration of the control loop. The xPC Target blockset

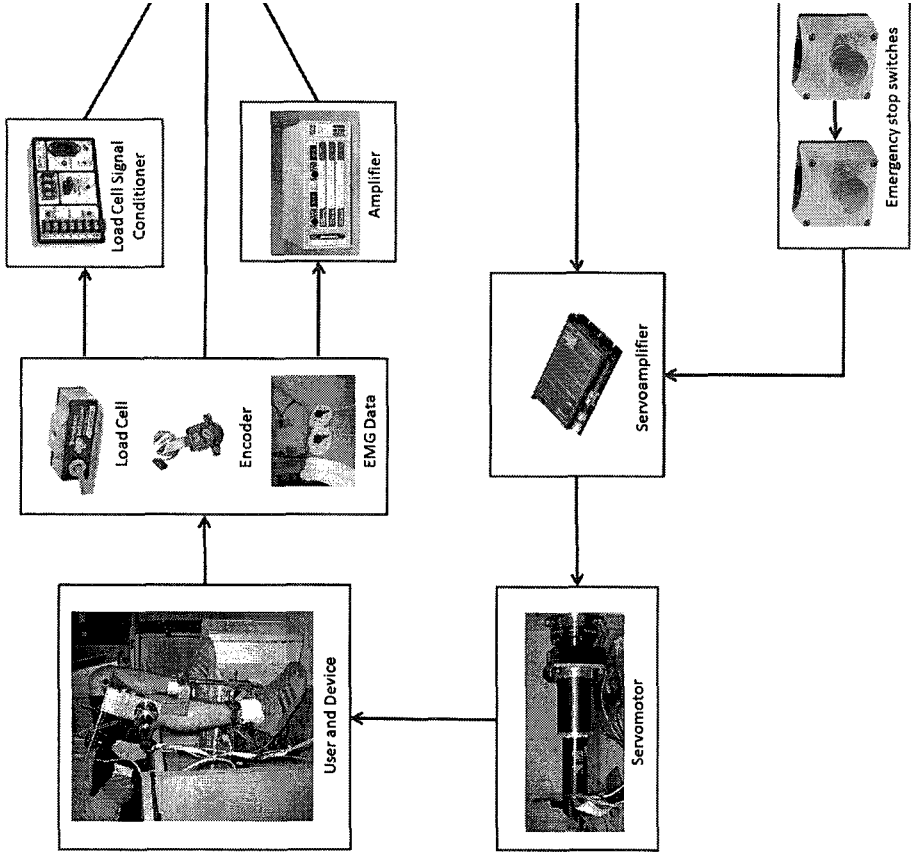

Figure 3.9: The control system architecture.

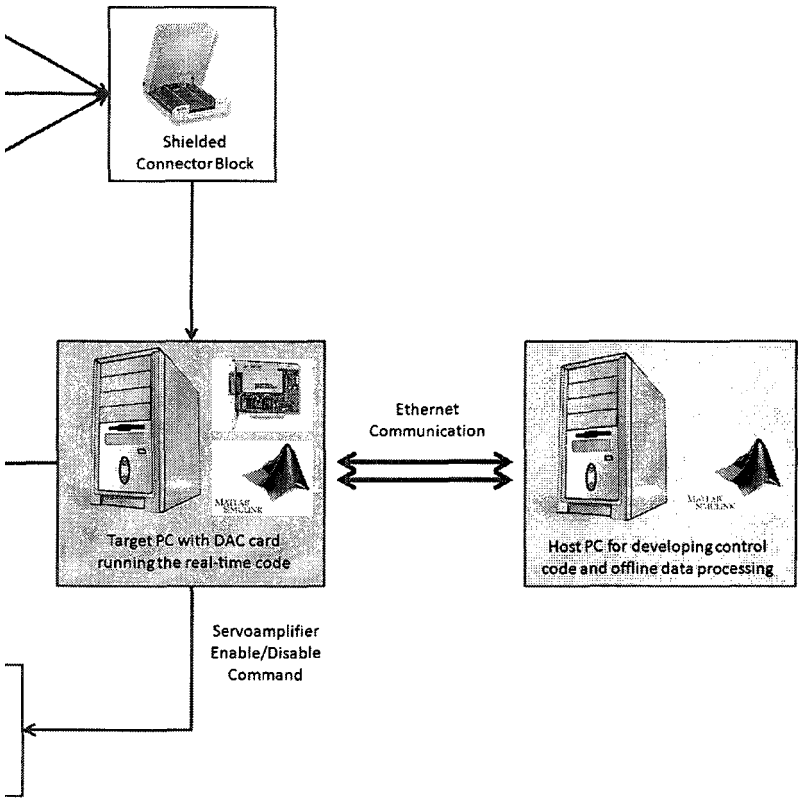
Shielded
Connector Block
Ethernet
Communication
Target PC with DAC card
running the real-time code
Host PC for developing control
code and offline data processing
Servoamplifier
Enable/Disable
Command

for Simulink provides the software required to communicate with the data acquisition card (DAC) used to acquire data from the sensors and send command signals to the servoamplifier.

Matlab's Real-Time Workshop is then used to automatically generate C-based control code from the Simulink model. This code is downloaded onto and executed from a target PC running xPC Target's real-time operating system. Using a target PC with a Pentium IV 1.4 GHz processor, a loop rate of 2 kHz is easily achieved. All data are locally logged on the target PC at a frequency of 2 kHz, and transferred to the host PC after the completion of the experiment.

A National Instruments PCI 6259 DAC (32 analog inputs, 4 analog outputs, 48 programmable digital I/O's, and 2 counters) is used as the input/output interface between the sensors/actuator and the control computer (i.e., the target PC). The DAC card is installed on the target PC, and an NI SCB-68 shielded connector block is used to route all signals to and from the DAC card.

3.2.9 Controller Implementation

Both the muscle amplification and assistance regulation controllers described in Sections 2.3.1 and 2.3.2, respectively, require modification when implemented on the experimental apparatus. This modification, along with the implementation of the control loop can be seen in Figure 3.10.

The modification consists of an additional first order low pass filter for the virtual torque. The filtered virtual torque signal is then used as the input into the virtual impedance model. This additional step was not necessary during simulation. However, it is essential for avoiding oscillations and ensuring the stability of the control loop when either the muscle amplification or ARC is implemented on the experimental apparatus.

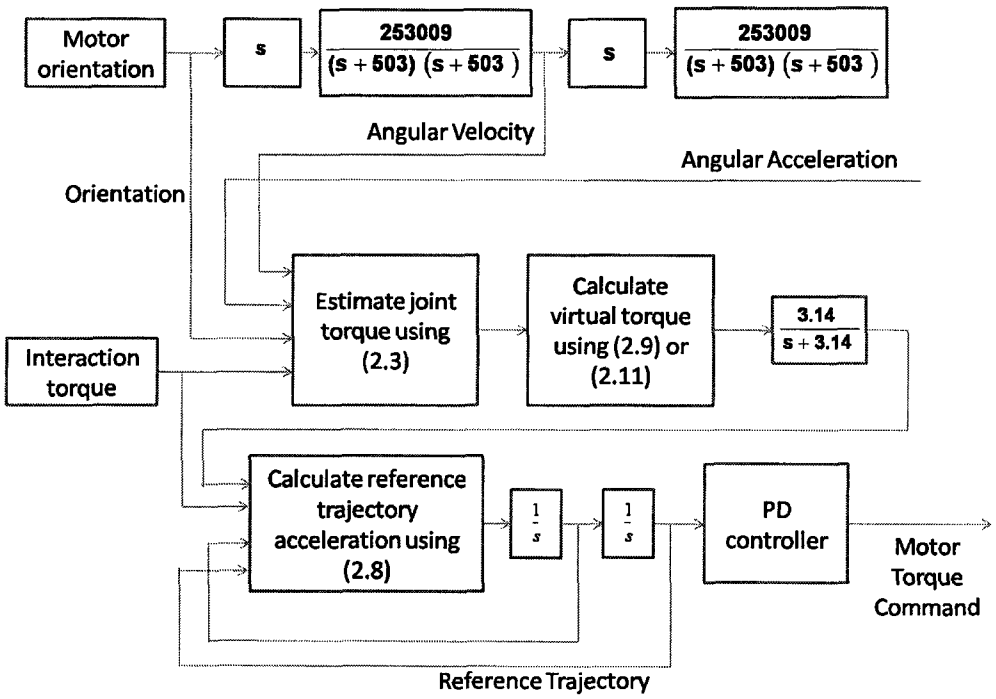

Figure 3.10: Block diagram of the control loop implemented on the experimental apparatus.

its dynamic characteristic (e.g., the small amount of backlash in the gear transmission), rather than a fundamental limitation imposed by the control strategy.

For the sake of consistency, filter bandwidths were subsequently fixed at 5 Hz and 0.5 Hz in the remainder of the verification and validation experiments.

Joint Torque Estimation

The joint torque estimates required for the MAC and ARC were obtained via the inverse dynamics technique discussed in Section 2.2. The angular velocity and acceleration estimates required to estimate joint torque were obtained by differentiating and filtering the encoder measured orientation as shown in Figure 3.10. Euler differentiation was used to estimate angular velocity and acceleration. Filter bandwidths of 80 Hz were used because they correspond to approximately 10 times the maximum bandwidth of a typical human joint [60].

Reference Trajectory Tracking Controller

The reference trajectory generated from the virtual impedance model was tracked using a standard proportional derivative (PD) controller. The output of the PD controller was limited between 0 and 5 volts - with 2.5 volts corresponding to a zero torque command - and the resultant value was relayed to the servoamplifier using an analog output from the DAC. Proportional and derivative gains of 0.25 V/deg and 0.009 Vs/deg were used in all experiments.

An example of the tracking performance is shown in Figure 3.11 (a). This experiment consisted of forearm flexion and extension that are representative of the types of motion considered in the verification and validation experiments described in the following chapter. The tracking error throughout the entire test is plotted in Figure 3.11 (b).

The filter bandwidth was chosen experimentally by repeating a simple forearm flexion experiment numerous times using the procedure described in Section 4.1 with varying filter bandwidths. The results of the experiments indicated that filter bandwidths above 7 Hz for the MAC and 1 Hz for the ARC resulted in excessive oscillations or instability. More specifically, at frequencies close to these limits, users were able to use the device but small-amplitude oscillations between 10-40 Hz persisted continuously and active effort was required to damp out large oscillation due to sudden motions. For frequencies well past these limits, the orthosis was unstable, and large oscillations would be observed on startup. In these situations, it was necessary for the user to quickly depress the emergency push-button to the stop the current supply to the motor and regain control over the orthosis. However, using a filter bandwidth under 2 Hz for the MAC also resulted in undesirable behaviour as users could feel the effects of the filter-induced time delay and complained of an *unnatural feel.*

Interestingly, small filter bandwidths did not have a detrimental effect on the performance of the ARC. In fact, users did not indicate a similar type of discomfort even when filter bandwidths of 0.1 Hz were used. This is likely because the large time delays ensured that the user had sufficient time to adapt their behaviour when the orthosis initially provided assistance. Additional details about this phenomenon are discussed in Chapter 5.

It is also important to note the bandwidth of a typical human joint varies between 4 - 8 Hz [60]. Thus, it would be desirable for the virtual torque filter bandwidths to exceed this range. However, the experimental results indicate that a virtual torque filter bandwidth of 5 Hz for the MAC and 0.5 Hz for the ARC is necessary to ensure an oscillation-free user-device interaction. The low filter bandwidths imply that only low frequency motions will be assisted by the orthosis. While undesirable, the experimental results suggest that this is a fundamental limitation that cannot be overcome. However, its origin is not known, and it is possible that this limitation is specific to this particular apparatus and

The maximum tracking error was found to be 0.11 degrees, while the root mean squared (RMS) error calculated to be 0.04 degrees. In general, both the maximum tracking and RMS errors tended to remain below 0.25 and 0.08 degrees, respectively, in most experiments.

The virtual torque input and virtual impedance model together specify the desired amount of assistance to provide to the user. Given that both these quantities determine the servomotor reference trajectory, it is reasonable to state the reference trajectory implicitly specifies the desired amount of assistance that the user should be provided with. Accordingly, perfectly tracking the reference trajectory implies that the orthosis provides the user with the desired amount of assistance. Conversely, large tracking errors indicate a discrepancy between the actual assistance provided to the user and the desired amount of assistance that should have been provided to the user. By extension, the excellent tracking results observed in Figure 3.11 - which are indicative of most experiments performed - imply that tracking errors cannot contribute to inconsistent controller behaviours such as those discussed in Section 4.2.4.

Ethics Clearance and Informed Consent

The experiments conducted with the experimental apparatus were reviewed and received ethics clearance through the Carleton University Research Ethics Committee in accordance to the Tri-Council Policy Statement for Ethical Conduct for Research Involving Humans. Only healthy individuals between the ages of 18 and 55 were allowed to participate in the study. Individuals with any previous history of serious shoulder, elbow, wrist, ankle, knee, or hip injuries, or who suffered from any disorders or conditions that resulted in knee weakness were excluded from the experiment.

Potential candidates for the experiments were contacted directly by the author and were provided a letter of information that described the purpose, procedure, risks, and conditions for participation. Interested individuals were then screened to ensure that they met the criteria for participating in the experiments. Those that passed the screening

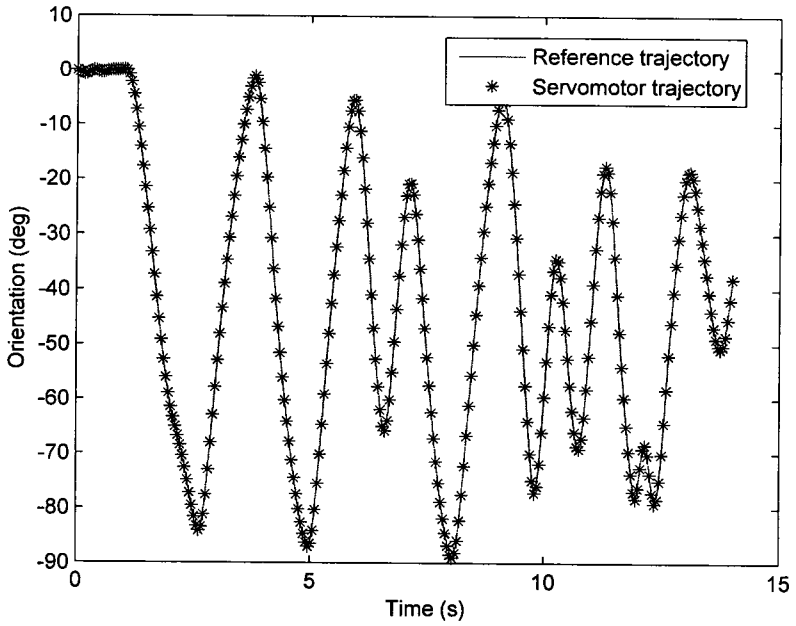

(a) Tracking performance

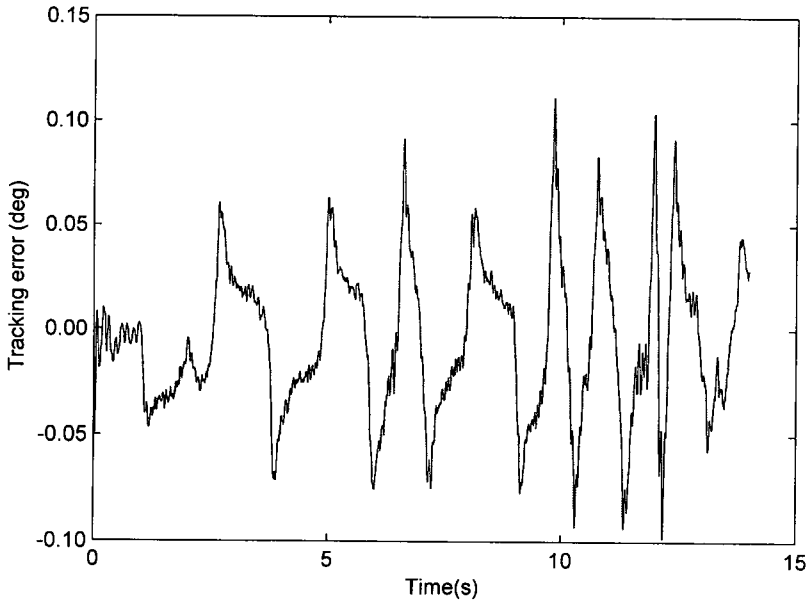

(b) Tracking error

Figure 3.11: Servomotor position controller tracking performance.

procedure were required to sign a consent form prior to starting the experiments. The participants consisted of co-workers of the author.

Participants were not provided with any compensation or benefits for participating in the experiment. Additionally, they were allowed to withdraw from the experiment (or from certain portions of the experiment) at any time, and without any consequences. By consenting to participate in the experiment, participants also agreed to allow the research data to be used in scientific reports, presentations, and publications under the condition that all reasonable precautions would be taken to maintain their anonymity.

Chapter 4

Controller Verification with Elbow Extension Experiments

The previous chapter described the design of a single DOF experimental platform developed for comparing the performance of the ARC and MAC. This platform was developed for assisting knee flexion and extension. However, numerous elbow extension verification experiments were conducted prior to the knee extension experiments to ensure correct controller implementation, and to assess whether the control loop remained stable when operated using IDB joint torque estimates.

Only one individual, the author, participated in the verification tests, and all tests were limited to forearm extension experiments. Limiting tests to forearm extension offered a safer and more controlled experimental setting since elbow motion is more easily and precisely controlled than knee motion, and because the orthosis could remain attached to a fixed base rather than being fully attached to the user. Fixing the orthosis to a base also made it possible to better align the joint and orthosis centres of rotation, and this helped avoid the problems with joint locking (see Section 3.2.2 for more information about joint locking). Figure 4.1 shows an image of the experimental setup used to conduct the experiments. An image of the user performing a test run can be seen in Figure 4.2.

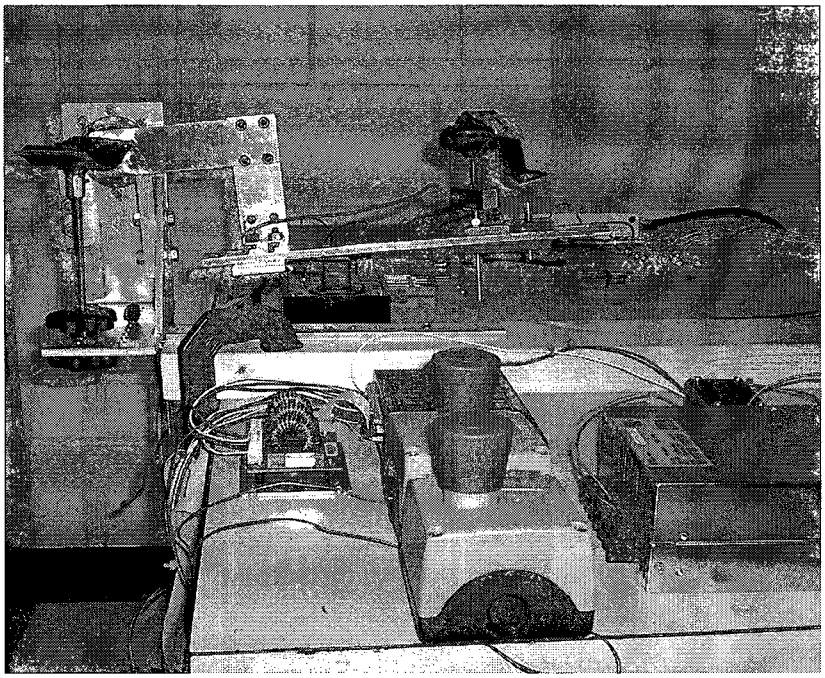

Figure 4.1: Image of the experimental setup used to conduct the elbow extension experiments.

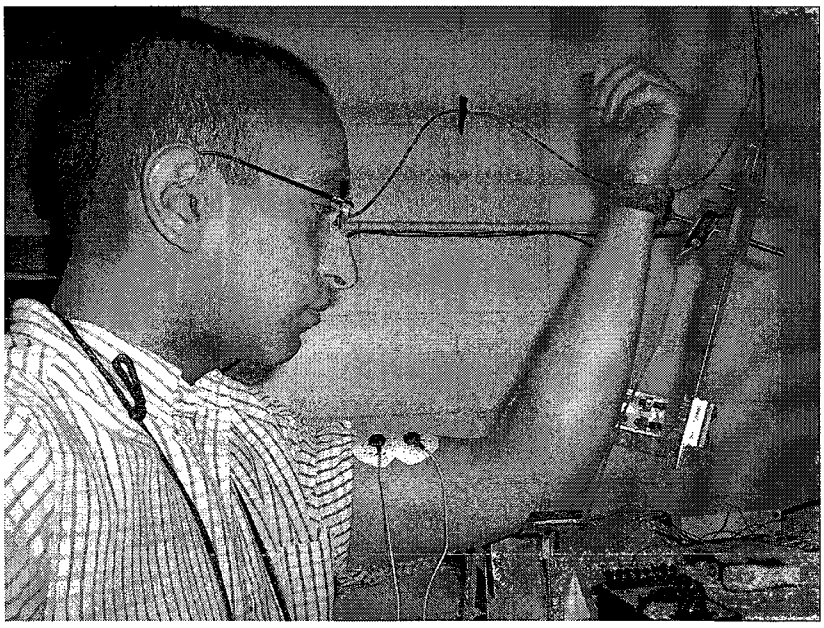

Figure 4.2: Monitor output seen by user during elbow extension experiments.

4.1 Method

The user observed a computer monitor that displayed the measured and desired elbow joint trajectories as two horizontal lines that scrolled vertically along the screen. One line scrolled according to a pre-programmed trajectory, while the second line provided feedback about the current joint angle measured using the servomotor encoder. An image of the monitor output is shown in Figure 4.3. The goal of each test run was to follow the desired elbow joint trajectory as closely as possible while being assisted (or resisted) by the orthosis. The distance between the two vertical scrolling lines provided a visual cue of the tracking error, and the user was required to keep the distance between both lines a minimum at all times throughout each test run.

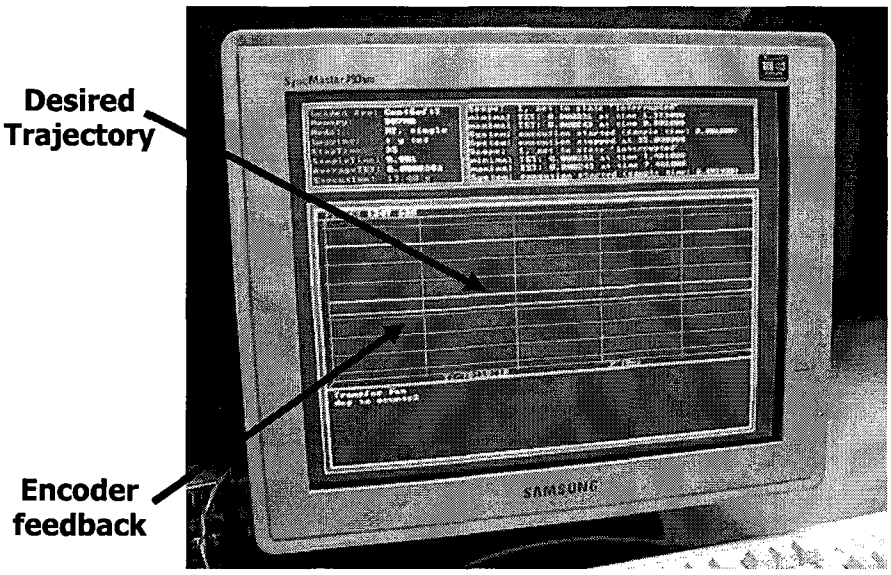

Figure 4.3: Monitor output seen by user during elbow extension experiments.

The desired trajectory used in all test runs was a smoothed constant velocity (8 deg/s) extension of 66.5 degrees. This particular type of motion was chosen for safety reasons - the robot moved away from the user's body at all times - and because it was relatively easy for the user to track. Close tracking of the desired trajectory is essential because comparisons between the ARC and MAC are only valid when conducted for similar

joint angle trajectories. When comparing controller performance for similar joint angle trajectories, the differences in the muscle joint torque required to track the same motion under both the MAC and ARC can be attributed directly to the differences between both controllers.

The user was asked to repeat numerous test runs at each of the three test conditions summarized in the list below.

- No assistance - the virtual torque term in the impedance controller was set to zero.
- Muscle amplification - the virtual torque term in the impedance controller was chosen to generate muscle amplification behaviour.
- Assistance regulation - the virtual torque term in the impedance controller was chosen to generate assistance regulation behaviour.

The user repeated the experiments a minimum of five times prior to data collection. Five repetitions were found to be sufficient to enable to user to properly adapt to each new test condition in most cases. Joint angle, interaction force, and EMG data were measured during all test runs and at each test condition.

EMG Data Collection

All EMG data collected during the verification experiments were recorded and processed according to procedure described in Section 3.2.6. Electrodes were placed on the belly of the bicep and tricep muscles. Amplification gains of 20,000 and 50,000 were used for the raw tricep and bicep EMG signals, respectively. An image of the electrode placement over the bicep muscles is shown in Figure 4.4.

Unless otherwise stated, all references to muscle, bicep, or tricep activation data in the remainder of this chapter refer to the EMG data collected and processed according the procedures described in this section and in Section 3.2.6.

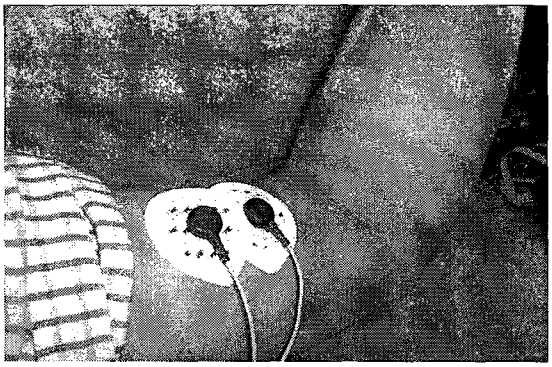

Figure 4.4: EMG electrode placement over bicep muscles.

Joint Torque Estimation

Forearm motion was modelled as an inverted pendulum, and model parameters were estimated using the guidelines provided in [35, 36]. The equation shown below was used to estimate the muscle-generated elbow joint torque:

$$\hat{\tau}_m = 0.08\ddot{\hat{\theta}}_e + 0.2\dot{\hat{\theta}}_e - 1.7\sin\hat{\theta}_e + 0.25\hat{F}_{int} \tag{4.1}$$

where $0.25\hat{F}_{int}$ is the estimated interaction torque, $\hat{F}_{int}$ is the measured interaction force, and $\hat{\theta}_e$ is the measured elbow orientation. Since joint motion was assumed to be concentric with orthosis motion, joint angle was assumed to be equal to the encoder-measured servomotor orientation.

Unless otherwise stated, all references to estimated joint torque in the remainder of this chapter refer to the IDB joint torque estimates obtained using (4.1).

Virtual Impedance Model

As discussed in Section 2.3.1, the virtual impedance model defines the desired impedance of the orthosis, and determines how much the user is assisted (or resisted) while wearing the orthosis. The virtual impedance model used during the verification experiments was specified as,

$$0.2\ddot{\theta}_{ref} + 6\dot{\theta}_{ref} - 13.5\sin\theta_{ref} = 0.25\hat{F}_{int} + \tau_v \tag{4.2}$$

where θ_{ref} is the reference trajectory, and τ_v is an additional input that can be used to control the magnitude and timing of the assistance provided to the user. The virtual torque input, τ_v, was specified as (2.9) when implementing the MAC, and as (2.11) when implementing the ARC.

The inertia and viscous damping coefficients of the virtual impedance model were chosen to be positive to increase the closed-loop joint impedance, and the gravitational torque component in (4.2) was used to simulate a 5.5 kilogram mass acting directly at the user's wrist. The additional resistance to joint motion provided by the virtual impedance model was necessary for inducing easily distinguishable changes in estimated joint torque between the no assistance, muscle amplification, and assistance regulation test conditions.

Controller Gains

The amplification gain, α, for the MAC was set to 1 (i.e., the assistance provided by the orthosis should have equalled the torque generated by the user). The choice of $\alpha = 1$ ensured that the change in user effort between the no assistance and muscle amplification was easy to distinguish.

The gains of the ARC (i.e., of (2.11)) were tuned to ensure that it provided the same amount of maximum assistance as the MAC. Ensuring that both controllers provided the same maximum assistance allowed for a consistent comparison between both controllers. After several preliminary experiments, it was determined that using $\beta = 8$ and $\sigma_u = 7$ Nm ensured that the ARC provided the same amount of maximum assistance as the MAC.

4.2 Results and Discussion

4.2.1 Variations in Joint Angle, Estimated Joint Torque, and Muscle Activation between Different Test Runs

Ten test runs were completed at each test condition because the user could not track the desired trajectory precisely (e.g., with a root mean square tracking error less than 0.25 degrees) or consistently (e.g., with similar tracking error profiles between different test runs). Variations in joint angle, estimated joint torque, and muscle activation data between test runs were noticeable, but reasonably bounded. Joint angle variations among the ten different test runs conducted at the *no assistance* test condition can be seen in Figure 4.5 (a). In general, variations in joint angle and torque were smaller than the corresponding variations in muscle activation data. An example of this behaviour can be seen in Figure 4.6 (a) which shows tricep activation data corresponding to the ten test runs shown in Figure 4.5 (a).

The significant inter-test run variations in muscle activation can be attributed primarily to the inherently low signal-to-noise ratio (SNR) of the EMG data [62]. The EMG data from these experiments were especially susceptible to noise since the resistance provided by the orthosis did not induce substantial muscle activity. The fact that it was possible to use large amplification gains (20000 - 50000) without saturating the amplifier output is a strong indication that the muscle activity during the experiments was moderate; typically, raw EMG signals are only amplified by a gain of 1000 in studies where maximum muscle

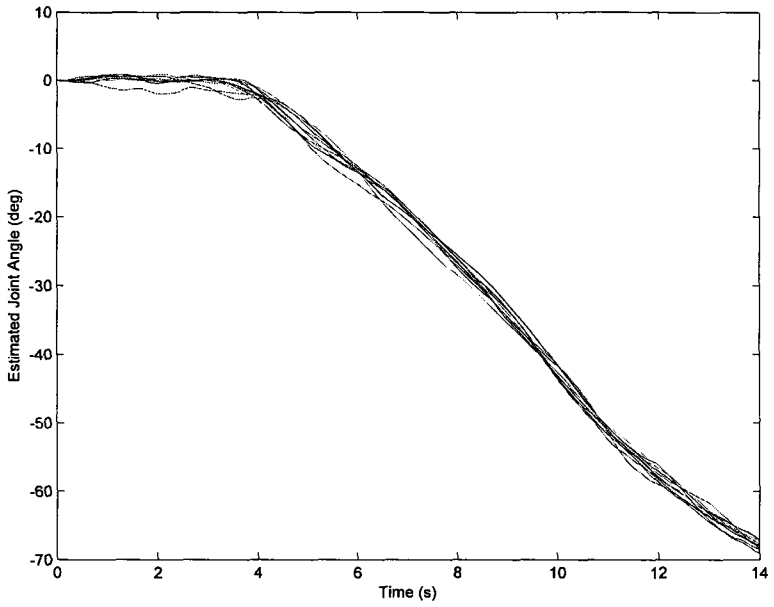

(a) Variations in joint angle for 10 different test runs performed at the no assistance test condition. Maximum deviation with respect to the desired trajectory is limited below 3 degrees in most test runs.

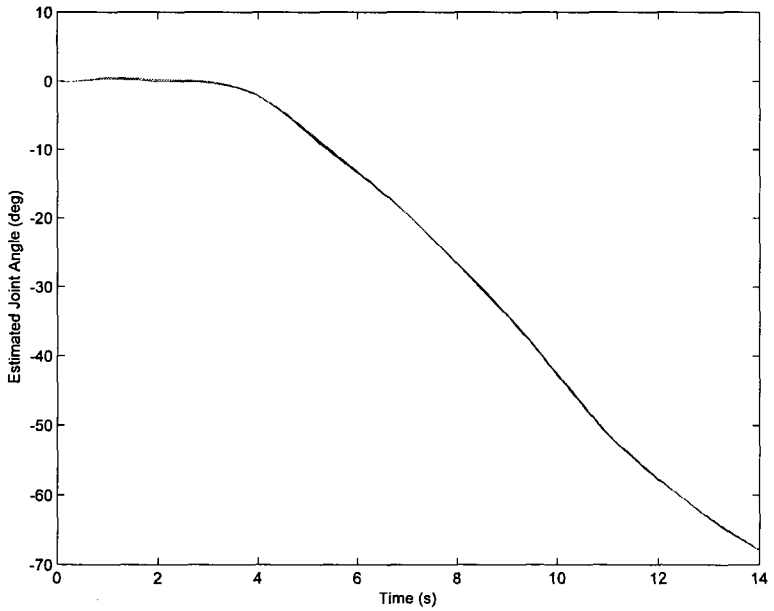

(b) Averaged joint angle trajectories using data 7,8,9 and 10 test runs. The difference between averaging over 7 and 10 test runs is minimal.

Figure 4.5: Joint angle (i.e., elbow orientation) data from 10 forearm extension test runs completed at the no assistance test condition.

contraction is recorded [8, 20, 61]. Experiments with higher orthosis resistance (or using large external loads) would provide more reliable muscle activation data, but were avoided to ensure the safety of the user and to avoid damaging the experimental apparatus.

It is also important to note that muscle activation data are indicative of muscle force rather than joint torque. Accordingly, any given joint motion can be generated using many different flexor and extensor muscle activation patterns. Thus, some of the variations in the muscle activation data shown in 4.6 (a) could be attributed to differences in muscle activation patterns between different test runs.

4.2.2 Averaging Data over Several Test Runs

Joint angle, torque, and muscle activation data were averaged using data from ten test runs in order to mitigate the effects of inter-test run variations. This averaged data was then used to compare the performance of the ARC and MAC. The minimum number of experiments required for averaging the data was not known ahead of time. As such, the two error measures shown below were used to compare the difference between averaging over seven and ten test runs.

$$| \text{ Max Error } | = \max\{|\bar{x}_{10}(t) - \bar{x}_{7}(t)|\} \tag{4.3}$$

where $\bar{x}_{10}(t)$ is the averaged data value at time t calculated using data from ten consecutive test runs, and $\bar{x}_{7}(t)$ is the averaged data value at time t calculated using data from the first seven test runs.

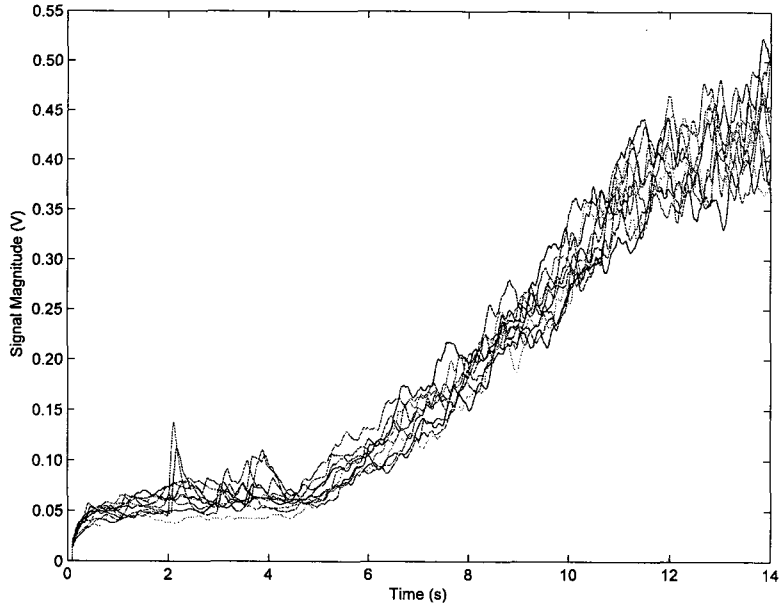

(a) Variations in tricep muscle activation for 10 different test runs performed at the no assistance test condition.

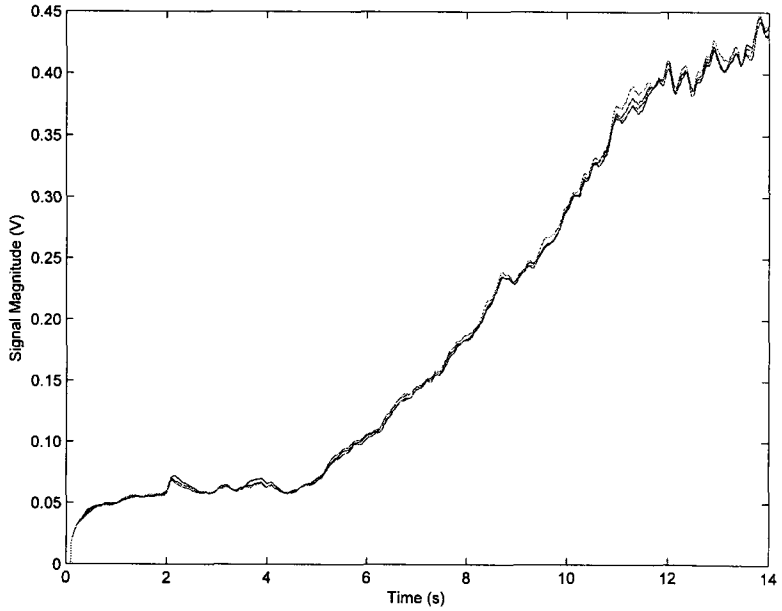

(b) Averaged tricep muscle activation data using 7,8,9 and 10 test runs. The difference between averaging over 7 and 10 test runs is minimal.

Figure 4.6: Tricep activation data from 10 forearm extension test runs completed at the no assistance test condition.

$$RMSE_7 = \sqrt{\frac{\sum_{t=0}^{T}(\bar{x}_{10}(t) - \bar{x}_7(t))^2}{T}} \tag{4.4}$$

where T is the duration of the experiment.

Both error measures were calculated for each data type, and at each test condition, and the results are summarized in Table 4.1. The quantity Max in Table 4.1 corresponds to the maximum of the absolute value of the averaged data. In all cases, Max is significantly larger than both |Max Error| and $RMSE_7$. This indicates that the difference between averaging over seven and ten test runs is substantially smaller than the magnitude of the signal itself. Accordingly, it was deemed unnecessary to use more than 10 test runs in averaging the data.

Figures 4.5 (b) and 4.6 (b) show the averaged joint angle and muscle activation data for the no assistance test condition. Visual inspection of both figures confirms that the difference between averaging data between seven and ten test runs is virtually insignificant. Similar results were observed for the estimated joint torque and bicep muscle activation data, and at all three test conditions. The averaged joint angle, estimated joint torque and muscle activation data for all three test conditions is presented in Figures 4.7 through 4.10.

4.2.3 Comparing the MAC and ARC

As with the simulation results discussed in Section 2.4.2, there are three points worth noting regarding the data presented in Figures 4.7 through 4.10.

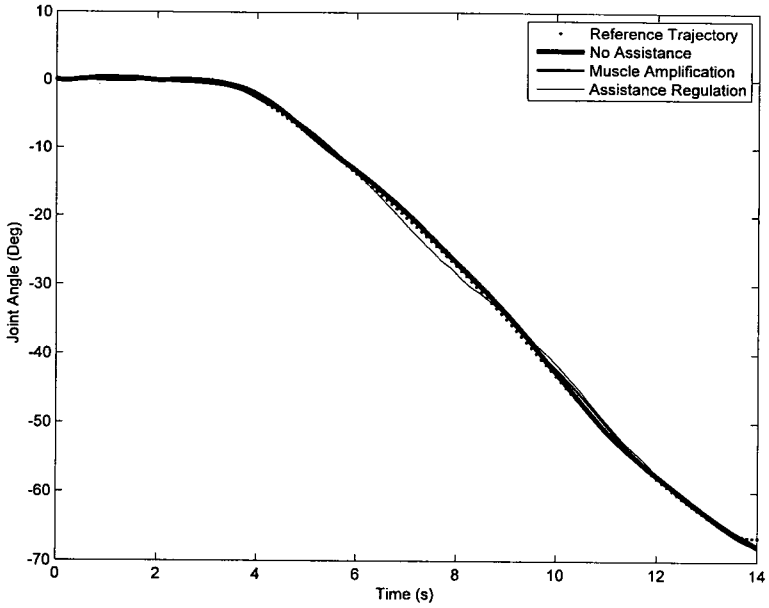

Figure 4.7: Averaged joint angle data, $\bar{\hat{\theta}}_e$, from ten test runs completed at each test condition.

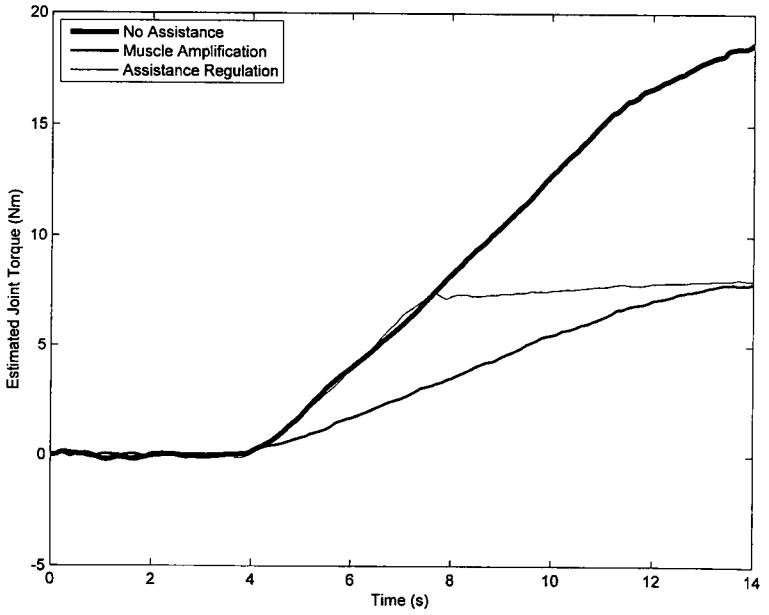

Figure 4.8: Averaged estimated joint torque, $\bar{\hat{\tau}}_m$, data from ten test runs completed at each test condition.

Table 4.1: Comparing the difference between averaging elbow extension experiment data using 7 and 10 data sets.

Test Condition	Data Type	| Max Error |	$RMSE_7$	Max
No Assistance	Estimated Joint Torque	0.19 Nm	0.07 Nm	18.58 Nm
	Joint Angle	0.38 deg	0.17 deg	67.85 deg
	Tricep Activation	16 mV	4 mV	446 mV
	Bicep Activation	26 mV	6 mV	440 mV
Muscle Amplification	Estimated Joint Torque	0.09 Nm	0.04 Nm	7.90 Nm
	Joint Angle	0.35 deg	0.14 deg	67.71 deg
	Tricep Activation	7 mV	4 mV	224 mV
	Bicep Activation	4 mV	2 mV	96 mV
Assistance Regulation	Estimated Joint Torque	0.27 Nm	0.11 Nm	8.11 Nm
	Joint Angle	0.71 deg	0.33 deg	68.2 deg
	Tricep Activation	12 mV	6 mV	211 mV
	Bicep Activation	7 mV	3 mV	110 mV

1. It is clear that both the MAC and ARC allowed the user to track their intended motion. This can be observed in Figure 4.7 which shows that the user was able to complete the same motion without assistance, and with assistance (using both types of controllers). However, this figure also indicates that deviation from the desired trajectory is largest at the assistance regulation test condition. In fact, the largest

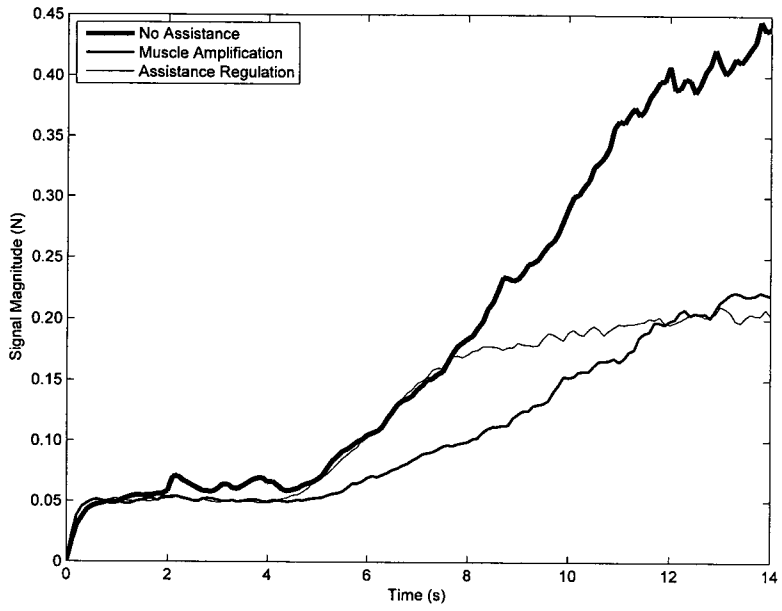

Figure 4.9: Averaged tricep activation data from ten test runs completed at each test condition.

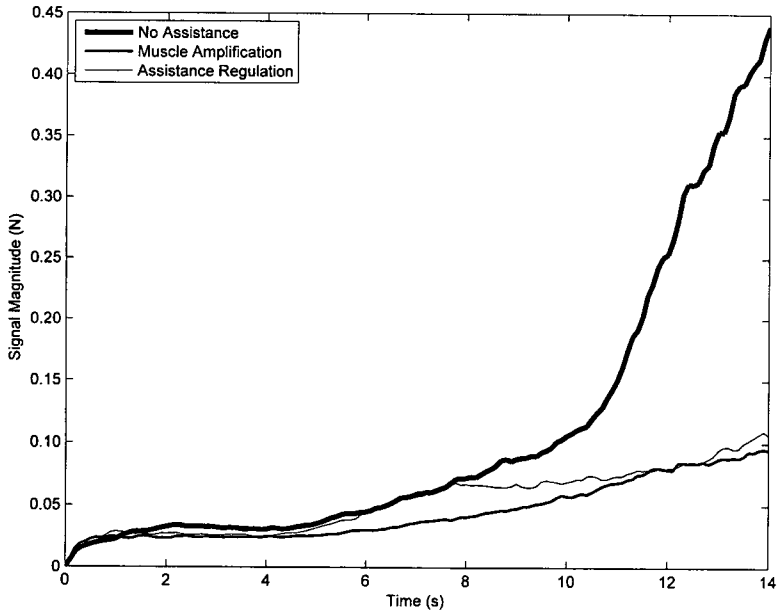

Figure 4.10: Averaged bicep activation data from ten test runs completed at each test condition.

deviations tended to occur near the moment when the orthosis first provided the user with some assistance. It was necessary for the user to modulate his behaviour in order to accommodate the assistance provided by the orthosis, and this tended to result in the larger tracking errors observed at the assistance regulation test condition.

2. It is also clear that the MAC provided excessive assistance. This can be observed in Figure 4.8 when comparing the estimated joint torque data from the assistance regulation and muscle amplification test conditions. The ARC required the user to generate 46% more joint torque on average to perform the same motion. The muscle activation data in Figures 4.9 and 4.10 similarly indicate that the ARC encouraged more user effort. Activation of both muscles tended to saturate in a similar manner to the estimated joint torque once the ARC began to supply the user with assistance approximately 7.5 seconds into the test run.

3. The similarity between the estimated joint torque curves of the no assistance and assistance regulation test conditions from 0 - 7.5 seconds in Figure 4.8 is also worth noting. This similarity implies that the ARC did not provide unnecessary assistance (or resistance) while the estimated joint torque remained below the upper assistance trigger. This notion is also supported by the muscle activation data in Figures 4.9 and 4.10, which shows equivalent similarities between the no assistance and assistance regulation test conditions prior to the point that the user was assisted by the orthosis. As such, it is reasonable to assume that by setting the assistance triggers close to the user's actual joint torque limits, the ARC ensures that assistance is provided only when required.

The large increase in bicep muscle activity at the no assistance test condition is indicative of muscle co-contraction, the simultaneous contraction of both the flexor and extensor muscles of the joint. Muscle co-contraction can be observed in a variety of normal and abnormal circumstances, but is most pronounced when the nervous system reacts to destabilizing external forces [63]. Since the simulated mass in the virtual impedance model behaves precisely like a destabilizing external force, it is not unreasonable to observe the

large increase in bicep activation at the no assistance test condition as shown in Figure 4.10. Furthermore, there is evidence to suggest that muscle co-contraction is a strong function of the magnitude of the destabilizing external force [63]. Accordingly, it is equally reasonable to see little muscle co-contraction at the muscle amplification and assistance regulation test conditions. The assistance provided by the orthosis when using the MAC or ARC effectively reduces the magnitude of the destabilizing force.

The interaction force measured at the user-device interface indicates how hard the orthosis pushed against the user (or vice-versa). The averaged interaction forces measured at each test condition are plotted in Figure 4.11. Large, positive force values imply that the orthosis had a strong tendency to extend the joint, and consequently, that more user effort was required to resist that tendency. Thus, a comparison of the interaction force trajectories at the muscle amplification and assistance regulation test conditions provides yet another indication that the ARC encourages more user effort than the MAC.

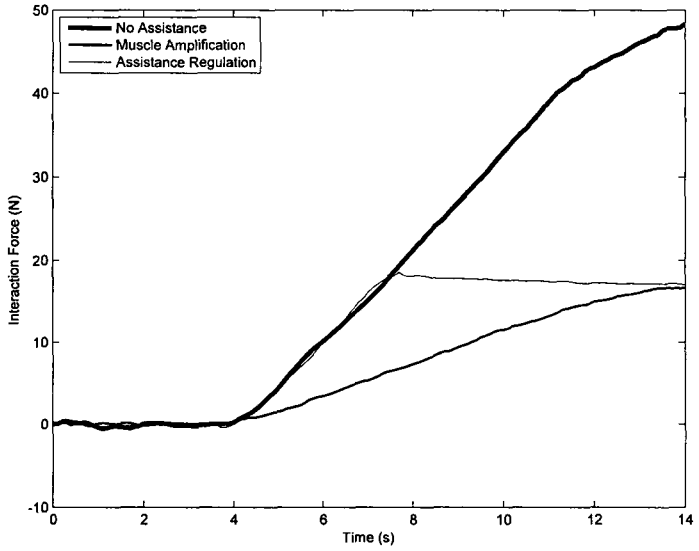

Figure 4.11: Averaged interaction force measurements from ten test runs completed at each test condition.

Figure 4.8 also indicates that the ARC is effective at regulating user effort close to the upper assistance trigger of 7 Nm. As in the simulation results presented in Section 2.4.2, some steady-state joint torque tracking error is inevitable when using the ARC. In fact, this error is necessary since assistance can only be provided if there is some tracking error.

4.2.4 Joint Torque Estimation Uncertainty and its Implications on the Closed-Loop Joint Dynamics

Joint torque estimation uncertainty due to joint angular velocity and acceleration may be approximated by multiplying the largest angular velocities and accelerations observed during all test runs (0.28 rad/s and 6.22 rad/s^2, respectively) by the assumed parameter estimation errors. This approach yields a joint torque estimation uncertainty of ± 0.58 Nm when assuming the parameter estimation errors to be twice the magnitude of the nominal parameter estimates used in (4.1). Assuming such large parameter estimation errors is reasonable given that the results in [33] and [64] suggest that the time variation in joint model parameters can sometimes exceed three times their initial (or nominal) values. These large changes in model parameters reflect the nonlinear joint viscoelastic properties discussed in Section 2.1.

Variations in forearm mass (typically between 2.1% and 3.2% of total body mass [41]) and forearm centre of mass position (typically located between 41% and 44% of total forearm length from the elbow joint [41]) may be used to approximate the joint torque estimation uncertainty due to forearm mass and centre of mass offset parameter estimation errors. Given the body mass, forearm length, and maximum extension angle, estimation uncertainty may approximated by,

$$\text{Uncertainty} = \frac{\pm\left((0.032)(0.44)m_b g L_f \sin(\theta_{max}) - (0.021)(0.041)m_b g L_f \sin(\theta_{max})\right)}{2}$$

where m_b is the total body mass, L_f is the forearm length, and θ_{max} is the maximum extension angle. Assuming a body mass of 71 kg, forearm length of 0.34 m, and a forearm extension of 66.5 degrees, forearm mass and centre of mass parameter estimation errors yield a joint torque estimation uncertainty of approximately ± 0.94 Nm in the tests discussed in this chapter. Combining the different sources of estimation uncertainty results in a total (maximum) uncertainty of approximately $\pm$ 1.5 Nm. This corresponds to an uncertainty of approximately $\pm 19\%$ at the muscle amplification and assistance regulation test conditions, and $\pm 8\%$ at the no assistance test condition. This level of uncertainty is reasonable given that even more complicated EMG-based joint torque/muscle force estimation methods are subject to similar levels of uncertainties (see [4,20,22,61] for examples).

One of the goals of the verification experiments was to assess the stability of the MAC and ARC when operated using inaccurate joint torque estimates. The results from the verification experiments indicated that limiting the assistance bandwidth as discussed in Section 3.2.9 was sufficient to guarantee the stability of both controllers for the set of controller parameters used. However, additional experiments with different controller parameters would be necessary to determine whether the assistance bandwidth filter unconditionally guarantees the stable operation of both controllers.

While the results of these experiments suggest that controller performance is not significantly affected by inaccurate joint torque estimates, joint torque estimation inaccuracies are still undesirable since they act as disturbances that create discrepancies between the desired and actual assistance provided to the user. An example of this behaviour can be observed by comparing (the averaged) peak joint torques at the no assistance and amplification test conditions shown in Table 4.1. These values were found to be 18.65 Nm and 7.86 Nm, respectively. Since an amplification gain of 1 was used, a peak estimated joint torque value of 9.33 Nm rather than 7.86 Nm would be expected at the muscle amplification test condition. This difference of 1.47 Nm is substantial (even relative

to the inter-test run variations in estimated joint torque). It is most likely a result of using inaccurate joint torque estimates in the control loop since no other experiment parameters could have contributed to it. It is difficult to explain this particular outcome without knowing the true parameters of the joint dynamic model. However, the analysis below qualitatively describes how using inaccurate joint torque estimates could result in similar types of discrepancies between the desired and actual assistance provided to the user.

As discussed in Section 2.1, joint dynamics are known to be non-linear functions of joint angle and velocity and muscle activation levels [33]. However, experimental evidence suggests that joint dynamics are adequately estimated as second-order linear time-invariant systems for small variations in joint angle and muscle activation [65]. The experiments considered in this thesis do not satisfy these assumptions. However, using these assumptions greatly simplifies the analysis below, and provides valuable insight into how inaccurate joint estimates affect the closed-loop joint dynamics.

Using assumptions and developments similar to the ones discussed in Section 2.3.1, and neglecting the use of the assistance bandwidth filter discussed in Section 3.2.9, the linearized closed-loop joint dynamics under muscle amplification are given by,

$$(J_e + K_1)\ddot{\theta}_e + (b_e + K_2)\dot{\theta}_e - (C_e + K_3)\theta_e = \alpha\hat{\tau}_m + \tau_m + \epsilon \tag{4.5}$$

where θ_e is the elbow angle, J_e, b_e, and C_e define the linearized dynamic model of the joint, K_1, K_2, and K_3 are the virtual impedance model parameters used to generate the desired closed-loop joint impedance, τ_m is the muscle-generated joint torque, α is the amplification gain of the MAC, $\hat{\tau}_m$ is the IDB estimate of the muscle-generated joint torque, and ϵ is an additive disturbance that alters the closed-loop joint dynamics. A variety of different factors can generate disturbances that alter the closed-loop joint dynamics. Some of

these factors include: estimating joint angular velocity and acceleration by differentiating the angular position; misalignment of the joint and orthosis axes of rotation; reference trajectory tracking errors; and, the motion of the passive joint. The sum of all these disturbances would likely be small in magnitude under normal circumstances, and has been represented as a single additive disturbance (i.e., as ϵ) for the purposes of this analysis.

The equation below describes the closed-loop joint dynamics that would be observed if joint torque was perfectly estimated and $\epsilon = 0$,

$$(J_e + K_1)\ddot{\theta}_e + (b_e + K_2)\dot{\theta}_e - (C_e + K_3)\theta_e = (1 + \alpha)\tau_m \tag{4.6}$$

In practice, J_e, b_e, and C_e would be unknown and would be estimated through experiments or using guidelines from sources such as [35] and [36]. As such, the IDB joint torque estimate can be specified as,

$$\hat{\tau}_m = (J_e + \triangle_1)\ddot{\theta}_e + (b_e + \triangle_2)\dot{\theta}_e - (C_e + \triangle_3)\theta_e - (\tau_{int} + \triangle_4) \tag{4.7}$$

where $\triangle_1$, $\triangle_2$, and $\triangle_3$, represent additive parameter estimation errors that are generated during the parameter estimation process, and $\triangle_4$ represents the combined (additive) noise and estimation inaccuracy in the interaction torque measurement. An expression for the closed-loop joint dynamics can be obtained by substituting (4.7) into (4.5).

$$(J_e + K_1 - \alpha\triangle_1)\ddot{\theta}_e + (b_e + K_2 - \alpha\triangle_2)\dot{\theta}_e - (C_e + K_3 + \alpha\triangle_3)\theta_e = (1+\alpha)\tau_m - \alpha\triangle_4 \quad (4.8)$$

The implications of using inaccurate joint torque estimates may be observed by comparing (4.6) with (4.8), and are summarized below.

- Large parameter estimation errors can lead to instability when $(J_e + K_1 - \alpha\triangle_1)$, $(b_e + K_2 - \alpha\triangle_2)$, and/or $(C_e + K_3 + \alpha\triangle_3)$ reach sufficiently large negative values. Defining more specific bounds on the maximum allowable parameter estimation errors is difficult without knowing how the user compensates for these errors. Such bounds could only be approximated if the transfer function that represents τ_m (i.e., the controller employed by the user to control joint motion) is known. The human motor behavior model described by (2.14) is one example of such a model. A rough approximation of the maximum allowable parameter estimation errors can be obtained by estimating the parameters k_p, k_i, and f of (2.14), and substituting the Laplace transform of (2.14) into (4.8).

- Equation (4.8) suggests that the sign of the parameter estimation error matters. In general, underestimating the values of J_e, b_e, and C_e (i.e., having negative values of $\triangle_1$, $\triangle_2$, and $\triangle_3$) is better because it makes $(J_e + K_1 - \alpha\triangle_1)$, $(b_e + K_2 - \alpha\triangle_2)$, and $(C_e + K_3 + \alpha\triangle_3)$ more positive.

- Using inaccurate joint torque estimates creates a discrepancy between the desired and actual closed-loop joint impedance. This effectively creates a discrepancy between the desired and actual assistance provided to the user, because the parameter estimation errors change the input-output relationship between the joint torque and joint angle. Furthermore, the magnitude of the discrepancy is directly linked to the magnitude of the parameter estimation error and the magnitude of α.

- Large values of α can only be used if the parameter estimation errors are small. This is a phenomenon that was observed during experimentation. For example, setting $\alpha = 1$ with $K_1 = 0.075$, $K_2 = 1$, and $K_3 = 0$ would typically result in an unstable user-device interaction. However, setting $\alpha = 1$ with $K_1 = 0.2$, $K_2 = 4$, and $K_3 = 0$ would allow stable operation of the orthosis.

- Joint torque estimation errors vary in proportion to the motion of the joint. They cannot be represented by a simple bias or scaling factor. Large joint angular velocities and accelerations will induce large estimation errors, and this must be taken into account when using these estimates for comparing controller performance.

- Noise in the force sensor used to estimate interaction torque directly drives the joint. Accordingly, this noise could result in oscillatory user-device interactions, particularly when the parameter estimation errors cause the closed-loop joint dynamics to approach the brink of stability. This behavior too, was observed during the experiments. Furthermore, low frequency errors in estimating the interaction torque (i.e., due to incorrect estimates of L_f in (3.1) or due to the motion of the passive joint) will directly contribute to creating a discrepancy between the desired and actual assistance provided to the user. Depending on the sign of error, the user may be over or under-assisted by the (low frequency) interaction torque estimation errors. It is also important to note that the effects of interaction torque estimation errors and noise become more prevalent as α becomes larger.

While the discussion above has focussed solely on the MAC, it is important to note that using inaccurate joint torque estimates in the assistance regulation control loop result will also result in the same problems.

4.3 Summary

The ultimate goal of this research was to develop an AD controller that allowed the user to control the motion of the orthosis with no pre-defined joint trajectories, and provided the user with assistance only when assistance was required. Another goal of this research was to prove that such a controller would be more effective at encouraging user effort - an essential element for optimizing rehabilitation therapy - than the commonly used MAC. The experimental results presented in this chapter provide evidence that the ARC presented in this thesis is capable of achieving both these goals.

In addition to confirming many of the benefits and behaviours predicted in simulation, the verification experiments also confirmed that the controller was properly implemented, and that it was possible to implement both the ARC and MAC using IDB joint torque estimates. However, using inaccurate joint torque estimates may result in discrepancies between the desired and actual assistance provided to the user.

Chapter 5

Validation Experiments with Knee Extension

The previous chapter described elbow extension experiments conducted to verify the performance of the ARC. The results of these experiments suggested that the ARC is capable of regulating user effort and that it is better suited for rehabilitation applications of wearable robots. However, the experiments described in the previous chapter were only conducted with one participant (the author), and the orthosis was not fully attached to the participant during the experiments. This chapter presents results for knee flexion experiments conducted with six different participants. These experiments were used to confirm the simulation and experimental results discussed in Chapters 2 and 4, and to gauge the users' subjective perceptions regarding the use of the ARC over the MAC. All tests were limited to constant speed knee joint extensions. The start and end position of the lower leg during each experiment is shown in Figure 2.1.

5.1 Method

Six healthy male participants between the ages of 23 and 26 and with heights and masses ranging between from 165 and 198 cm and 70 and 113 kg, respectively, participated in the experiments. The participant recruitment, screening, and informed consent processes described in the Section 3.2.9 were followed with all participants. Any individuals with neurological disorders or knee injuries that might effect their ability to perform the

experiments were refrained from participating in the experiments.

The experimental procedure used during the elbow flexion experiments (see Section 4.1 for details) was used to conduct the knee flexion experiments described in this chapter. As with the elbow flexion tests, each user was asked to track a desired knee motion. A visual cue of tracking error was provided through a monitor output that presented vertical scrolling lines corresponding the the desired and actual knee orientation. The desired trajectory used in all test runs was a smoothed constant velocity (8 °/s) extension of 66.5°.

The user was asked to repeat a maximum of three test runs at each of the three test conditions summarized in the list below.

- No assistance - the virtual torque term in the impedance controller was set to zero.
- Muscle amplification - the virtual torque term in the impedance controller was chosen to generate the muscle amplification behaviour.
- Assistance regulation - the virtual torque term in the impedance controller was chosen to generate the assistance regulation behaviour.

Each user repeated the experiments a minimum of two times prior to data collection. Two repetitions were found to be adequate to enable the user to sufficiently adapt to each new test condition in most cases. However some participants required more practice, particularly with the no assistance test condition during which the orthosis provided the largest amount of resistance. Joint angle, interaction force, and EMG data were measured during all test runs and at each test condition. Users were not allowed large numbers of practice runs, and only three test runs were completed at each test condition during the data collection process in order to keep the length of the experiment under 1.5 hours. In general, the review of the experimental and safety procedures, and the installation and calibration of the device, EMG electrodes, and controller parameters typically required 30-45 minutes. The remainder of the experiment was devoted to completing the practice

and data collection test runs at each test condition.

Figure 5.1 shows the orthosis fitted onto one of the participants. Preliminary experiments with the first participant indicated that completing the tests while sitting on a chair was too difficult, especially if the participant's feet were touching the ground. Accordingly, all remaining tests were done with participants sitting on a table as shown in Figure 5.1.

EMG Data Collection

All EMG data collected during the verification experiments was recorded and processed according to the procedure described in Section 3.2.6. Electrodes were placed on the belly of the medial vastus (extensor) and biceps femoris (flexor) muscles. In general, there are more muscles involved in controlling knee motions. However, the type of knee motion considered in this experiment is most strongly correlated to the activity in the medial vastus and biceps femoris muscles [66]. Raw EMG signals were amplified by gains ranging between 20000 and 100000. The largest amplification value that avoided saturation of the amplifier output was used for each individual and each muscle.

Unless otherwise stated, all references to muscle, flexor, or extensor activation data in the remainder of this chapter refer to the EMG data collected and processed according the procedures described in this section and in Section 3.2.6.

Joint Torque Estimation

Knee motion was modelled according to (2.1), and joint torque was estimated by solving for τ_m in this equation. The inertia and viscous damping parameters of (2.1) were specified as $J_k = 0.22$ kg·m^2 and $b_k = 1.71$ Nm/(rad/s) for all participants. These values correspond to the estimated knee joint inertia and damping parameters for a healthy 78 kg male provided in [18]. The values of J_k and b_k would undoubtedly have varied between the different

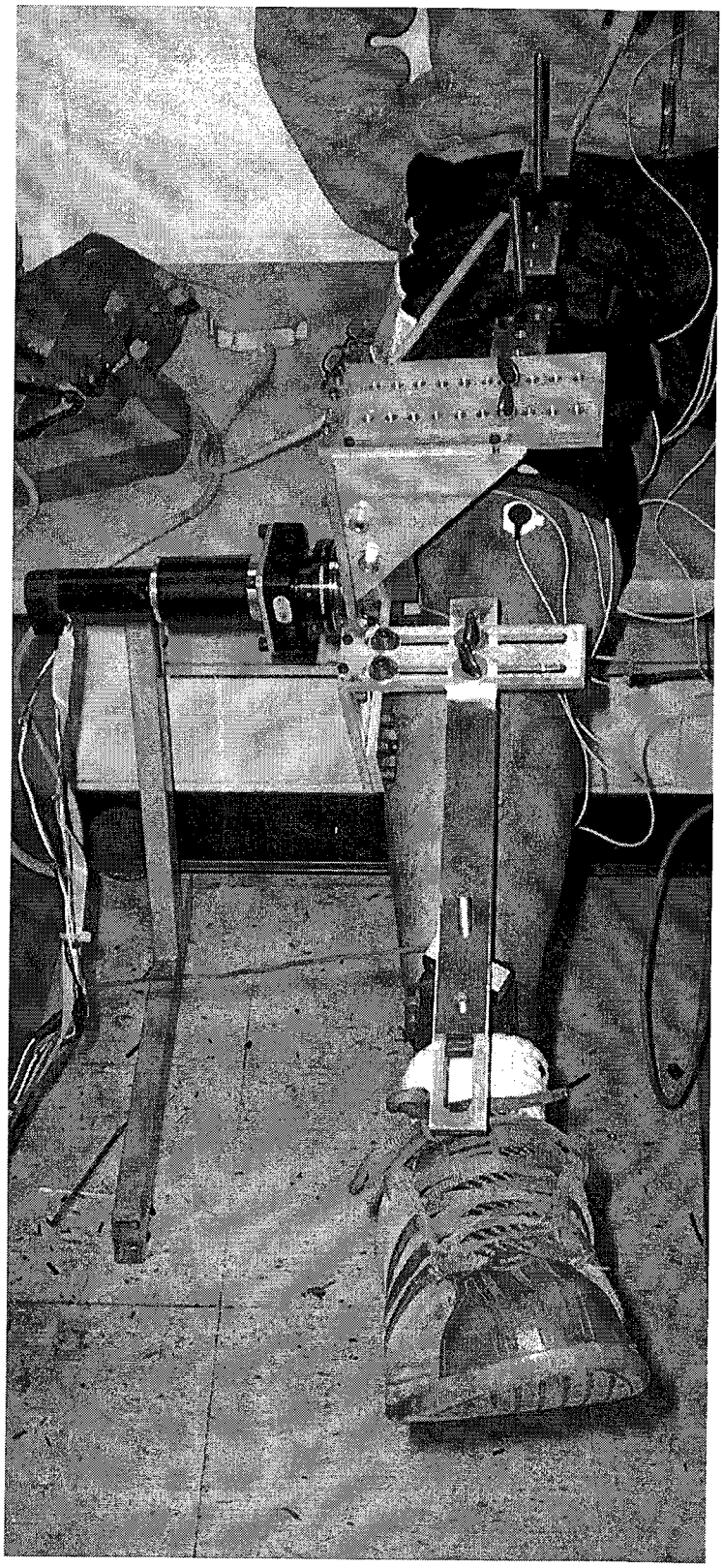

Figure 5.1: The orthosis fitted onto one of the knee flexion experiment participants.

individuals who participated in the experiment. However, it was not possible to estimate user-specific values of either model parameter because the current feedback provided by the servomotor amplifier was too noisy and inaccurate to be used to estimate motor torque; and without accurate estimates of motor torque, it was not possible to employ system identification techniques (e.g., such as those used in [18]) to estimate user-specific values of joint inertia and damping. It is also important to note that the values of J_k and b_k likely had a minimal impact on joint torque estimation accuracy. This is because the motions considered during the experiment consisted of constant speed extensions conducted at relatively low speeds. The values of lower leg mass, m_k, and centre of mass offset, L_k, have a substantial impact on joint torque estimation accuracy and were estimated for each user. Information about each user's weight and height, and the averages of body segment mass and centre of mass position provided in [41] were used to determine user-specific values of m_k and L_k.

Interaction torque (i.e., τ_{int} in (2.1)) was modelled according to (3.1). The value of L_f in (3.1) was measured for each individual and tended to vary between 0.25 and 0.3 m.

Virtual Impedance Model

The virtual impedance model used during the verification experiments was specified as,

$$0.2\ddot{\theta}_{ref} + 6\dot{\theta}_{ref} + 9.81\sin\theta_{ref} = \tau_{int} + \tau_v \tag{5.1}$$

where θ_{ref} is the reference trajectory, and τ_v is used to control the assistance provided to the user. The virtual torque input, τ_v, was defined by (2.9) when implementing the MAC, and by (2.11) when implementing the ARC.

As in the elbow flexion experiments described in the previous chapter, the parameters of the virtual impedance model were purposely chosen to substantially increase the inertial, viscous, and gravitational loading perceived by the user. This was necessary because it allowed changes in estimated joint torque between the no assistance, muscle amplification, and assistance regulation test conditions to be easily distinguished.

Controller Gains

The amplification gain, α, for the MAC was set to 1. This implied that the orthosis should provide half the torque required to complete any particular motion. The choice of $\alpha = 1$ ensured that the change in user effort between the no assistance and muscle amplification test conditions was sufficiently large to be easily discerned by the user and in the data collected during the experiment.

The gains of the ARC were determined experimentally for each user. Both the difference gain, β, and upper assistance trigger, σ_u, were chosen such that the ARC provided the same amount of assistance as the muscle amplifying controller towards the end of the desired trajectory. This meant that the maximum assistance provided by both controllers was the same. It was necessary to choose the ARC gains in this way in order to ensure a consistent comparison between both controllers. The values of β and σ_u used for each participant are summarized in Table 5.1.

5.2 Results and Discussion

Six healthy males participated in the experiments. The adjustment mechanisms included in the orthosis design (see Section 3.2.1 for details) were found to be sufficient to accommodate the reasonably large variations in body morphology that existed within the group of participants. However, the offset mass of the servomotor did result in a twisting moment

Table 5.1: The assistance regulation controller gains used for all six participants of the knee extension validation experiments.

Participant Number	β	σ_u (Nm)
1	4	7
2	5	8.5
3	5	9
4	5	7.5
5	5	8.5
6	5	8

about the hip that tended to cause the device to slip at the connection points. The effect of this twisting moment was mitigated through the use of a 2.2 kg counterweight that provided an opposing twisting moment that balanced the twisting moment generated by the servomotor. The counterweight, and its placement can be seen in Figure 5.2. While no participants were injured during the experiments, some participants did note minor discomfort generated as a result of the tightening of the velcro straps around the thigh and ankle.

Figure 5.2: The location of the counterweight used to balance the servomotor's offset mass.

Particular attention was given to aligning the axes of rotation of the orthosis and joint during the fitting process. However, some motion of the passive translational joint, the passive DOF added to the mechanical design to accommodate differences in joint and orthosis axes of rotation (see Section 3.2.2 for details), was observed in all participants. Visual inspection of the passive joint suggested that it tended to move closer to the orthosis centre of rotation as the user approached the flexion limits of the device.

Problems with joint locking were not observed during the muscle amplification and assistance regulation test conditions, or when the user rotated their lower leg with the motor inactive. However, joint locking was observed at the no assistance test condition. Visual inspection indicated that the natural motion of the passive joint was hindered in these situations, and that the entire orthosis tended to move vertically with respect to the knee joint (due to slip and rotation at the connection points). This vertical motion likely caused the orthosis and joint axes of rotation to become misaligned, as users complained of a sudden and large resistance to continued extension in these situations. Typically, this behaviour was only observed when the resistance provided by the orthosis was close to its peak. This suggests that an increase in static or sliding friction may have limited the motion of the passive joint whenever the user exerted a large force against the lower leg frame of the orthosis. This problem was resolved by asking each participant to resist the vertical motion of the orthosis by pushing down on the upper leg frame of the orthosis during the duration of the test run. This solution was sufficient to allow each participant to successfully perform test runs at the no assistance test condition.

The number of test runs performed at each test condition by each participant are summarized in Table 5.2. All participants indicated that controlling knee motion to precisely follow a desired trajectory under the loading conditions considered during the experiments required reasonable physical and mental effort. Most participants noted that it became quite challenging to maintain the level of focus required to successfully complete a test run beyond 45 minutes of working with the orthosis. As a result, some participants

were not able to complete 3 successful test runs at all test conditions.

Table 5.2: The number of knee extension test runs completed by each participant.

Participant Number	No Assistance	Muscle Amplification	Assistance Regulation
1	3	3	2
2	3	3	3
3	3	3	3
4	3	2	3
5	2	3	3
6	3	3	3

Due to the lack of practice, and the difficulty in precisely controlling knee motion in general (in comparison to elbow motion), the tracking errors observed in these experiments tended to be larger than those observed in the elbow flexion experiments. Figures 5.3 and 5.4 show the averaged knee joint trajectories at all test conditions for Participants 5 and 6. Comparison of these two figures with Figure 4.7 clearly indicates that the tracking error in the knee flexion experiments was larger than in the elbow flexion experiments. These figures, like the rest of the figures shown in this chapter present data that has been averaged over the total number of test runs completed at each test condition by each participant. Only the data for Participants 1 and 6 has been presented in this chapter. This is because Participant 1 was least able to track the desired trajectory while Participant 6 was best able to track the desired trajectory; all other participants were able to track the desired trajectory with an accuracy somewhere in between. It is also important to note that tracking errors tended to be largest at the no assistance condition because participants were required to simultaneously focus on completing the test run, and pushing down on the upper leg frame of the orthosis to avoid problems with joint locking. While the tracking errors are larger than in the elbow extension experiments, the results from the validation experiments again confirm that both the MAC and ARC allow the user to control their

joint motion fairly precisely.

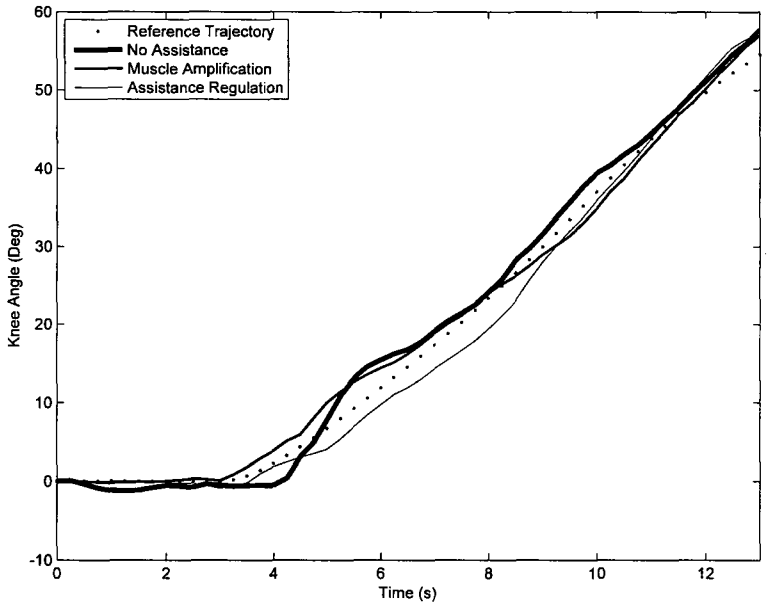

Figure 5.3: Averaged knee angle trajectories at all test conditions for Participant 1.

Figures 5.5 and 5.6 show the estimated joint torque data for Participants 1 and 6. Comparisons of these figures with Figure 4.8 shows the same trends observed in the elbow extension tests - even though both the MAC and ARC provide nearly the same maximum level of assistance towards the end of the test run, the ARC encourages significantly more user effort since it does not provide assistance throughout the entire motion. Figure 5.6 also shows that the estimated joint torque trajectories at the assistance regulation and no assistance test conditions are nearly the same up to the point that the orthosis provides the user with additional assistance (i.e., approximately 7 seconds into the test). These results suggest that choosing the assistance triggers appropriately (i.e., close to the user's joint torque limits) ensure that the ARC would provide the user with assistance only when the user actually required assistance. As with the knee angle trajectories, the estimated joint torque trajectories from all other participants showed trends similar to those shown

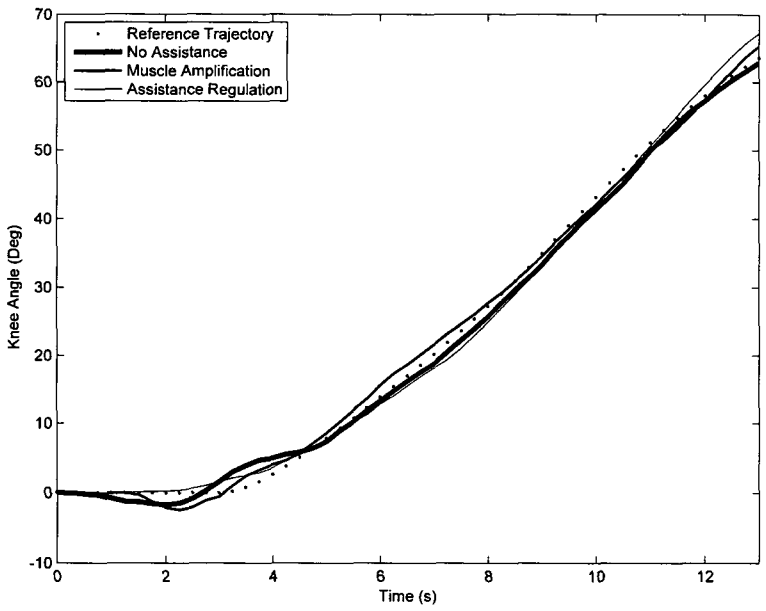

Figure 5.4: Averaged knee angle trajectories at all test conditions for Participant 6.

in Figures 5.5 and 5.6.

The difference between the estimated joint torque trajectories for the assistance regulation and no assistance test conditions for the first seven seconds in Figure 5.5 can be attributed to the tracking errors seen in Figure 5.3. Figure 5.3 shows that Participant 1 was consistently lagging the desired motion for the assistance regulation test condition and consistently leading the desired motion for the no assistance test condition. Since the resistance provided by the orthosis was a function of the joint angle (see the gravitational torque term in (5.1)), Participant 1 was subject to less orthosis resistance when lagging the desired motion, and more orthosis resistance when leading the desired motion. This implies, as Figure 5.5 also shows, that less joint torque would have been required to sustain the knee angle trajectory followed at the assistance regulation test condition.

Figures 5.7 and 5.8 show the extensor muscle activation data at all test conditions for

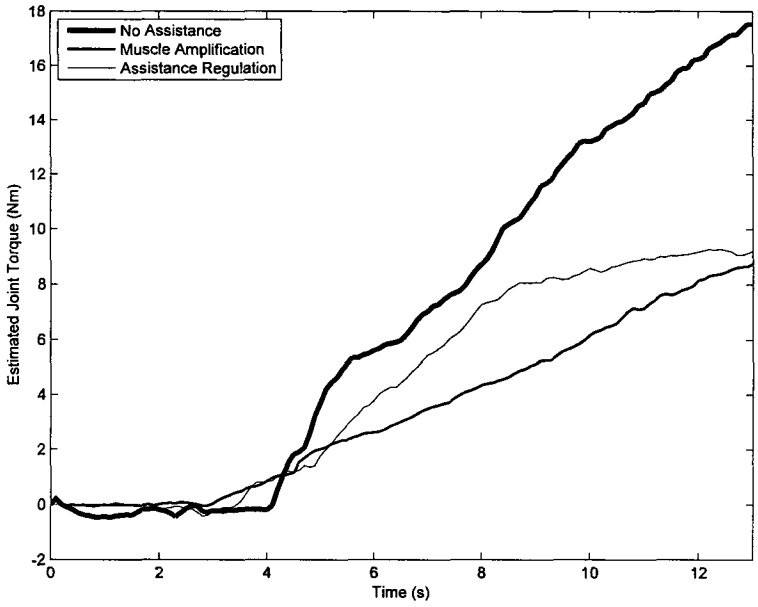

Figure 5.5: Averaged estimated joint torque data at all test conditions for Participant 1.

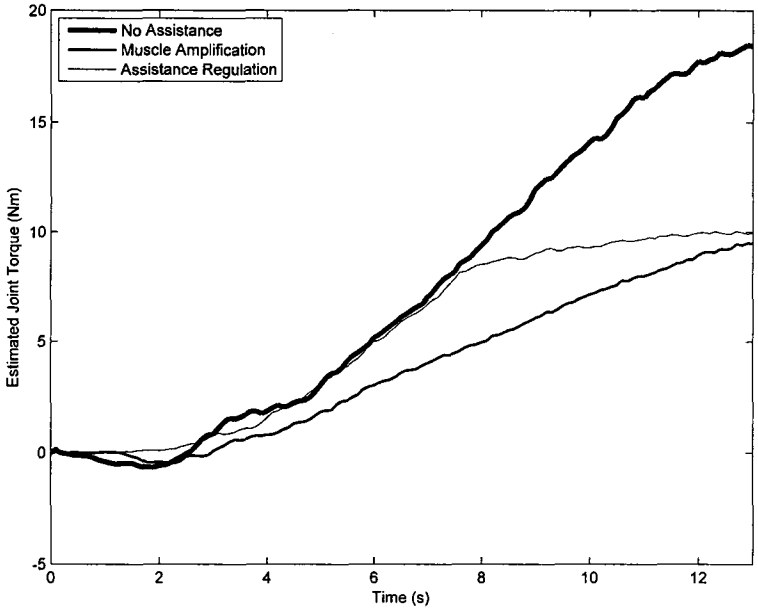

Figure 5.6: Averaged estimated joint torque data at all test conditions for Participant 6.

Participants 1 and 6. Flexor muscle activation data for Participants 1 and 6 are shown in Figures 5.9 and 5.10. Raw EMG data for Participant 1 were collected using the 3M RedDot electrodes. The Duo-Trode electrodes from MyoTronics Inc. were used for all other participants since there were no more 3M RedDot electrodes available. Figures 5.7 and 5.9 show muscle activation data that is consistent with the estimated joint torque data shown in Figure 5.6, and with the qualitative assessments of effort provided by Participant 1. Extensor muscle activation levels (see Figure 5.7) were highest at the no assistance condition, and higher at the assistance regulation test condition in comparison with the muscle amplification test condition.

Interestingly, the results in Figure 5.9 also suggest that flexor muscle activation at both the assistance regulation and muscle amplification test conditions was higher than at the no assistance test condition. It is difficult to determine whether this data suggests a change in the spatio-temporal muscle activation pattern as a result of using either the MAC or ARC, or whether it simply reflects the inter-test run variations in muscle data that were also observed in the elbow extension experiments (e.g., see Figure 4.6 for an example of the inter-test run variations in tricep activation during the elbow extension experiments). More knee extension tests at each test condition would need to be completed to see whether using either controller results in changes in muscle activation patterns similar to those discussed in [4].

Figures 5.8 and 5.10 show the averaged extensor and flexor muscle activation data for Participant 6. The data in this figure is not consistent with the estimated joint torque data shown in Figure 5.6, or with the qualitative assessments of effort provided by the participant. The extensor muscle activation data, in particular, does not show higher muscle activity at the assistance regulation test condition in comparison to the muscle amplification test condition. Additionally, this behavior can not be attributed to changes in muscle activation patterns either, since Figure 5.10 does not show increased flexor muscle activation at the assistance regulation test condition. Similar types of inconsistency

between the participant's perception of effort and the estimated joint torque data, and the corresponding flexor and extensor muscle activation data were observed for all participants who were tested using the Myotronics Duo-Trode electrodes (i.e., all participants except Participant 1). Thus, either the electrodes may have been faulty (i.e., too dry), or there may have been a problem in applying and using this particular brand of electrodes. No other aspects of the EMG data recording and processing procedures were altered when using the Duo-Trode electrodes instead of the 3M RedDot electrodes.

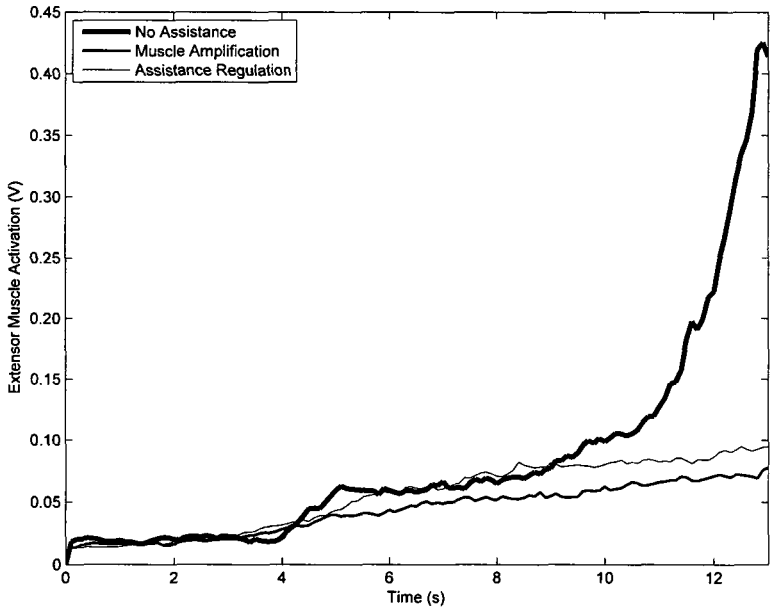

Figure 5.7: Averaged extensor muscle activation data at all test conditions for Participant 1.

The interaction force data measured during the experiments provides an indirect measure of user effort that can also be used to compare controller performance. As noted in Chapter 4, interaction force measurements provide an indication of how hard the orthosis pushed against the user (or vice-versa). Recording large, negative force values during knee extension imply that the orthosis was providing a large resistance to the user's intent to further extend the knee joint. This is the behaviour that was observed at the no assistance

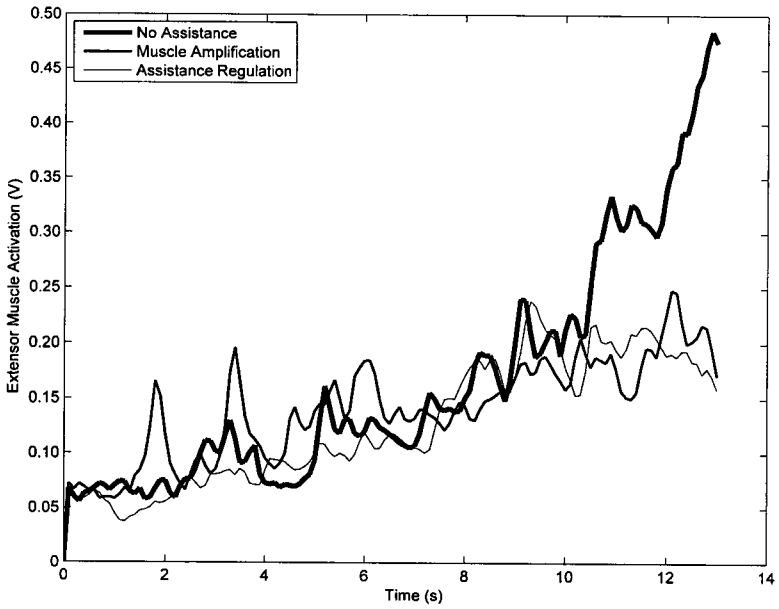

Figure 5.8: Averaged extensor muscle activation data at all test conditions for Participant 6.

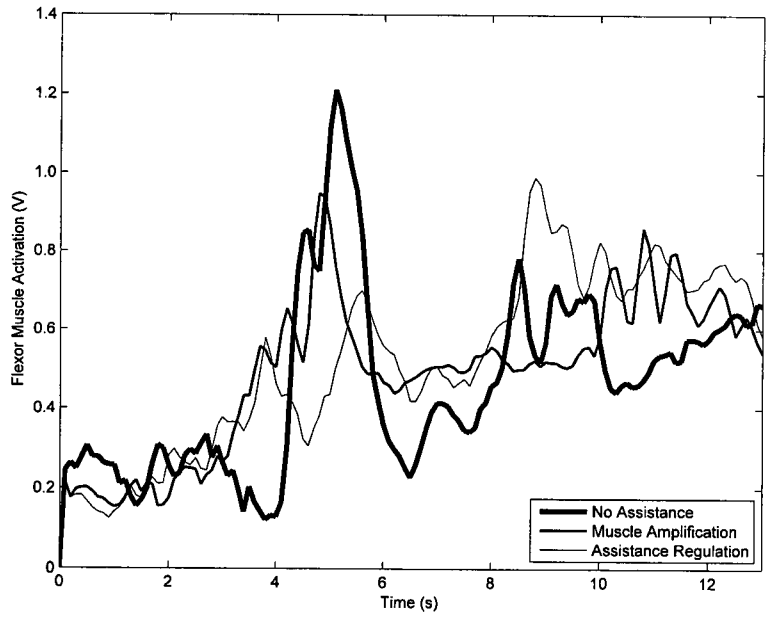

Figure 5.9: Averaged flexor muscle activation data at all test conditions for Participant 1.

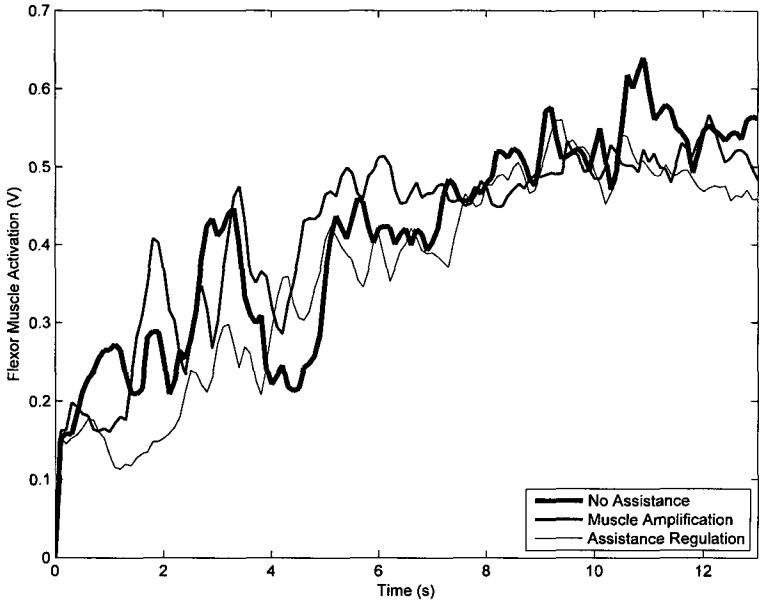

Figure 5.10: Averaged flexor muscle activation data at all test conditions for Participant 6.

test condition with all participants, and it is consistent with the increased gravitational loading generated by the virtual impedance model used during the tests.

Averaged interaction force data for Participants 1 and 6 are provided in Figures 5.11 and 5.12. This data also clearly shows that the ARC elicits more user effort than the MAC. Both participants faced a much larger resistance from the orthosis throughout the entire test when the ARC was used. This implies that both participants would have needed to exert more effort to follow the desired trajectory while facing the added resistance. Thus, even though the muscle activation data for Participant 6 may not reflect this, the interaction force data in Figure 5.12 does clearly show that Participant 6 would have needed to exert more effort to complete the motion when using the ARC instead of the MAC. It is noted that the averaged interaction force data for the remaining participants also showed the same general trends observed in Figures 5.11 and 5.12. This suggests that the inconsistency between muscle activation and estimated joint torque data discussed

above likely reflects a problem with the EMG data collection process.

The fact that the measured interaction force was quite small during the muscle amplification test condition is also consistent with how the virtual impedance model was specified. The estimated lower leg mass (i.e., the value of m_k in (2.1)) ranged between 4.1 and 4.8 kg for all six participants. However, (5.1) simulated the presence of an additional 4 kg mass located 0.25 cm from the orthosis centre of rotation. Thus, the simulated mass effectively made the user feel as though their lower leg was twice as heavy when using the orthosis, i.e., the perceived gravitational loading while wearing the orthosis was approximately twice the actual gravitational loading generated by the user's lower leg. Since the motions considered during the experiment required little acceleration and were performed at relatively low speeds, the participant's joint torque was primarily spent overcoming the perceived gravitational loading. Accordingly, specifying $\alpha = 1$ for the MAC meant that participant needed to generate only half the amount of joint torque required to overcome the perceived gravitational loading at the no assistance test condition. In other words, the participant would have effectively felt only half of the perceived gravitational loading under muscle amplification. As such, the simulated mass provided little or no resistance to the user under muscle amplification, and this explains why the measured interaction forces were so small during the muscle amplification test condition.

5.2.1 Participant Comments Regarding the Use of the MAC and ARC

Participants were questioned about the perceived ease of use and their sense of comfort when using the ARC instead of the MAC. In general, all participants agreed that the MAC felt easier to use and more natural to work with. This perception is also reflected in the tracking error data which suggests that on average, participants were better able to track the desired knee motion when using the MAC instead of the ARC. The fact that most participants required more training test runs when using the ARC also suggests further evidence of this. When asked why, most participants indicated that there was some

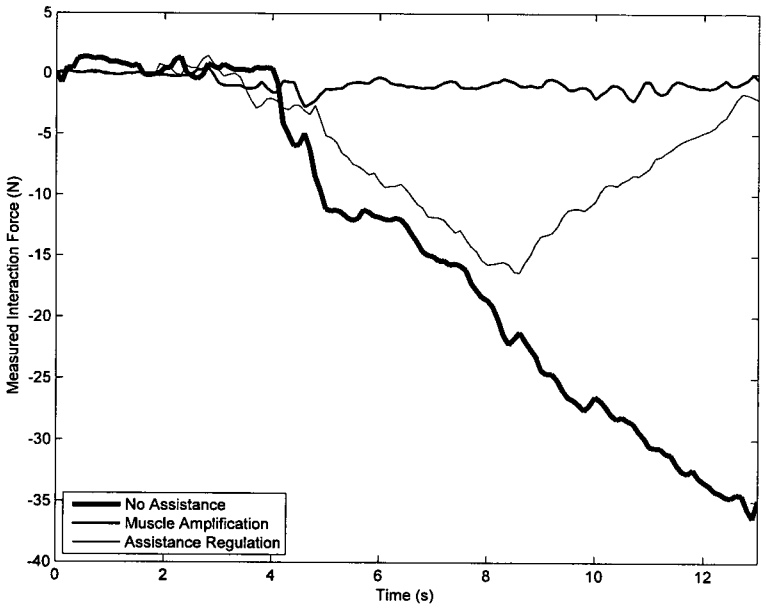

Figure 5.11: Averaged interaction force data at all test conditions for Participant 1.

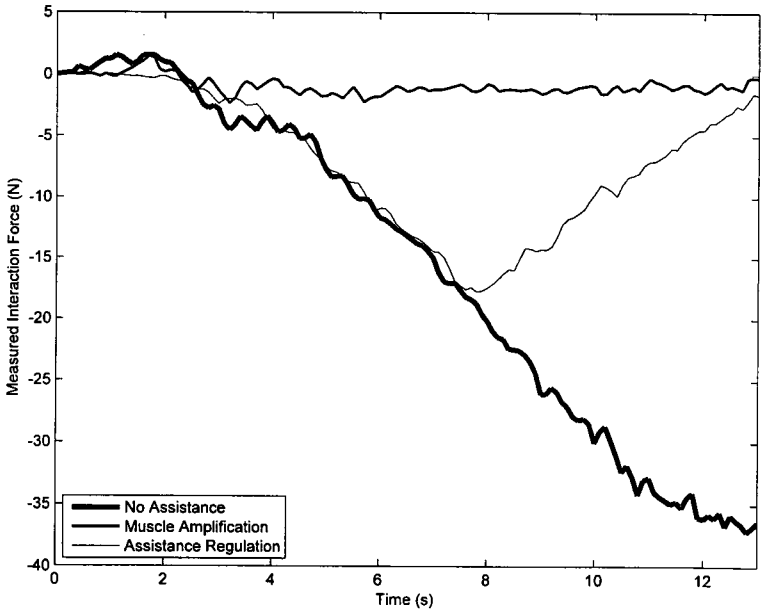

Figure 5.12: Averaged interaction force data at all test conditions for Participant 6.

challenge involved in modulating their own effort to accommodate the added assistance provided by the orthosis when the assistance trigger of the ARC was first surpassed. However, all participants also indicated that it took very little time to become accustomed to the added assistance once the trigger was surpassed and that with sufficient practice with using the ARC, it too would feel as natural as the MAC. Additionally, no participants suggested that the ARC was too difficult (either physically or mentally) to be used continuously. These comments suggest that it may be necessary to design new methods for applying assistance more gradually when using the ARC. These comments also provide a possible reason for why such low virtual torque filter bandwidths were required when using the ARC (see Section 3.2.9 for details); using low filter bandwidths effectively results in assistance being applied in a more gradual manner.

All participants indicated that distinguishing the no assistance test condition from the other two test conditions was easy. Similarly, all participants also indicated that the ARC required more effort than the MAC. However, three of the six participants also indicated that the difference between the assistance regulation and muscle amplification test conditions did not feel substantial. It is important to note though, that perceptions of effort must be treated with caution. This is especially the case in the validation experiments described in this chapter, because participants were not able to try the MAC and ARC simultaneously. Participants performed tests with each controller sequentially and had to rely on a memory of a previous test run when making the comparison. As discussed above, differences in tracking error between test runs completed at different test conditions would have subjected the participant to different levels of orthosis resistance. This too, makes subjective indications of user effort more difficult to trust, since the user's perception of effort is partly linked to how closely the desired motion was tracked. This emphasizes the importance of using controlled experiments to compare controller performance rather than relying on subjective perceptions of user effort to qualify the effectiveness of one AD controller over another.

It is also important to note that all participants were tested with the same sequence of test conditions. Thus, it is possible that training effects may also have biased participant perceptions about ease of use and the effort required when using the ARC. However, additional tests with random test sequences would be necessary to determine the relative importance of training effects.

5.2.2 Comparing the ARC to other AD controllers

In general, few researchers in the field of AD control address the need to ensure active user participation during AD usage. In fact, the EMG-driven forearm orthosis controller described in [19] is among the few controllers designed to intelligently regulate assistance based on the user's need for assistance. In [19], the reference trajectory generated by an impedance controller was actively manipulated to provide the user with more assistance anytime a therapist-specified EMG threshold was exceeded. The controller ensured active user participation since the user was forced to initiate and sustain any motion that did not cause this threshold to be exceeded. However, the controller did not allow for precise regulation of user effort, and was vulnerable to factors like muscle co-contraction and muscle fatigue.

Another drawback of that approach - and of similar approaches such as those in [18] - was that the orthosis was controlled using fixed impedance controller gains. Fixed impedance controller gains, like fixed amplification gains, are undesirable since they generate a specific input-output relationship between joint torque and angle. Since the user's joint torque capacity remains constant regardless of the activity's torque requirements, low gains will ensure sufficient user effort during the completion of one task. However, the same gains may be insufficient for assisting the user in completing a higher intensity task. Similarly, high gains will ensure sufficient assistance during the completion of high-intensity tasks, but the same gains will provide excessive assistance for low-intensity tasks; this particular behaviour is most clearly observed in the simulation results presented in Figures 2.5 and 2.7.

The tradeoffs with using fixed controller gains can be overcome by using different gains for different tasks. However, using task-dependent controller gains introduces a new set of control and sensing challenges. ADs are usually designed to assist users in a wide range of tasks with highly variable torque requirements. Thus, simply defining the appropriate gains for each task is itself a significant challenge. Furthermore, using task-dependent controller gains introduces additional control complexity and sensing and computation overhead due to the need to identify the task being performed and the appropriate controller gains to associate with the identified task. However, the ARC is not completely immune from this problem either - a full body exoskeleton employing assistance regulation would require additional sensors to allow proper distinguishing of the appropriate gait phase or the presence of unmodelled external loads. However, the performance of the ARC is substantially more robust than many other AD controllers with respect to changes in tasks and/or task intensities.

Some researchers have tried using time-varying impedance controller gains as a means for regulating user effort. In [3] and [23] for example, both the desired trajectory and desired exoskeleton impedance were obtained from the output of a neuro-fuzzy controller trained to simultaneously minimize position and EMG tracking errors during a dedicated controller training process. The amount of assistance provided to the user was controlled by specifying the desired EMG activity during the training period. This approach was suitable for coarsely regulating user effort. However, the training process required several minutes, and needed to be repeated for different assistance levels and external loads. Additionally, retraining would be necessary any time electrode positions were varied. Furthermore, controller performance could not be guaranteed in the event of muscle fatigue or for other situations outside the range of the training data.

Another EMG-based approach to assistance regulation is described in [37]. In this case, the assistance provided to the user (i.e., the support level) was defined using an EMG-based

user effort measure that compared the muscle activation induced by a particular activity with and without assistance from the orthosis. A proportional controller was then used to regulate this measure, the support level, to a desired value. The proportional controller was shown to be effective at regulating the support level during walking motions. However, the support level calculation required a priori knowledge about expected EMG activation levels of the activity when no assistance was provided by the orthosis. This approach to assistance regulation is effectively task-dependent, since some explicit information about the nature of the task is required in order to appropriately regulate user effort. As such, this approach is subject to the same challenges associated with using task-dependent amplification or impedance gains described above.

The following list summarizes how the ARC presented in this thesis addresses many of the drawbacks of the different assistance regulation approaches discussed above.

- Controller performance is not diminished by factors such as muscle co-contraction or fatigue since EMG data is not used to define the amount of assistance to provide the user, or to predict the intended motion of the user.
- The drawbacks of using fixed amplification and impedance controller gains are avoided since the virtual torque term, rather than the controller gains themselves, are used to control the amount of assistance provided to the user.
- The ability to regulate assistance, and hence, user effort, is independent of the task that the user is performing, provided that joint torque is accurately estimated. This is because the ARC only provides assistance when the muscle joint torque exceeds either the upper or lower assistance trigger. In contrast, typical AD controllers are designed to constantly provide a fraction of the predicted user effort at all times. These controllers naturally provide excessive assistance when a user performs a task that he or she is fully capable of performing without any assistance.

5.3 Summary

This chapter presented the results of knee flexion experiments carried out with six healthy male participants. The goal of these tests was to confirm the behaviours and benefits of using the ARC suggested by the simulation results presented in Chapter 2, and the elbow extension experiments discussed in Chapter 4. Notwithstanding some of the minor variations seen between participants, the results of the validation experiments again confirmed that the ARC, when its gains are properly specified, is capable of achieving its intended goal of simultaneously allowing the user to remain in control of the orthosis-assisted limb motion and providing assistance only when assistance is required. The knee angle trajectories, estimated joint torque data, and interaction force data collected during the experiments all support this claim. While muscle activation data for Participant 1 supports this claim, it is likely that problems with the EMG data collection process contributed to the inconsistent muscle activation data observed in all other participants.

The qualitative assessments of the participants recorded during the experiments also provided some valuable information. While all participants agreed that the MAC was preferable over the ARC because it felt easier to use, all participants also agreed that the ARC could easily be used continuously for long periods of time after sufficient practice. Finally, the comments from the participants also suggested that making the ARC provide assistance in a more gradual manner would also help make it easier to use.

Chapter 6

Conclusion and Recommendations

The need to physically and mentally engage the user during rehabilitation therapy is well recognized in RART. Researchers in this area have already pursued the design of *assist as needed* control strategies for controlling the robots used in RART. However, most of these approaches effectively consist of ad-hoc methods for parameter adaptation or feed forward compensation of standard position or impedance controllers. While effective, these approaches to assistance regulation rely on defining a desired trajectory for the robot and, by consequence, for the joint or limb being assisted. As such, these approaches are not likely to be flexible enough to address the intrinsic variability and complexity in completing even the most common activities of daily living because it is impractical to design a trajectory for every conceivable situation that takes into account both the patient's intended motion and all other environmental inputs (e.g., variable terrain, obstacles, etc.). Additionally, RART is typically conducted using a video-game-like interface and with robots that are not fully interfaced with the user (e.g., robots with a fixed-base that cannot be worn by a user). Thus, RART can not faithfully represent the activities of daily living for which functional recovery is desired, and is not easily provided in representative contexts and environments (e.g., in the user's home rather than in a hospital or clinic). Though there is no direct evidence available to date, it is likely that RART would be most effective if it was designed to assist the user in performing the actual task that requires recovery or compensation, rather than a simulated version of that task.

Actuated ADs such as wearable powered orthoses and exoskeletons are designed to assist users in performing a wide range of different tasks. These devices can be fully interfaced with the user, and can be used in representative contexts and environments. Furthermore, their motion does not have to be prescribed ahead of time. They rely on user-supplied input signals such as EMG or interaction force measurements for generating their motion commands. As such, ADs can overcome many of the limitations of RART. However, most ADs are designed and controlled to amplify user strength. They are effective at helping users perform high intensity tasks with relative ease. However, they drastically reduce the effort required to perform low intensity tasks. As such, prolonged use of ADs that amplify user strength may result in unanticipated detrimental effects such as muscle atrophy. Furthermore, it is well known that patient involvement in rehabilitation therapy is essential for both facilitating and optimizing functional recovery. Thus, muscle amplification is clearly not suitable for use in rehabilitation application of wearable ADs. Such ADs must strike a balance between providing the immediate assistance required to perform a task and promoting neuromuscular recovery over the long term by gently and persistently challenging the user. The first step in achieving this goal is to control powered ADs to selectively assist users based on their need for assistance.

As noted above, many researchers in the field of RART have already considered the problem of assistance regulation. However, none of these approaches are easily transferable to ADs since they explicitly assume that the desired motion of the user (or device) are known ahead of time. Accordingly, the primary objective of this research was to design an AD controller that assisted the user only when the user required assistance, and that did so without requiring the motion of the user (or device) to be known ahead of time. This objective was subject to constraints on the simplicity of the controller's implementation and calibration, and on using the same types of actuators and sensors typically used on other ADs. The simulation and experimental results presented in Chapters 2,4, and 5 suggest that the ARC presented in this thesis satisfies the primary research objective. Figures 4.8, 4.9, 4.10, 5.6, and 5.7 suggest that the ARC does not provide assistance until

either assistance trigger is surpassed. This, in turn implies, that the ARC will provide assistance only when required, if the assistance triggers are properly specified to be just below the user's actual joint torque limits.

The secondary objective of this research was to demonstrate that an AD controller that provides assistance only when required would encourage more user effort than a MAC. This too, was demonstrated by the simulation and experimental results in Chapters 2, 4, and 5. In chapter 3, for example, it was shown that the ARC requires the user to generate 46% more joint torque on average when performing constant speed elbow extension motions. In these tests, both the MAC and ARC were tuned to provide the same level of maximum assistance. These results imply that the ARC provided the immediate assistance required to perform the task, but encouraged substantially more user effort the MAC. In general, the ARC will always encourage more user effort because it provides assistance only if the user's effort is estimated to exceed a pre-defined threshold.

In addition to the primary research conclusions discussed above, the list below summarizes several other important conclusions drawn from the simulation and experimental results.

1. The simulation results in Chapter 2 suggest that the benefits of the ARC are not limited to slowly-varying motions. The ARC encourages more user effort even during dynamic motions. This can be observed by comparing the ARC and MAC joint torque trajectories for the sinusoidal knee motion simulations presented in Section 2.4.2.

2. Simulation results also suggest that the performance of the ARC is not task or task intensity dependent. The same controller gains were equally effective in both the high and low intensity knee motion simulations discussed in chapter 2.

3. Both the simulation and experimental results suggest that ARC does not limit the user's ability to control the orthosis-assisted joint motion. This can be inferred from the user's ability to track the desired trajectory in both simulation and during the knee

and elbow extension experiments. However, the experimental results also suggest that tracking error was larger when using the ARC. The participants of the knee flexion experiments suggested that it was necessary for them to adjust their behaviour when the orthosis first started to provide additional assistance, and that this made it more difficult to track the desired trajectory.

4. The experimental results in Chapters 4 and 5 indicate that the assistance bandwidth filter (see Section 3.2.9 for details) was sufficient to guarantee stable operation of the orthosis for the set of controller parameters used during the experiments. Additionally, the results also suggest that it is possible to generate stable user-device interactions even when using inaccurate IDB joint torque estimates in the control loop. However, the analysis presented in Section 4.2.4 indicates that large joint dynamic model parameter estimation errors and/or amplification gains can contribute to unstable user-orthosis interactions, and that joint torque estimation errors result in discrepancies between the actual and desired assistance provided to the user.

5. Finally, while all knee extension experiment participants suggested that the MAC felt easier and more natural to use, no participants felt that the ARC was too uncomfortable or challenging to use continuously. All participants agreed that they would be equally comfortable with using the ARC after a sufficient amount of practice.

6.1 Future Work and Recommendations

The simulation and experimental results suggest that the ARC presented in this thesis may be more suitable than the MAC for rehabilitation applications of wearable ADs. However, the experiments discussed in this thesis were only performed with healthy individuals. Accordingly, it is important to validate controller performance with the population group that is most likely to use such devices. The ARC, like the MAC, allows the user to remain in full control of the orthosis-assisted limb motion. While this is advantageous, it also puts the onus on the user to ensure the stability of the user-orthosis interaction. Additional

experiments would be necessary to determine whether users suffering from motor skill impairments are equally quick and able to adapt to the intermittent assistance provided by the ARC. Furthermore, it must be noted that increased user effort does directly correlate to functional recovery. Clinical trials comparing the effectiveness of the ARC, MAC, and traditional rehabilitation therapies in terms of function restoration would be necessary to determine if the ARC is capable of increasing the rate and/or extent of functional recovery.

Additional experiments with dynamic motions are also necessary. The simulation results suggest that the ARC results in slower closed-loop joint responses, and as noted in Section 4.2.4, joint torque estimation inaccuracies are much larger when joint angular accelerations and velocities are large. Both factors imply that the ARC may be more challenging to use during highly dynamic motions. Such tests were not conducted as a part of this research because it was difficult for users to closely track dynamic motions using either the MAC or ARC. The large tracking errors in these tests would have made it difficult to compare the performance of both controllers. However, additional tests using highly dynamic motions are necessary to quantify the closed-loop joint bandwidth that can be achieved while using the ARC, and to compare it to the joint bandwidth of healthy human joints.

The mechanical design of the experimental apparatus developed to validate controller performance is sufficient for performing simple knee flexion and extension experiments. However, the design needs to be improved before it can be used for sit-to-stand, and walking experiments. The design requires a better solution for balancing the twisting moment generated by the offset servomotor mass, and the coupling between the upper leg frame and the user's thighs needs to be re-designed to ensure that the device does not slip when the user walks. The long motor and sensor wires extending to the DAC connector block and power supply may also pose a limitation when performing walking and stair climbing experiments. It may be necessary to develop an embedded control system using a microcontroller or embedded PC and wearable power supply (e.g., batteries) in order to

perform these experiments.

List of References

[1] M. Kitchener, T. Ng, H. Y. Lee, and C. Harrington, "Assistive technology in medicaid home- and community-based waiver programs.," *Gerontologist*, vol. 48, pp. 181–189, Apr 2008.

[2] A. M. Dollar and H. Herr, "Active orthoses for the lower-limbs: Challenges and state of the art," in *Proc. IEEE 10th International Conference on Rehabilitation Robotics ICORR 2007*, pp. 968–977, 13–15 June 2007.

[3] K. Kiguchi, R. Esaki, T. Tsuruta, K. Watanabe, and T. Fukuda, "An exoskeleton system for elbow joint motion rehabilitation," in *Proc. IEEE/ASME International Conference on Advanced Intelligent Mechatronics AIM 2003*, vol. 2, pp. 1228–1233, 20–24 July 2003.

[4] T. Hayashi, H. Kawamoto, and Y. Sankai, "Control method of robot suit hal working as operator's muscle using biological and dynamical information," in *Proc. IEEE/RSJ International Conference on Intelligent Robots and Systems (IROS 2005)*, pp. 3063–3068, 2–6 Aug. 2005.

[5] C. Fleischer and G. Hommel, "Embedded control system for a powered leg exoskeleton," *Embedded Systems Modeling, Technology, and Applications*, pp. 177–185, 2006.

[6] G. S. Sawicki, K. E. Gordon, and D. P. Ferris, "Powered lower limb orthoses: applications in motor adaptation and rehabilitation," in *Proc. 9th International Conference on Rehabilitation Robotics ICORR 2005*, pp. 206–211, 28 June–1 July 2005.

[7] H. Kazerooni, J. L. Racine, L. Huang, and R. Steger, "On the control of the berkeley lower extremity exoskeleton (bleex)," in *Proc. IEEE International Conference on Robotics and Automation ICRA 2005*, pp. 4353–4360, 18–22 April 2005.

[8] R. Song, K. Y. Tong, X. L. Hu, and X. J. Zheng, "Myoelectrically controlled robotic system that provide voluntary mechanical help for persons after stroke," in *Proc. IEEE 10th International Conference on Rehabilitation Robotics ICORR 2007*, pp. 246–249, 13–15 June 2007.

[9] J. A. Kleim and T. A. Jones, "Principles of experience-dependent neural plasticity: implications for rehabilitation after brain damage.," *J Speech Lang Hear Res*, vol. 51, pp. S225–S239, Feb 2008.

[10] N. Hogan, H. I. Krebs, B. Rohrer, J. J. Palazzolo, L. Dipietro, S. E. Fasoli, J. Stein, R. Hughes, W. R. Frontera, D. Lynch, and B. T. Volpe, "Motions or muscles? some behavioral factors underlying robotic assistance of motor recovery.," *J Rehabil Res Dev*, vol. 43, no. 5, pp. 605–618, 2006.

[11] E. T. Wolbrecht, V. Chan, D. J. Reinkensmeyer, and J. E. Bobrow, "Optimizing compliant, model-based robotic assistance to promote neurorehabilitation," *IEEE Transactions on Neural Systems and Rehabilitation Engineering*, vol. 16, pp. 286–297, June 2008.

[12] R. Colombo, F. Pisano, S. Micera, A. Mazzone, C. Delconte, M. C. Carrozza, P. Dario, and G. Minuco, "Robotic techniques for upper limb evaluation and rehabilitation of stroke patients," *IEEE Transactions on Neural Systems and Rehabilitation Engineering*, vol. 13, pp. 311–324, Sept. 2005.

[13] H. Krebs, J. Palazzolo, L. Dipietro, M. Ferraro, J. Krol, K. Rannekleiv, B. Volpe, and N. Hogan, "Rehabilitation robotics: Performance-based progressive robot-assisted therapy," *Autonomous Robots*, vol. 15, pp. 7–20, July 2003.

[14] L. E. Kahn, W. Z. Rymer, and D. J. Reinkensmeyer, "Adaptive assistance for guided force training in chronic stroke," in *Proc. 26th Annual International Conference of the IEEE Engineering in Medicine and Biology Society IEMBS '04*, vol. 1, pp. 2722–2725, 1–5 Sept. 2004.

[15] R. Riener, L. Lunenburger, S. Jezernik, M. Anderschitz, G. Colombo, and V. Dietz, "Patient-cooperative strategies for robot-aided treadmill training: first experimental results," *IEEE Transactions on Neural Systems and Rehabilitation Engineering*, vol. 13, pp. 380–394, Sept. 2005.

[16] S. K. Banala, S. K. Agrawal, and J. P. Scholz, "Active leg exoskeleton (alex) for gait rehabilitation of motor-impaired patients," in *Proc. IEEE 10th International Conference on Rehabilitation Robotics ICORR 2007*, pp. 401–407, 13–15 June 2007.

[17] B. Weinberg, J. Nikitczuk, S. Patel, B. Patritti, C. Mavroidis, P. Bonato, and P. Canavan, "Design, control and human testing of an active knee rehabilitation orthotic device," in *Proc. IEEE International Conference on Robotics and Automation*, pp. 4126–4133, 10–14 April 2007.

[18] G. Aguirre-Ollinger, J. E. Colgate, M. A. Peshkin, and A. Goswami, "Active-impedance control of a lower-limb assistive exoskeleton," in *Proc. IEEE 10th International Conference on Rehabilitation Robotics ICORR 2007*, pp. 188–195, 13–15 June 2007.

[19] D. S. Andreasen, S. K. Alien, and D. A. Backus, "Exoskeleton with emg based active assistance for rehabilitation," in *Proc. 9th International Conference on Rehabilitation Robotics ICORR 2005*, pp. 333–336, 28 June–1 July 2005.

[20] E. E. Cavallaro, J. Rosen, J. C. Perry, and S. Burns, "Real-time myoprocessors for a neural controlled powered exoskeleton arm," *IEEE Transactions on Biomedical Engineering*, vol. 53, pp. 2387–2396, Nov. 2006.

[21] J. Rosen, M. Brand, M. B. Fuchs, and M. Arcan, "A myosignal-based powered exoskeleton system," *IEEE Transactions on Systems, Man and Cybernetics, Part A*, vol. 31, pp. 210–222, May 2001.

[22] C. Fleischer and G. Hommel, "Emg-driven human model for orthosis control," *Human Interaction with Machines*, pp. 69–76, 2006.

[23] K. Kiguchi, M. H. Rahman, and M. Sasaki, "Neuro-fuzzy based motion control of a robotic exoskeleton: considering end-effector force vectors," in *Proc. IEEE International Conference on Robotics and Automation ICRA 2006*, pp. 3146–3151, 15–19 May 2006.

[24] J. E. Pratt, B. T. Krupp, C. J. Morse, and S. H. Collins, "The roboknee: an exoskeleton for enhancing strength and endurance during walking," in *Proc. IEEE International Conference on Robotics and Automation ICRA '04*, vol. 3, pp. 2430–2435, Apr 26–May 1, 2004.

[25] J. L. Emken, S. J. Harkema, J. A. Beres-Jones, C. K. Ferreira, and D. J. Reinkensmeyer, "Feasibility of manual teach-and-replay and continuous impedance shaping for robotic locomotor training following spinal cord injury," *IEEE Transactions on Biomedical Engineering*, vol. 55, pp. 322–334, Jan. 2008.

[26] A. LeBlanc, C. Lin, L. Shackelford, V. Sinitsyn, H. Evans, O. Belichenko, B. Schenkman, I. Kozlovskaya, V. Oganov, A. Bakulin, T. Hedrick, and D. Feeback, "Muscle volume, mri relaxation times (t2), and body composition after spaceflight.," *J Appl Physiol*, vol. 89, pp. 2158–2164, Dec 2000.

[27] G. Venture, Y. Nakamura, K. Yamane, and M. Hirashima, "Identification of limbs joint passive visco-elasticity: A comparison of two experimental methods," in *International Symposium on Skill Science*, pp. pp. 31–37, 2007.

[28] F. W. Brinckmann P. and L. W., *Muscoskeletal Biomechanics*, ch. Translation and rotation in a plane, pp. 28–32. Thieme, 2002.

[29] G. Venture, K. Yamane, Y. Nakamura, and T. Yamamoto, "Indentification of human limb viscoelasticity using robotics methods to support the diagnosis of neuromuscular diseases," *The International Journal of Robotics Research*, p. 0278364909103786, 2009.

[30] T. E. Milner and C. Cloutier, "The effect of antagonist muscle co-contraction on damping of the wrist joint during voluntary movement," in *Proc. IEEE 17th Annual Conference Engineering in Medicine and Biology Society*, vol. 2, pp. 1247–1248, 20–23 Sept. 1995.

[31] T. E. Milner, "Dependence of elbow viscoelastic behavior on speed and loading in voluntary movements," *Experimental Brain Research*, vol. 93, pp. 177–180, Feb. 1993.

[32] J. B. MacNeil, R. E. Kearney, and I. W. Hunter, "Time-varying identification of the neuromuscular system. i. human joint dynamics," in *Proc. Fifteenth Annual Northeast Bioengineering Conference*, pp. 147–148, 27–28 March 1989.

[33] D. J. Bennett, J. M. Hollerbach, Y. Xu, and I. W. Hunter, "Time-varying stiffness of human elbow joint during cyclic voluntary movement.," *Exp Brain Res*, vol. 88, no. 2, pp. 433–442, 1992.

[34] K. C. Hayes and H. Hatze, "Passive visco-elastic properties of the structures spanning the human elbow joint.," *Eur J Appl Physiol Occup Physiol*, vol. 37, pp. 265–274, Dec 1977.

[35] C.-C. Lin, M.-S. Ju, and C.-W. Lin, "The pendulum test for evaluating spasticity of the elbow joint.," *Arch Phys Med Rehabil*, vol. 84, pp. 69–74, Jan 2003.

[36] E. V. Biryukova, V. Y. Roschin, A. A. Frolov, M. E. Ioffe, J. Massion, and M. Dufosse, "Forearm postural control during unloading: anticipatory changes in elbow stiffness.," *Exp Brain Res*, vol. 124, pp. 107–117, Jan 1999.

[37] H. Kawamoto, S. Lee, S. Kanbe, and Y. Sankai, "Power assist method for hal-3 using emg-based feedback controller," in *Proc. IEEE International Conference on Systems, Man and Cybernetics*, vol. 2, pp. 1648–1653, 5–8 Oct. 2003.

[38] G. Field and Y. Stepanenko, "Model reference impedance control of robotic manipulators," in *Proc. IEEE Pacific Rim Conference on Communications, Computers and Signal Processing*, vol. 2, pp. 614–617, 19–21 May 1993.

[39] D. A. Lawrence, "Impedance control stability properties in common implementations," in *Proc. IEEE International Conference on Robotics and Automation*, pp. 1185–1190, 24–29 April 1988.

[40] T. Tsumugiwa, R. Yokogawa, and K. Yoshida, "Stability analysis for impedance control of robot for human-robot cooperative task system," in *Proc. IEEE/RSJ International Conference on Intelligent Robots and Systems (IROS 2004)*, vol. 4, pp. 3883–3888, 28 Sept.–2 Oct. 2004.

[41] C. Clauser, J. McConville, and J. Young, "Weight, volume, and center of mass of segments of the human body," tech. rep., (AMRL Technical Report 69-70). Wright-Patterson Air Force Base, OH: Aerospace Medical Research Laboratories, 1969.

[42] J. L. Emken, R. Benitez, A. Sideris, J. E. Bobrow, and D. J. Reinkensmeyer, "Motor adaptation as a greedy optimization of error and effort.," *J Neurophysiol*, vol. 97, pp. 3997–4006, Jun 2007.

[43] D. J. Reinkensmeyer, E. Wolbrecht, and J. Bobrow, "A computational model of human-robot load sharing during robot-assisted arm movement training after stroke," in *Proc. 29th Annual International Conference of the IEEE Engineering in Medicine and Biology Society EMBS 2007*, pp. 4019–4023, 22–26 Aug. 2007.

[44] D. G. Caldwell, "Robotic actuation: organic and inorganic power systems," in *Proc. IEE Colloquium on Robot Actuators*, pp. 6/1–6/5, 7 Oct 1991.

[45] P. Beyl, J. Naudet, R. Van Ham, and D. Lefeber, "Mechanical design of an active knee orthosis for gait rehabilitation," in *Proc. IEEE 10th International Conference on Rehabilitation Robotics ICORR 2007*, pp. 100–105, 13–15 June 2007.

[46] A. Zoss, H. Kazerooni, and A. Chu, "On the mechanical design of the berkeley lower extremity exoskeleton (bleex)," in *Proc. IEEE/RSJ International Conference on Intelligent Robots and Systems (IROS 2005)*, pp. 3465–3472, 2–6 Aug. 2005.

[47] R. Holt, S. Makower, A. Jackson, P. Culmer, M. Levesley, R. Richardson, A. Cozens, M. M. Williams, and B. Bhakta, "User involvement in developing rehabilitation robotic devices: An essential requirement," in *Proc. IEEE 10th International Conference on Rehabilitation Robotics ICORR 2007*, pp. 196–204, 13–15 June 2007.

[48] S. Dong, K.-Q. Lu, J. Q. Sun, and K. Rudolph, "Rehabilitation device with variable resistance and intelligent control.," *Med Eng Phys*, vol. 27, pp. 249–255, Apr 2005.

[49] R. C. Juvinall and K. M. Marshek, *Fundementals of Machine Component Design.* John Wile and Sons, Inc., 3 ed., 2000.

[50] V. Wright and E. Radin, *Mechanics of human joints: physiology, pathophysiology, and treatment.* Informa Health Care, 1993.

[51] Z. D. Hollman J. H., Deusinger R. H. and M. M., "Estimation of knee joint surface rolling/gliding kinematics via instant center of rotation measurement," in *2000 Annual Americal Society of Biomechanics Meeting*, 2000.

[52] A. M. Bull and A. A. Amis, "Knee joint motion: description and measurement.," *Proc Inst Mech Eng H*, vol. 212, no. 5, pp. 357–372, 1998.

[53] C. R. Wheeless, *Wheeless' Textbook of Orthopaedics.* Data Trace Internet Publishing, 2008.

[54] T. P. Andriacchi, G. B. Andersson, R. W. Fermier, D. Stern, and J. O. Galante, "A study of lower-limb mechanics during stair-climbing.," *J Bone Joint Surg Am*, vol. 62, pp. 749–757, Jul 1980.

[55] R. Riener, M. Rabuffetti, and C. Frigo, "Joint powers in stair climbing at different slopes," in *Proc. First Joint [Engineering in Medicine and Biology 21st Annual Conf. and the 1999 Annual Fall Meeting of the Biomedical Engineering Soc.] BMES/EMBS Conference*, vol. 1, p. 530, 13–16 Oct. 1999.

[56] D. P. and H. T., "Obesity is not associated with increased knee joint torque and power during level walking," *Journal of Biomechanics*, vol. 36, pp. 1355–1362(8), September 2003.

[57] R. Riener, M. Rabuffetti, and C. Frigo, "Stair ascent and descent at different inclinations.," *Gait Posture*, vol. 15, pp. 32–44, Feb 2002.

[58] J. E. Earl, S. J. Piazza, and J. Hertel, "The protonics knee brace unloads the quadriceps muscles in healthy subjects.," *J Athl Train*, vol. 39, pp. 44–49, Mar 2004.

[59] "Shunt calibration of a strain gage sensor," tech. rep., PCB Piezotronics, 2002.

[60] K. Kong and M. Tomizuka, "Flexible joint actuator for patient's rehabilitation device," in *Proc. 16th IEEE International Symposium on Robot and Human interactive Communication RO-MAN 2007*, pp. 1179–1184, 26–29 Aug. 2007.

[61] J. R. Potvin and S. H. M. Brown, "Less is more: high pass filtering, to remove up to 99muscle force estimates.," *J Electromyogr Kinesiol*, vol. 14, pp. 389–399, Jun 2004.

[62] M. B. I. Raez, M. S. Hussain, and F. Mohd-Yasin, "Techniques of emg signal analysis: detection, processing, classification and applications.," *Biol Proced Online*, vol. 8, pp. 11–35, 2006.

[63] M. Darainy and D. J. Ostry, "Muscle cocontraction following dynamics learning.," *Exp Brain Res*, vol. 190, pp. 153–163, Sep 2008.

[64] G. F. Inbar, "Modeling the human elbow joint dynamics: estimation of joint stiffness with different loads and movement velocities," in *Proc. First Regional Conference. IEEE Engineering in Medicine and Biology Society and 14th Conference of the Biomedical Engineering Society of India An International Meeting*, pp. 3/19–3/20, 15–18 Feb. 1995.

[65] J. Trainor, "Identification of time-varying human joint dynamics during an electrically stimulated twitch," Master's thesis, McGill University, 1994.

[66] H. Kawamoto and Y. Sankai, "Comfortable power assist control method for walking aid by hal-3," in *Proc. IEEE International Conference on Systems, Man and Cybernetics*, vol. 4, p. 6pp., 6–9 Oct. 2002.

Appendix A

Informed Consent

Evaluating Assistive Control Algorithms for a Powered Knee Orthosis

Principal Researcher: Aliasgar Morbi

Department of Mechanical and Aerospace Engineering

Carleton University

ME 3129

1125 Colonel By Drive

Ottawa ON

K1S 5B6

E-mail Address: amorbi@connect.carleton.ca

Telephone: 613-520-2600 x1684

This research is being conducted under the supervision of the following professors:

Name: Mojtaba Ahmadi

Department/School: Mechanical and Aerospace Engineering, Carleton University

E-mail Address: mahmadi@mae.carleton.ca

Telephone: 613-520-2600 x4057

Name: Robert Langlois

Department/School: Mechanical and Aerospace Engineering, Carleton University

E-mail Address: rlangloi@mae.carleton.ca

Telephone: 613-520-2600 x5714

Name: Adrian D.C. Chan

Department/School: Systems and Computer Engineering, Carleton University

E-mail Address: adcchan@sce.carleton.ca

Telephone: 613-520-2600 x1535

Purpose:

Most assistive devices and rehabilitation robots provide users with a fixed amount of support, or force users through predefined trajectories. Both these approaches are not optimal from the point of view of rehabilitation therapy. Providing the user assistance only when required (i.e., the 'assist as needed' approach to rehabilitation therapy) has been proven to maximize both the speed and extent of a user's recovery. Accordingly, the goal of this project is to experimentally evaluate new assistive control algorithms designed specifically to facilitate and accelerate user recovery.

The new algorithms considered in this research are designed to automatically modulate the magnitude and timing of the assistance provided to the user in relation to the user's need for assistance. The primary goal of the research is to characterize how well these new algorithms achieve their intended purpose. The control algorithms will be tested using a powered orthosis created specifically for conducting the research.

Procedure:

By checking the boxes below,

[ ] I understand that some portions of the experiment will require that I wear a powered orthosis that generates an external torque about my knee (or elbow) joint capable of assisting/amplifying (or resisting) my natural knee (or elbow) motion.

[ ] I understand that my muscle activity, knee joint flexion/extension angle, and the interaction force between my lower leg and the powered knee orthosis may be measured and recorded while I complete some of the tasks described in the Session Activities section below. I confirm that I have read through the Letter of Information, and am familiar and comfortable with the methods used to measure and record these quantities.

[ ] I understand that the study will be stopped immediately if the principal researcher notices any unusual readings during the experiment. The principal researcher is not a physician and cannot make a medical diagnosis. I will be asked to contact my family physician. The principal researcher will contact my physician in writing explaining why the experiment was stopped. I may not return to the study or undertake any further experiments without the written consent of my physician.

Session Activities

The list below indicates the activities that will take place and/or that I may be asked to participate in during the course of my session with the principal researcher.

The session will take place at Carleton University in either the Applied Dynamics Laboratory in the VSIM building or at the Advanced Biomechatronics Laboratory in the Mackenzie building. A typical session will include the following activities:

1. Experiment Overview and Safety Briefing (10-15 min)
2. Comparison Data Collection (15-30 min) - I will be asked to do the following types of motions/exercises without wearing the orthosis:
   (a) While sitting, I will be asked to move my lower leg up and down, or to maintain my lower leg at a specific angle for short periods of time. I may be asked to repeat the same motions with ankle weights not exceeding 15 lbs.

(b) I will be asked to stand from a sitting position, and/or sit from a standing position. Only muscle activity will be recorded during this portion of experiment.

3. Safety Feature Testing (10-15 min) - The orthosis will be mounted onto a testing apparatus and all limit switches, emergency stop switches and software safety features will be tested to ensure they function properly.

4. Range of Motion Adjustment (10-15 min) - The device will be fitted onto my leg, and the mechanical hard stop/limit switch positions will be adjusted to achieve the desired range of motion.

5. Range of Motion Adjustment (10-15 min) - The device will be fitted onto my leg, and the mechanical hard stop/limit switch positions will be adjusted to achieve the desired range of motion.

All the steps mentioned above, excluding Step 2 ii) will be followed if elbow flexion/extension experiments are conducted. Step ii) will be avoided since sitting to standing motions contribute no valuable information when conducting experiments with the elbow joint.

By checking the boxes below,

[ ] I agree that I am comfortable with participating in the session activities described above,

[ ] I understand that I have the right to choose which motions/exercises in steps 2 and 5 I wish to participate in during the course of the session,

[ ] I understand that the principal researcher may deny me the opportunity to participate in some activities listed in steps 2 and 5 due to safety concerns,

[ ] I agree to follow the safety protocols and precautions at all times throughout the session,

[ ] I understand that the principal researcher has the right to stop the experiment immediately in the event that I do not comply with the safety protocols and precautions,

and

[ ] I understand that a typical session may require approximately 1.5-2 hours of my time.

The principal researcher may request to take digital images of me while I participate in the experiment. These images may be used in publications related to this research, or for future research in assistive device/rehabilitation robot control. However, I understand that I have the option to participate in the experiment without providing consent for the taking and the use of any images. Please check ONLY ONE of the boxes below:

[ ] YES, I agree to allow these images to be taken during the experiment. I also agree to allow the principal researcher and supervisors to use these images in books, theses, academic journals, conferences, articles, course materials, and/or on web site publications related to this research, and to future research related to assistive device/rehabilitation robot control.

[ ] NO, I prefer that no images be taken during the experiment.

I may be asked to return for additional sessions, and will be informed of this at the end of the first session. I am in no way obligated to participate in these additional sessions.

Risks and Safety Precautions:

I understand that there is some minor physical risk associated with participating in this experiment. The weight of the orthosis, the reduction in range of motion when wearing the orthosis, possible skin irritation due to the use of strapping for securing the orthosis to the leg (or arm) and due to the use of the electrodes for measuring muscle activity, and the sensation of interacting with the orthosis may all prove to be minor sources of discomfort during the experiment.

I also understand that injuries resulting from over-extension or over-flexion of the knee (or elbow) joint are among the only physical risks anticipated during the experiment. I understand that a variety of safety features and precautions have been included in both the design of the device and the experiment in order to mitigate the possibility of over-extension or over-flexion.

By checking the box below,

[ ] I confirm that I am familiar with the safety features and precautions used to limit over-extension and over-flexion discussed in Appendix A of the Letter of Information.

By checking the boxes below, I agree to the use of the following safety precautions:

[ ] I agree to allow my range of motion (while wearing the orthosis) to be reduced via the use of adjustable hard stops and limit switches. I understand that this will reduce the likelihood of injuries due to over-extension and over-flexion.

[ ] I agree to allow the control software to automatically limit the maximum allowable motor torque when the hard stops/limit switches are being approached. I understand that this will help reduce the likelihood of the hard stops ever being engaged and of injuries occurring due to over-extension or over-flexion.

[ ] I agree to work with the principal researcher in choosing safe and appropriate speeds and intensity levels for any motions/exercises in steps 2 and 5 of the Session Activities,

[ ] I agree to wear appropriate clothing and use all the safety equipment that is provided to me by the principal researcher.

[ ] I agree to carry an "emergency stop" push button switch at all times during the experiment. I understand that depression of this switch will immediately power down the motor. I agree to use this switch any time I feel uncomfortable, unsafe, or when I am instructed to do so by the principal researcher.

[ ] I agree to allow the principal researcher to be in control of another "emergency stop"

push button switch at all times during the experiment. I understand that depression of this switch will immediately power down the motor, and I agree to allow the principal researcher to use this switch anytime he perceives a safety risk, or the likelihood of a safety risk.

[ ] I agree to follow any other precautions or safety measures that the principal researcher may explain to me during a session.

Personal Information:

[ ] I understand that I may be asked some questions to ascertain my suitability for participating in the experiment, or for completing some portions of the experiment. These questions will be related to my age, gender, and overall health/physical capacity. I may also be asked about my medical history related to previous shoulder, elbow, wrist, ankle, knee, and hip injuries, and/or any causes of knee muscle weakness.

[ ] I understand that I am allowed to refuse answering any questions. However, I also understand that refusing to answer some questions related to my medical history may make it difficult for the researchers to determine my suitability for the experiment, and that the researchers may be forced to stop me from participating in certain activities or the entire experiment due to safety concerns; in such an event, any information I have provided will be destroyed.

Benefits:

[ ] I understand that I will not be provided with any compensation or benefits for participating in this study. My participation in the experiment will help the researchers understand how to design better control algorithms for assistive devices.

Withdrawal:

[ ] I understand that participation in this study is strictly voluntary. I understand that I

am free to withdraw from the experiment at any time and without any consequences; any information I may have provided prior to withdrawal will be destroyed.

Anonymity and Confidentiality:

The results of this research may be published in a thesis, academic journals, conferences, articles, presentations, course materials, books, and/or on web site publications. None of the published results will contain information that directly reveals my identity. However,

[ ] I understand that information about my age, gender, and other pertinent medical information (e.g., previous history of injuries or other causes of knee muscle weakness) may be included in any such publications,

[ ] I also understand that the researchers will take all reasonable precautions to protect my identity if I have allowed images of my participation in the experiment to be included in any of the publication types mentioned above (e.g., covering my face, only showing images of my lower body, etc.). However, I understand that the researchers cannot fully guarantee my anonymity if any images are used in a publication.

[ ] I understand that the information I provide, any images taken during the experiment, and the data collected during the experiment may be kept for an indefinite period of time by the supervisors. I understand that the data may be used for comparison with data from future experiments and that both the data and images may be used in publications like a thesis, academic journals, articles, presentations, books, course materials, conferences, and/or on web site publications stemming from related future research in assistive device/rehabilitation robot control. Both the principal investigator and supervisors will retain soft copies of the data obtained from these experiments. Soft copies of the data will only be referenced by subject number, and will not contain any personally identifiable information. However, hardcopies of personal information, this consent form, and soft copies of the images will be kept by the supervisors.

I will be provided with a soft copy of the thesis or any other publications that result from the research upon request. I can also be provided with a soft copy of the experimental data from my session upon request.

Ethics Clearance:

This study has been reviewed and received ethics clearance through the Carleton University Research Ethics Committee in accordance to the Tri-Council Policy Statement for Ethical Conduct for Research Involving Humans. I will forward any concerns or questions regarding my involvement in this study to the chair of the committee. The chair's name and contact information is provided below:

Professor Antonio Gualtieri, Chair
Carleton University Research Ethics Committee
Office of Research Services
Carleton University
1125 Colonel By Drive
Ottawa, Ontario K1S 5B6
Tel: 613-520-2517
E-mail: ethics@carleton.ca

Consent for Participation in the Study

I hereby agree to participate in this study and consent to the use of this research data in scientific reports, presentations, and publications. I have read and understand the above explanation of the research procedure and all my questions have been answered to my satisfaction. I understand that I am free to withdraw from this research at any time and without any consequence.

Participant:

Signature:

Date:

Principle Researcher:

Signature:

Date: